

**Isolation, Identification and Bioactivity  
Evaluation of Mangiferin and Genkwanin  
5-O- $\beta$ -primeveroside in Gaharu Plant  
Parts and Finished Products for Gaharu  
Technologies Sdn Bhd**

A THESIS SUBMITTED IN FULFILMENT OF THE  
REQUIREMENTS FOR THE DEGREE OF MASTER OF  
PHILOSOPHY



**University of  
Nottingham**  
UK | CHINA | MALAYSIA

FACULTY OF SCIENCE  
UNIVERSITY OF NOTTINGHAM MALAYSIA CAMPUS  
AUG 2018

BY  
WILLIAM NGUI TET SHUNG

## **ACKNOWLEDGEMENTS**

First and foremost, I would like to express my most sincere gratitude to my supervisor, Dr. Lim Kuan Hon, for his patience and motivation throughout the period of this research and the writing of this thesis. I would also like to express my gratitude to my co-supervisor, Dr. Suresh Kumar MohanKumar, for his guidance in my cell culture works and bioassays. Their guidance has made this project a success.

This research would have been impossible without the help and support of my senior colleagues, Premanad Krishnan, Lee Fong Kai, Chan Zi Yang and Margret Chinoso Ezeoke. I would like to express my gratitude for their help and also for providing a supportive friendly environment. I also greatly appreciate the assistant provided by the staffs at the laboratory and Pharmacy Department, University of Nottingham Malaysia Campus.

Last but not least, my deepest gratitude for my parents for providing me support emotionally and financially. Without them, I would not have such an amazing opportunity to pursue higher education.

## ABSTRACT

Agarwood, produced from the trees of *Aquilaria* species, has been highly valued since ancient times for its commercial uses as well as medicinal properties such as antidiabetic, constipation and headache. HOGA Gaharu Tea products produced by Gaharu Technologies Sdn Bhd (GTSB) were claimed to be able to help reduce blood sugar levels and constipation. However, traditional recipes are generally not formulated based on scientific data, while beneficial claims are often not substantiated scientifically. Based on recent literature reviews, it has been found that the major phytochemicals responsible for the reported antidiabetic and laxative effects of *Aquilaria sinensis* are due to mangiferin (**1**) and genkwanin 5-O- $\beta$ -primeveroside (**4**), respectively (Hara et al., 2008; Ito et al., 2012). In the present study, both mangiferin (**1**) and genkwanin 5-O- $\beta$ -primeveroside (**4**) have been successfully isolated from the acetone and MeOH extracts of gaharu leaf material, along with naringenin (**2**) and iriflophenone 2-O- $\alpha$ -rhamnoside (**3**).

Through MTT assay, safe concentration ranges (above IC<sub>50</sub>) were determined for all test samples to be subjected to gluconeogenesis assay. Glucose concentration values ( $\mu$ M) are normalised by amount of protein ( $\mu$ g) present in each well as determined from the Bradford Protein assay. It has been shown that mangiferin in various concentrations showed significant glucose suppression effect, while genkwanin 5-O- $\beta$ -primeveroside was practically ineffective. Normalised gluconeogenesis assay has shown that leaf water extract, with the highest amount of mangiferin (6.00% w/w), exhibited the best glucose production-suppression activity (0.00035  $\mu$ M/ $\mu$ g) relative to

control (0.00254  $\mu\text{M}/\mu\text{g}$ ). This is followed by twig (0.00090  $\mu\text{M}/\mu\text{g}$ ) which contain 0.50% w/w of mangiferin. Bark (0.00223  $\mu\text{M}/\mu\text{g}$ ) and young shoot (0.00215  $\mu\text{M}/\mu\text{g}$ ) showed no significant glucose suppression activity compared to control, which correlated to the fact that mangiferin was undetectable in these two plant parts. As for the tea products, both Gaharu Tea and Gaharu Cool Tea showed comparable normalised glucose concentration values (0.00172 and 0.00183  $\mu\text{M}/\mu\text{g}$ , respectively), which correlated to the comparable amounts of mangiferin detected in Gaharu Tea (1.33% w/w) and Gaharu Cool Tea (1.66% w/w). Only 0.18% w/w of mangiferin was detected in GOGA Drink Powder, which corresponded well with the high normalised glucose concentration (0.00221  $\mu\text{M}/\mu\text{g}$ ) determined. Through HPLC quantitative analysis, the amounts of genkwanin 5-O- $\beta$ -primeveroside were also determined, i.e., leaf 0.55%, Gaharu Tea 0.15%, and Gaharu Cool Tea 0.11%. Genkwanin 5-O- $\beta$ -primeveroside was undetectable in twig, bark, young shoot, and GOGA Drink Powder. However, no significant gluconeogenesis assay results are associated with genkwanin 5-O- $\beta$ -primeveroside. From the product consumption perspective, each sachet of Gaharu Tea and Gaharu Cool Tea has comparable amount of mangiferin per serving (approximately 4.10 mg and 5.70 mg, respectively), whereas a bottle of GOGA Drink (300 ml/bottle, which is prepared by dissolving GOGA Drink Powder in water) has lesser amount of mangiferin per serving (0.36 mg). Therefore, it is speculated that consuming Gaharu Tea and Gaharu Cool Tea would result in better glucose suppression activity compared to GOGA Drink per serving.

# TABLE OF CONTENTS

<b>Acknowledgements</b> .....	ii
<b>Abstract</b> .....	iii
<b>Table of Contents</b> .....	v
<b>List of Abbreviations</b> .....	ix
<b>List of Figures</b> .....	xii
<b>List of Tables</b> .....	xiv
<b>List of Appendices</b> .....	xvi
<b>Chapter 1: Introduction</b> .....	1
1.1 Background.....	1
1.2 Agarwood and <i>Aquilaria</i> Species.....	2
1.2.1 <i>Aquilaria sinensis</i> .....	4
1.3 Traditional Medicinal Uses, Phytochemicals and Bioactivity of <i>Aquilaria</i> Species.....	5
1.3.1 Phytochemicals and Bioactivity of <i>Aquilaria</i> <i>sinensis</i> .....	7
1.4 Xanthones.....	8
1.4.1 General.....	8
1.4.2 Classification.....	9
1.4.3 Biological Activities of Xanthones.....	11
1.4.3.1 Mangiferin and Its Biological Activities.....	12
1.4.3.2 Antidiabetic Mechanism of Mangiferin.....	13
1.5 Flavonoids.....	17
1.5.1 General.....	17
1.5.2 Classification.....	17
1.5.3 Biological Activities of Flavonoids.....	20
1.5.3.1 Genkwanin 5-O- $\beta$ -primeveroside and Its Biological Activities.....	20

1.6 Diabetes Mellitus.....	21
1.6.1 Classification of Diabetes.....	22
1.6.1.1 Type 1 Diabetes.....	22
1.6.1.2 Type 2 Diabetes.....	23
1.6.2 Complications of Diabetes.....	23
1.6.3 Management of Diabetes Mellitus.....	24
1.6.3.1 Insulin.....	25
1.6.3.2 Oral Antidiabetic Drugs.....	26
1.6.3.3 Traditional Herbal Medicines As Antidiabetic Remedies.....	27
1.7 Gaharu Technologies Sdn Bhd (GTSB).....	29
1.8 Biological Assays.....	31
1.8.1 MTT Assay.....	31
1.8.2 Gluconeogenesis Assay.....	32
1.8.3 Bradford Protein Assay.....	33
1.9 Isolation, Purification and Structure Characterization of Natural Products.....	34
1.9.1 Vacuum Column Chromatography (VCC).....	35
1.9.2 Thin Layer Chromatography (TLC).....	36
1.9.3 Centrifugal Thin Layer Chromatography (CTLC).....	37
1.9.4 High Performance Liquid Chromatography (HPLC).....	38
1.9.5 Nuclear Magnetic Resonance (NMR).....	40
1.9.6 Mass Spectrometry (MS).....	42
1.10 Research Objectives.....	45
<b>Chapter 2: Experimental.....</b>	<b>46</b>
2.1 Plant Source and Gaharu Tea Products.....	46
2.2 Materials.....	46
2.3 General Experimental Procedures Used for Isolation, Purification, and Quantitative Analysis.....	47

2.4 Chromatographic Techniques.....	48
2.4.1 Column Chromatography (CC).....	48
2.4.2 Thin Layer Chromatography (TLC).....	49
2.4.3 Centrifugal Thin Layer Chromatography (CTLC).....	50
2.5 Spray Reagents.....	51
2.5.1 Aluminium Chloride (AlCl <sub>3</sub> ).....	51
2.5.2 10% Sulphuric Acid (H <sub>2</sub> SO <sub>4</sub> ).....	52
2.6 Extraction of Plant Materials.....	52
2.7 Isolation and Purification.....	52
2.7.1 Purification of Genkwanin 5-O-β-primeveroside by Reverse Phase HPLC.....	54
2.8 HPLC Quantitative Analyses of Mangiferin and Genkwanin 5-O-β- primeveroside.....	55
2.9 Compounds Data.....	56
2.10 Cell Culture.....	57
2.10.1 Cell Lines and Cell Culture .....	57
2.10.2 Total Dissolved Solid (TDS).....	57
2.10.3 MTT Assay.....	58
2.10.4 Gluconeogenesis Assay.....	59
2.10.5 Bradford Protein Assay.....	60
2.10.6 Statistical Analysis.....	63
<b>Chapter 3: Results</b> .....	<b>64</b>
3.1 Isolation and Identification of Compounds.....	64
3.1.1 Mangiferin (1).....	65
3.1.2 Naringenin (2).....	68
3.1.3 Iriflophenone 2-O-α-rhamnoside (3).....	70
3.1.4 Genkwanin 5-O-β-primeveroside (4).....	72
3.2 Extraction Yields from TDS.....	76

3.3 HPLC Quantitative Analyses of Mangiferin and Genkwanin 5-O- $\beta$ - primeveroside.....	78
3.4 Biological Assays.....	79
3.4.1 MTT Assay.....	79
3.4.2 Gluconeogenesis Assay.....	83
3.4.3 Bradford Protein Assay.....	86
3.4.4 Normalised Gluconeogenesis Assay.....	91
<b>Chapter 4: Discussion.....</b>	<b>95</b>
4.1 Isolation and Structure Determination.....	95
4.2 Biological Assays.....	96
<b>Chapter 5: Conclusion, Research Limitations and Future Works.....</b>	<b>102</b>
5.1 Conclusion.....	102
5.2 Research Limitations and Future Works.....	104
<b>References.....</b>	<b>106</b>
<b>Appendices.....</b>	<b>124</b>



## LIST OF ABBREVIATIONS

AChE	Acetylcholinesterase
AlCl <sub>3</sub>	Aluminium chloride
AMP	Adenosine monophosphate
AMPK	5' Adenosine monophosphate-activated protein kinase
ATP	Adenosine triphosphate
Bax	BCL2 associated X
Bcl-2	B-cell lymphoma 2
BGL	Blood glucose level
BSA	Bovine solution albumin
CaMKK $\beta$	Calcium-calmodulin-dependent kinase kinase $\beta$
cAMP	Cyclic adenosine monophosphate
CDCl <sub>3</sub>	Deuterated chloroform
CHCl <sub>3</sub>	Chloroform
CO <sub>2</sub>	Carbon dioxide
CoA	Coenzyme A
CRE	cAMP-response element
CREB	cAMP-response element-binding protein
CRTC2	CREB-regulated transcription coactivator 2
CTLC	Centrifugal thin layer chromatography
DAG	Diacylglycerol
DKA	Diabetic ketoacidosis
DMEM	Dulbecco's Modified Eagle's Medium
DMSO	Dimethyl sulfoxide
DNA	Deoxyribonucleic acid
DUSP4	Dual specific phosphatase 4
EGR1	Early growth response protein 1
FBS	Fetal bovine serum

FOXO1	Forkhead box O1
FRIM	Forest Research Institute Malaysia
G6Pase	Glucose-6-phosphatase
GLUT2	Glucose transporter protein 2
GLUT4	Glucose transporter protein 4
GSK-3 $\beta$	Glycogen synthase kinase 3 $\beta$
GTSB	Gaharu Technologies Sdn Bhd
H <sub>2</sub> O	Water
H <sub>2</sub> O <sub>2</sub>	Hydrogen peroxide
H <sub>2</sub> SO <sub>4</sub>	Sulphuric acid
HbA1c	Glycated haemoglobin
HIV-1	Human immunodeficiency virus-1
HPLC	High performance liquid chromatography
IC <sub>50</sub>	Half maximal inhibitory concentration
IDDM	Insulin-dependent diabetes mellitus
IUCN	International Union for Conservation of Nature
LC-MS	Liquid chromatography – mass spectrometry
LDL	Low-density lipoprotein
LKB1	Liver kinase B1
LTQ	Linear trap quadrupole
MeOH	Methanol
MTT	3-(4,5-dimethylthiazol-2-yl)-2,5-diphenyltetrazolium bromide
NADPH	Dihydronicotinamide adenine dinucleotide phosphate
NIDDM	Non-insulin-dependent diabetes mellitus
NMR	Nuclear magnetic resonance
NOE	Nuclear Overhauser effect
ODS	Octadecylsilane
PBS	Phosphate buffered saline
PEPCK	Phosphoenolpyruvate carboxykinase

R&D	Research & Development
R <sub>f</sub>	Retention factor
RIPA	Radioimmunoprecipitation assay
RPMI	Roswell Park Memorial Institute
RT-PCR	Reverse transcription polymerase chain reaction
S.D.	Standard deviation
SDS	Sodium dodecyl sulfate
SEM	Standard error of mean
Tak1	Transforming growth factor $\beta$ -activated kinase-1
TDS	Total dissolved solid
TGF	Transforming growth factor
Thr	Threonine
TLC	Thin layer chromatography
TMS	Tetramethylsilane
UV	Ultraviolet
VCC	Vacuum column chromatography

## LIST OF FIGURES

<b>Figure 1.1:</b> <i>Aquilaria sinensis</i> .....	4
<b>Figure 1.2:</b> Basic structures of basic xanthone and flavonoid skeleta.....	8
<b>Figure 1.3:</b> Chemical structure of mangiferin.....	12
<b>Figure 1.4:</b> Schematic diagram of the carbohydrate metabolism pathway for glycolysis and gluconeogenesis.....	14
<b>Figure 1.5:</b> Schematic diagram of the antidiabetic effect of mangiferin through AMPK activation.....	16
<b>Figure 1.6:</b> The 15-carbon skeleton of a flavonoid.....	18
<b>Figure 1.7:</b> Chemical structure of genkwanin 5-O- $\beta$ -primeveroside.....	21
<b>Figure 1.8:</b> HOGA Gaharu Tea, HOGA Fruit Tea, and GOGA Drink that are being sold in the market.....	29
<b>Figure 1.9:</b> Screenshot of the GTSB homepage about the health beneficial claims of the HOGA Gaharu Tea Products.....	30
<b>Figure 1.10:</b> Reduction of yellow tetrazolium dye MTT into purple formazan.....	32
<b>Figure 1.11:</b> Illustration on the conversion of Amplex Red reagent into resorufin in gluconeogenesis assay.....	33
<b>Figure 1.12:</b> VCC setup.....	36
<b>Figure 1.13:</b> TLC equipment and development process.....	37

<b>Figure 1.14:</b> Schematic view of a Chromatotron.....	37
<b>Figure 1.15:</b> Schematic diagram of a HPLC system featuring an automated sample collector.....	39
<b>Figure 1.16:</b> Schematic diagram of the formation of an electron ionization mass spectrum from a number (p) of molecules (M) interacting with electrons (e <sup>-</sup> ).....	43
<b>Figure 1.17:</b> Schematic diagram of an LC-MS (electrospray ionization interface) system.....	44
<b>Figure 2.1:</b> Isolation of compounds 1-4 from the leaves of <i>A. sinensis</i> .....	54
<b>Figure 2.2:</b> TDS calibration curve of Gaharu Tea.....	58
<b>Figure 2.3:</b> Standard glucose calibration curve.....	60
<b>Figure 2.4:</b> Standard protein calibration curve.....	62
<b>Figure 3.1:</b> <sup>1</sup> H NMR spectrum and the structure of compound <b>1</b> .....	66
<b>Figure 3.2:</b> HPLC profiling of the isolated sample (compound <b>1</b> ).....	67
<b>Figure 3.3:</b> <sup>1</sup> H NMR spectrum and the structure of compound <b>2</b> .....	69
<b>Figure 3.4:</b> <sup>1</sup> H NMR spectrum and the structure of compound <b>3</b> .....	71
<b>Figure 3.5:</b> <sup>1</sup> H NMR spectrum and the structure of compound <b>4</b> .....	73
<b>Figure 3.6:</b> HPLC chromatogram on the purification of genkwanin 5-O-β-primeveroside.....	74
<b>Figure 3.7:</b> MTT assays.....	79

<b>Figure 3.8:</b> Gluconeogenesis assays.....	83
<b>Figure 3.9:</b> Normalised gluconeogenesis assays.....	91
<b>Figure 4.1:</b> Normalised gluconeogenesis concentrations and mangiferin contents associated with the water extracts of different plant parts and tea products.....	98

## LIST OF TABLES

<b>Table 1.1:</b> Six major groups of xanthones.....	10
<b>Table 1.2:</b> Six major groups of flavonoids.....	18
<b>Table 2.1:</b> HPLC conditions used for quantitative analyses of mangiferin and genkwanin 5-O- $\beta$ -primeveroside.....	55
<b>Table 2.2:</b> Standard protein solution dilution.....	61
<b>Table 3.1:</b> Isolation yields of compounds from the leaves of <i>A. sinensis</i> .....	64
<b>Table 3.2:</b> <sup>1</sup> H NMR data of mangiferin ( <b>1</b> ) compared to those of literature.....	65
<b>Table 3.3:</b> <sup>1</sup> H NMR data of naringenin ( <b>2</b> ) compared to those of literature.....	68

<b>Table 3.4:</b> <sup>1</sup> H NMR data of iriflophenone 2-O- $\alpha$ -rhamnoside ( <b>3</b> ) compared to those of literature.....	70
<b>Table 3.5:</b> <sup>1</sup> H NMR data of genkwanin 5-O- $\beta$ -primeveroside ( <b>4</b> ) compared to those of literature.....	72
<b>Table 3.6:</b> TDS of two batches of water extracts of various plant parts and tea products.....	76
<b>Table 3.7:</b> Quantitative analysis of mangiferin and genkwanin 5-O- $\beta$ -primeveroside.....	78
<b>Table 3.8:</b> Total amount of protein determined for the gluconeogenesis assay for acetone extract, methanol extract, mangiferin, insulin, metformin, dexamethasone, vehicle control, and control.....	86
<b>Table 3.9:</b> Total amount of protein determined for the gluconeogenesis assay for genkwanin 5-O- $\beta$ -primeveroside, insulin, metformin, dexamethasone, vehicle control, and control .....	88
<b>Table 3.10:</b> Total amount of protein determined for the gluconeogenesis assay for bark, leaf, twig, young shoot, Gaharu Tea, Gaharu Cool Tea, GOGA Drink Powder and control.....	89
<b>Table 4.1:</b> Tea products composition.....	97
<b>Table 4.2:</b> Mangiferin content per serving of Gaharu Tea, Gaharu Cool Tea, and GOGA Drink.....	100

## LIST OF APPENDICES

<b>Appendix 1:</b> <i>Aquilaria sienensis</i> . A. Flowering twig. B. Inflorescence. C. Flower with part of calyx removed. D. Stigma. E. Petaloid appendages. F. Stamens (in front) with petaloid appendages (behind) .....	123
<b>Appendix 2</b> – <i>Aquilaria sienensis</i> . A. Fruiting bunch. B. Dehisced fruits with seeds hanging on long threadlike funicle. C. Longitudinal section of fruit. D. Seed. F. Hairs on seed surface.....	124
<b>Appendix 3</b> – <i>Aquilaria sinensis</i> . Stages of development from flower bud to mature fruit.....	125
<b>Appendix 4</b> – HPLC analysis of mangiferin (1) tested against standard mangiferin.....	126
<b>Appendix 5</b> – HPLC quantitative analysis of mangiferin in the water extracts of plant parts and tea products (by FRIM).....	127
<b>Appendix 6</b> – HPLC quantitative analysis of genkwanin 5-O- $\beta$ -primeveroside in the water extracts of plant parts and tea products (by Permulab Sdn Bhd).....	128
<b>Appendix 7</b> – LC-Orbitrap-MS (negative mode) of mangiferin (1).....	129
<b>Appendix 8</b> – LC-Orbitrap-MS (negative mode) naringenin (2).....	130
<b>Appendix 9</b> – LC-Orbitrap-MS (negative mode) iriflophenone 2-O- $\alpha$ -rhamnoside (3).....	131



# Chapter One

## Introduction

### 1.1 Background

Diabetes (or diabetes mellitus) is one of the major diseases that contributed to the morbidity and mortality rate worldwide. It is a chronic metabolic disorder related to insulin deficiency and/or insulin resistance. Treatments for diabetes include diet and lifestyle modifications, as well as pharmacological agents such as insulin and oral antidiabetic drugs. However, there are lots of documented side effects from taking these pharmacological agents. Besides that, not every diabetic community can afford to procure these pharmacological agents which need to be taken over a long time, if not for a whole life. All these conditions have led to the ongoing search for antidiabetic agents from natural sources.

Agarwood, also known as gaharu, is mainly produced by trees of *Aquilaria* species. Since ancient times, agarwood has been highly valued for its uses as incenses for religious purposes, perfumes, and also as traditional medicines (Feng et al., 2011). Uses of agarwood in traditional medicine recipes have claimed to possess an array of therapeutic and health promoting effects, where one of them was antidiabetic effect. However, traditional medicine recipes are generally not formulated based on scientific data. Chemical analyses are required to determine the bioactive phytochemicals that are responsible for the claimed bioactivities, and the isolated bioactive

phytochemicals need to be subjected to various bioassays to determine the activity and effect on a molecular level.

## **1.2 Agarwood and *Aquilaria* species**

*Aquilaria* is one of the genera under the Thymelaeaceae family. It is native to Southeast Asia region such as Laos, Vietnam, Malaysia, Borneo and etc. This genus, along with the *Gyrinops* genus, is best known for producing agarwood, which is the resinous heartwood of the *Aquilaria* tree. Agarwood is also known by other names such as gaharu, aloeswood, jinkoh, eaglewood and etc. The agarwood is formed in the tree when it is mechanically wounded and then infected by a certain dematiaceous fungus known as *Phaeoacremonium parasitica*. In response to that, the immune system of the tree will produce an oleoresin rich in volatile organic compounds to retard the fungal growth and activates the healing process (Crous et al., 1996). In nature, only 1 out of 10 *Aquilaria* trees produces agarwood. In recent decades, wild *Aquilaria* trees have declined to near extinction due to the fact that the tree has to be cut open in order to determine the content and quality of the resin, not to mention illegal tree cutting happening everywhere. Eight threatened species are currently included in the IUCN (International Union for Conservation of Nature 2010.3) red list (The World Bank, 2008). In order to satisfy the market needs for sustainable agarwood production, great efforts are taken such as cultivation of 6000 *A. crassna* trees in Phu Quoc Island, Vietnam and also researches in artificial inoculation technologies (Nakashima et al., 2005). The business involving “the wood of gods” is no small trade as the price range can

go from USD100/kg for low grade up to USD100,000/kg for superiorly pure grade. Agarwood is highly-priced and valued due to its characteristic fragrance and beneficial properties. It has been used as incense for centuries in Hindu and Buddhist ceremonies. In the perfume industry, the essential oil of agarwood is highly demanded owing to its unique blend of balsamic and sandalwood-ambergris smell. Besides that, its medicinal properties are highly appreciated and applied into Ayurvedic, Tibetan and Chinese traditional medicines for an array of therapeutic effects such as relieve cough, gastric problems, high fever as well as being sedative, carminative and cardiogenic (Naef, 2011).

There are around fifteen species of *Aquilaria* distributed throughout tropical Asia, these 15 species are *A. apiculata*, *A. baillonii*, *A. banaensae*, *A. beccariana*, *A. brachyantha*, *A. cumingiana*, *A. filaria*, *A. hirta*, *A. khasiana*, *A. malaccensis*, *A. microcarpa*, *A. rostrata*, *A. sinensis*, *A. subintegra*, and *A. crassna*. Out of these fifteen species of *Aquilaria* tree, only the agarwood of *A. sinensis*, *A. malaccensis* (*A. agallocha*) and *A. crassna* are exploited commercially (Naef, 2011). Up to date, five *Aquilaria* species have been found scattered from lowland forests up to hill forests in Malaysia. These five species are *A. beccariana*, *A. hirta*, *A. malaccensis*, *A. microcarpa* and *A. rostrata* (Lee et al., 2013). Three species originated from Indochina were introduced into Malaysia for the purpose of agarwood production. These three species are *A. crassna*, *A. sinensis* and *A. subintegra*, which are mostly planted in plantation (Forestry Department Peninsular Malaysia, 2015).

### 1.2.1 *Aquilaria sinensis*

*A. sinensis* tree may grow up to 20 m tall. The bark is smooth and greyish-brown or light grey in colour, while the twig is covered with short fine hairs. The leaves are characterised by elliptic or obovate, 2.8 – 6 cm wide and 5 – 9 cm long with 15 – 20 pairs of vein. Inflorescences are a terminal or subterminal umbel with 6 – 9 flowers. The flowers are greenish-yellow. Its puberulous pedicels are up to 4 – 10 mm in length. The calyx tube is 3 – 5 mm long. The fruit is a green ovoid-shaped capsule, which can measure up to 1.6 – 2 cm wide and 3 – 4 cm long. The seed is dark brown colour, ovoid and covered with short fine hairs. It can measure up to 7 mm wide and 15 mm long (Sam and Noordin, 2017). For more detailed illustration of the flower, fruit and the stages of fruit development of *A. sinensis*, please refer Appendices 1-3.

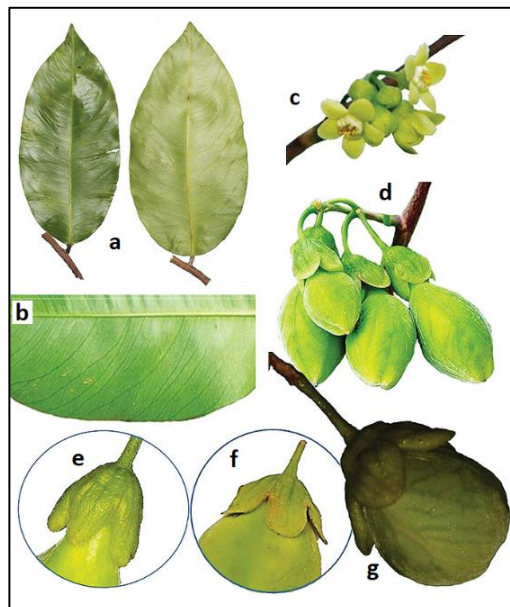


**Figure 1.1** – *A. sinensis*. (a) Upper and lower surfaces of the leaf; (b) veins structure on the lower surface of the leaf; (c) inflorescences; (d) fruits; (e)

calyx tube with big calyx lobes, clutching on the base of the fruit; (f) sometimes the calyx lobes are slightly curved upward; (g) fruit of *A. crassna*, which has similar calyx to that of *A. sinensis* (Forestry Department Peninsular Malaysia, 2015).

### **1.3 Traditional medicinal uses, phytochemicals and bioactivity of *Aquilaria* species**

Agarwood is used not only as incense for religious ceremonies or perfume for centuries, but it also has imperative role in traditional medicines across different cultural backgrounds from Middle East to Asia. Agarwood extract has been used as one of the active ingredients in Thai traditional medicine such as “Krisanaglan”, which was used as antidiarrheal, antispasmodic, and cardiovascular enhancer for patient that has fainted. The extract was also used in other Thai traditional medicines that was used to treat dysentery and skin diseases (Kamonwannasit et al., 2013). It was also reported that the resin of agarwood was traditionally used in India to treat gout, paralysis, snakebite, and vomiting. (Borris et al., 1988). *A. sinensis* was part of the mixtures of a traditional Chinese herbal cataplasm, Xiaozhang Tie used to treat cirrhotic ascites (Xing et al., 2012). Besides that, it was also applied in traditional medicine used to treat bruises and fractures (Zhou et al., 2008). In an ethno-medicinal study conducted in Bangladesh, *A. malaccensis* was found to have been traditionally used by the *Manipuri* tribal community to treat rheumatism (Rana et al., 2010). A review article by Adam et al. (2018) presented that the

leaves of *A. crassna* were used to treat constipation, diabetes, headache, and high blood pressure.

In recent decades, a lot of research has been done on the scientific nature of traditional agarwood application as well as developing new products that have pharmacological activity from agarwood. Up to date, more than 300 phytochemicals have been isolated and identified from numerous species from the *Aquilaria* genus. In some review articles, Chen et al. (2012) have presented 132 phytochemicals, whereas in Wang et al. (2018) another 154 new phytochemicals were presented since 2010. Most of the isolated phytochemicals can be categorised into 2-(2-phenyl)-4H-chromen-4-one derivatives, aromatics, flavonoids, terpenoids, triterpenes, sesquiterpenes, etc. Aquimavitalin, a new phorbol ester isolated from the ethanolic extract of *A. malaccensis*, was reported to possess potential antiallergic activity (Korinek et al., 2016). Aqueous extracts of fermented green tea with *Aquilariae lignum* (*A. malaccensis*), which contain phytochemicals such as benzylacetone, *p*-methoxybenzylacetone, hydrocinnamic acid, agarospirol, agarofuran, and dihydroagarofuran, have shown antidiabetic effect in high fat-fed mouse (Lee et al., 2015).  $\beta$ -Caryophyllene, a sesquiterpene isolated from the essential oil of *A. crassna*, has shown selective anticancer, antioxidant and antimicrobial activities (Dahham et al., 2015). Iriflophenone 3-C- $\beta$ -D-glucoside was reported as one of the major active compounds in *A. crassna* leaf with antidiabetic activity (Putalun et al., 2013). Kaempferol 3,4,7-trimethyl ether, isolated from the leaf of *A. subintegra*, has shown to possess AChE inhibitory activity

(Bahrani et al., 2014). Specific phytochemicals from *A. sinensis* as well as their bioactivities are discussed in the subsequent section (1.3.1).

### **1.3.1 Phytochemicals and bioactivity of *Aquilaria sinensis***

Four fragrant sesquiterpenes, which are 4-hydroxyl-baimuxinol, 7 $\beta$ -H-9(10)-ene-11,12-epoxy-8-oxoeremophilane, 7 $\alpha$ -H-9(10)-ene-11,12-epoxy-8-oxoeremophilane, and neopetasane, were isolated from *A. sinensis* and these phytochemicals (except 4-hydroxyl-baimuxinol) have shown potential acetylcholinesterase (AChE) inhibitory activity, which is the principal pharmacotherapy mechanism of drugs used to treat Alzheimer's disease (Yang et al., 2014). Mangiferin and genkwanin 5-O- $\beta$ -primeveroside were reported to be the major phytochemicals responsible for the laxative effect of the ethanolic extract of *A. sinensis* and *A. crassna* (Hara et al., 2008; Kakino et al., 2010; Ito et al., 2012). Four new compounds, which are aquilarisinin, aquilarisin, hypolaetin 5-O- $\beta$ -D-glucuronopyranoside, and aquilarixanthone, together with another four known compounds, including mangiferin, iriflophenone 2-O- $\alpha$ -L-rhamnopyranoside, iriflophenone 3-C- $\beta$ -D-glucoside, and iriflophenone 3,5-C- $\beta$ -D-diglucoopyranoside were isolated from 70% aqueous ethanolic extract of *A. sinensis* leaves. All eight of these compounds were reported to exhibit  $\alpha$ -glucosidase inhibitory activity, of which mangiferin showing the most potent activity (Feng et al., 2011). A novel benzophenone glucoside (aquilarinoside A) and a new flavonoid (7- $\beta$ -D-glucoside of 5-O-methylapigenin), along with eight known compounds, including iriflophenone,

mangiferin, 5-O-xylosylglucoside of 7-O-methylapigenin, 5-O-xylosylglucoside of 7,4'-di-O-methylapigenin, 5-β-D-glucoside of 7,3'-di-O-methyluteolin, luteolin, genkwanin, and hydroxygenkwanin were isolated from the leaves of *A. sinensis*. All these compounds (except 5-O-xylosylglucoside of 7,4'-di-O-methylapigenin and 5-β-D-glucoside of 7,3'-di-O-methyluteolin) showed anti-inflammatory activity in the neutrophils respiratory burst assay (Qi et al., 2009). Pranakhon et al. (2015) have isolated five compounds from the methanolic extract of *A. sinensis* leaves, which include 5-hydroxy-7,4'-dimethoxyflavone, genkwanin, protocatechuic acid, iriflophenone 3-C-β-glucoside, and mangiferin. All these compounds were found to lower the fasting blood glucose activity through mechanism such as enhancement of glucose uptake activity.

## **1.4 Xanthoness**

### **1.4.1 General**

Mangiferin is the major xanthone-type compound that was isolated from *Aquilaria* species and was found to be a main active constituent for the antidiabetic effect of *Aquilaria* species. Xanthoness are secondary metabolites that occur commonly in higher plant families, fungi and lichen (Negi et al., 2013). The molecular formula of a basic xanthone structure is C<sub>13</sub>H<sub>8</sub>O<sub>2</sub> and its structure is closely related to that of flavonoid (Figure 1.2).



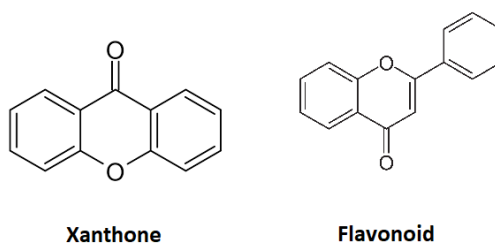


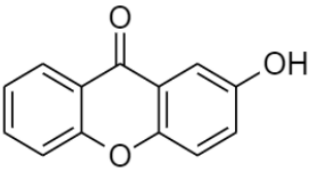
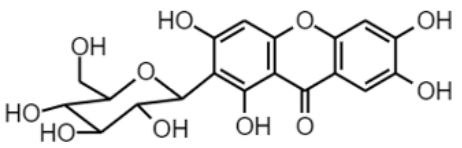
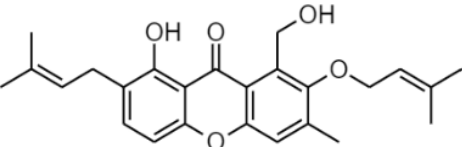
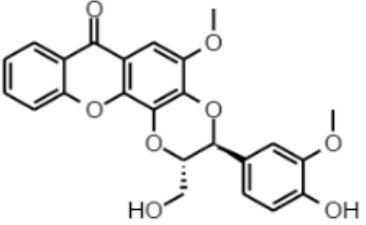
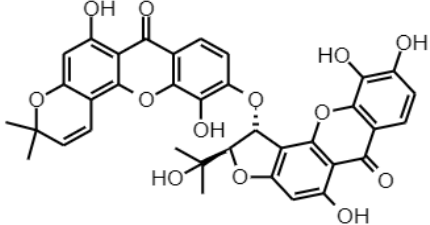
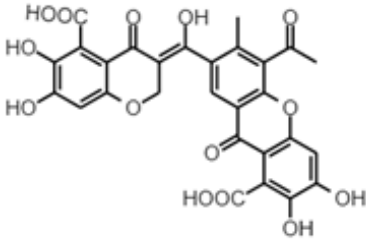
**Figure 1.2** – Basic structures of basic xanthone and flavonoid skeleta.

Flavonoids are found commonly in nature whereas xanthenes are mainly occurring in limited number of families such as Clusiaceae, Gentianaceae, Guttiferae, Moraceae, Polygalaceae (Negi et al., 2013) and Thymelaeaceae (in which *Aquilaria* species belong). Most xanthenes isolated from higher plants are mainly associated with the families Clusiaceae (55 species in 12 genera) and Gentianaceae (28 species in 8 genera) (Vieira and Kijjoa, 2005). Xanthenes are sometimes found as mono- or poly-methyl ethers, as parent polyhydroxylated compounds, or even as glycosides (Hostettmann and Miura, 1977).

#### 1.4.2 Classification

Xanthenes isolated from natural sources can be classified into six major groups based on their structure. These six major groups are simple oxygenated xanthenes, xanthone glycosides, prenylated xanthenes, xanthonolignoids, bisxanthenes, and miscellaneous xanthenes. Table 1.1 shows an example for each of the six major groups of xanthenes.

**Table 1.1** – Six major groups of xanthenes.

Group	Characteristics	Example
Simple oxygenated xanthenes	Hydroxy, methoxy, or methyl groups	 <p>2-hydroxyxanthone</p>
Xanthone glycosides	C- or O-glycosides	 <p>Mangiferin</p>
Prenylated xanthenes	Prenyl group (C <sub>5</sub> )	 <p>Isoemicicellin</p>
Xanthonolignoids	Benzyl ether moiety	 <p>Kielcorin</p>
Bisxanthenes	Two xanthone moieties	 <p>Jacarelhyperol A</p>
Miscellaneous xanthenes	Substituents not belonging to any of the five groups	 <p>Xanthofulvin</p>

### 1.4.3 Biological activities of xanthenes

Naturally occurring xanthenes have emerged as an important class of organic compound due to their outstanding biological and pharmacological activities. It has been observed that most plant-based chemotherapeutic agents contain xanthenes as one of the active constituents. As mentioned above, naturally occurring xanthenes are rare and only limited to a number of families. Xanthenes belonging to the family Gentianaceae are best known for their bitter taste and are used in some traditional remedies to treat fever and loss of appetite (Negi et al., 2013). Bellidifolin (extracted from *Swertia japonica*) and Swerchirin (extracted from *Swertia longifolia* and *Swertia chirayita*) are reported to have strong hypoglycaemic activity (Bajpai et al., 1991; Basnet et al., 1995; Shekarchi et al., 2010). *Swertia paniculata*, which is widely distributed throughout the temperate region above 5000 ft sea level at Western Himalayas, is used as bitter tonic in the Indian system medicine to treat certain mental disorder such as melancholia (Prakash et al., 1982). Extract of *Swertia hookeri* has been found to possess antimicrobial activity and also can be used as mood elevator (Ghosal et al., 1980). Swertifrancheside isolated from *Swertia franchetiana*, along with other compounds such as triterpene and protolichesterinic acid isolated from other natural sources, were found to be potent inhibitors of the DNA polymerase activity of HIV-1 reverse transcriptase. (Pengsuparp et al., 1995). A herbal formulation known as Ayush-64 which is used to treat malaria contain the extract of *Swertia chirata* (Neena et al., 2000). An O-glycoside xanthone known as norswertianolin which is isolated from *Swertia purpurascens*, has

been reported to cause anticonvulsant activity and central nervous system depression in albino rats and mice (Ghosal et al., 1974). Eight out of twenty xanthenes isolated from *Swertia mussotii* are reported to have significant inhibition on hepatitis B virus DNA replication (Cao et al., 2013). The various biological activities shown by mangiferin are discussed in the subsequent section (1.4.3.1).

#### 1.4.3.1 Mangiferin and its biological activities

Mangiferin (2-β-D-glucopyranosyl-1,3,6,7-tetrahydroxyxanthen-9-one) is a natural C-glucoside xanthone, which can be found abundantly in various parts of mango tree (*Mangifera indica*, family Anacardiaceae) (Biswas et al., 2015). Some other plant sources where mangiferin can be isolated include *Aquilaria* species, *Bombax malabaricum*, *Gentiana lutea*, and *Swertia chirata*. The molecular formula of mangiferin is C<sub>19</sub>H<sub>18</sub>O<sub>11</sub>, and it has a molecular weight of 422.34 g/mol. The chemical structure of mangiferin is illustrated in Figure 1.3.

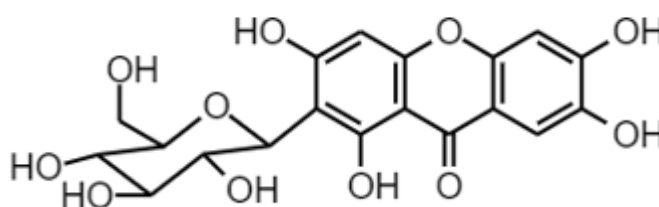


**Figure 1.3** – Chemical structure of mangiferin.

Mangiferin has been reported to possess an array of therapeutic effects such as antidiabetic, anti-inflammatory, antioxidant and laxative. The most studied

and prominent bioactivity associated with mangiferin is antidiabetic activity. Mangiferin was reported to have antihyperglycemic effect on streptozotocin-induced diabetic rats (Li et al., 2010), lowers blood lipids which is beneficial for type 2 diabetes and metabolic disorder (Huang et al., 2006), as well as modulating multiple targets: protein tyrosine phosphatase 1B (Hu et al., 2007), glucose transporter protein 4 (GLUT4) (Miura et al., 2001), and  $\alpha$ -glucosidase (Feng et al., 2011). These findings supported mangiferin to be a potentially useful antidiabetic agent. Mangiferin has also been reported to possess anti-inflammatory and antioxidant properties, such as regulation of the Bcl-2 and Bax pathway (Luo et al., 2015) as well as decreasing oxidative stress damage (Kavitha et al., 2013). The laxative effect of mangiferin has been reported to be caused by activation of the acetylcholine receptors (Kakino et al., 2010).

#### **1.4.3.2 Antidiabetic mechanism of mangiferin**

Gluconeogenesis is a metabolic pathway where glucose is synthesised from pyruvate and other non-carbohydrate precursors such as amino acid, glycerol, and lactate (Rang et al., 2003). It is the reverse process of glycolysis where glucose is broken down into pyruvate. Figure 1.4 illustrates the carbohydrate metabolism pathway for glycolysis and gluconeogenesis.

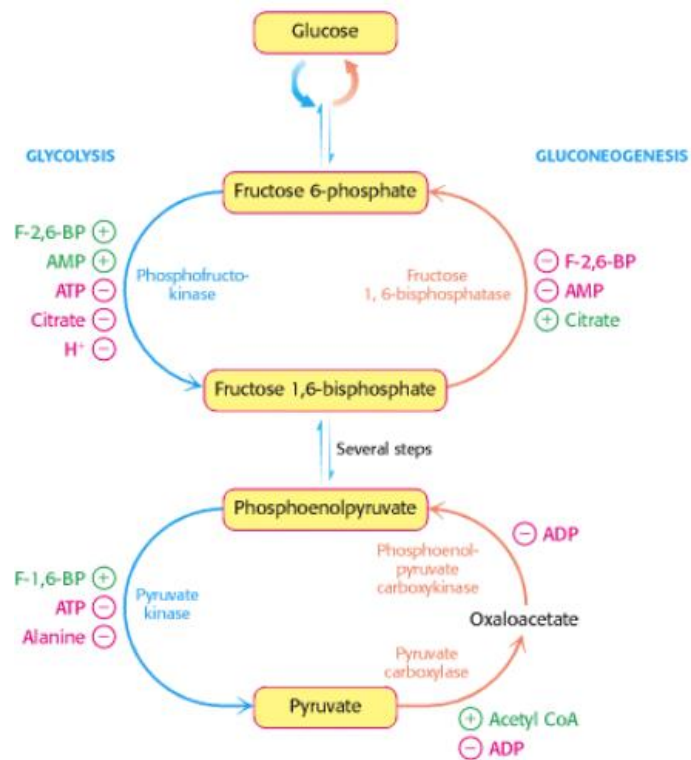


**Figure 1.4** – Schematic diagram of the carbohydrate metabolism pathway for glycolysis and gluconeogenesis (Raval et al., n.d.).

5' Adenosine monophosphate-activated protein kinase (AMPK) is a major regulator of metabolic homeostasis and cellular energy sensor (Zhang et al., 2009). It is a heterotrimeric complex made up of a catalytic ( $\alpha$ ) and two regulatory ( $\beta$  and  $\gamma$ ) subunits (Hardie et al., 2006). Phosphorylation of threonine (Thr)-172 within the  $\alpha$  subunit is the prerequisite for AMPK activation. Three upstream kinases are known to phosphorylate Thr-172, these are: liver kinase B1 (LKB1), calcium-calmodulin-dependent kinase kinase  $\beta$  (CaMKK $\beta$ ) and transforming growth factor (TGF)- $\beta$ -activated kinase-1 (Tak1) (Zhang et al., 2009).

Mangiferin is known to possess antidiabetic properties. Multiple studies have concluded that the antidiabetic property of mangiferin comes from the

activation of AMPK (Zhang et al., 2009; Wang et al., 2016). Several versions of AMPK activation mechanism by mangiferin were reported. One report suggested that mangiferin stimulate AMPK by increasing the AMP/ATP (adenosine monophosphate/adenosine triphosphate) ratio (Niu et al., 2012). Another study showed that the AMPK stimulation activity of mangiferin could be blocked partially by a CaMKK $\beta$  inhibitor, suggesting AMPK activation by mangiferin may involve the CaMKK $\beta$  (Han et al., 2015).

There are two metabolic pathways that lead to the antidiabetic effect upon activation of AMPK by mangiferin. First of all is the increase in basal glucose consumption which is AMPK-dependent. Mangiferin has shown to stimulate membrane translocation of GLUT4 to the plasma membrane (Girón et al., 2009). Besides that, mangiferin has also shown to increase glucose and pyruvate oxidation as well as ATP production in muscle cells (Apontes et al., 2014). Both of these mechanisms lead to increased glucose uptake.

The second metabolic pathway which mangiferin causes antidiabetic effect is through gluconeogenesis suppression, which is also AMPK-dependent. There are two pivotal enzymes involved in the completion of the gluconeogenesis pathway. Phosphoenolpyruvate carboxykinase (PEPCK) is involved in the conversion of oxaloacetate into phosphoenolpyruvate at the early stage of gluconeogenesis (Méndez-Lucas et al., 2014), whereas as glucose-6-phosphatase (G6Pase) is responsible for hydrolysing glucose 6-phosphate into free glucose and a phosphate group (Ghosh et al., 2002). When transcriptions factors such as cAMP-responsive element-binding protein (CREB)-regulated

transcription coactivator 2 (CRTC2) and forkhead box O1 (FOXO1) bind to the CRE in the genes of PEPCK and G6Pase, expression of these two enzymes is induced. However, activation of AMPK suppresses the binding of these two transcription factors, leading to the downregulation of PEPCK and G6Pase, which translate to the reduction of gluconeogenesis in the liver (Zhang et al., 2009). Besides that, AMPK activation also increases phosphorylation of glycogen synthase kinase 3 $\beta$  (GSK-3 $\beta$ ), which reduces the transcriptional activity of CRE and gene expression of PEPCK-C in the liver, thus reducing gluconeogenesis (Horike et al., 2008). Figure 1.5 shows the overall antidiabetic effect of mangiferin upon activation of AMPK.

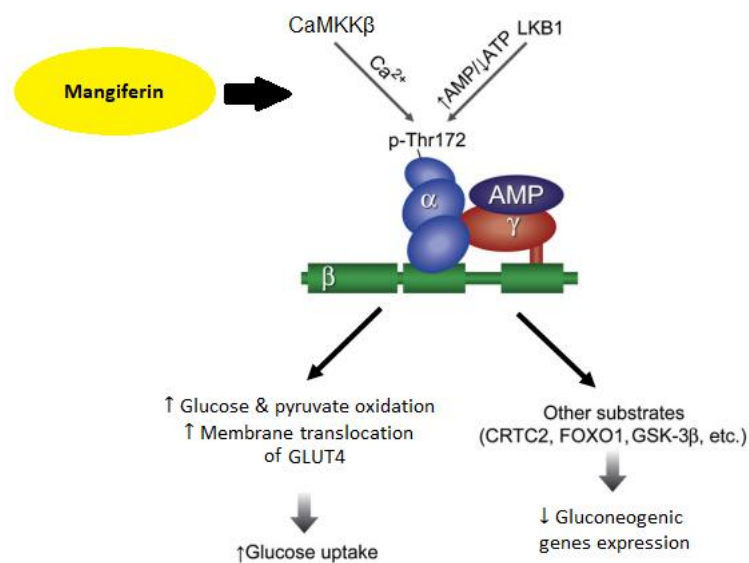


**Figure 1.5** – Schematic diagram of the antidiabetic effect of mangiferin through AMPK activation. Increase in AMP/ATP ratio will activate LKB1, whereas increase in intracellular calcium will activate CaMKK $\beta$ . Activation of these upstream kinases will activate AMPK through phosphorylation of Thr-172 (Zhang et al., 2009).



## 1.5 Flavonoids

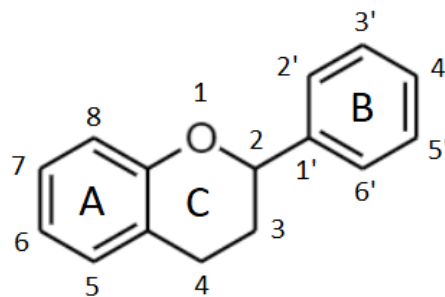
### 1.5.1 General

Genkwanin 5-O- $\beta$ -primeveroside is one of the major flavonoid compounds that was isolated from *Aquilaria* species and was found to be the main active constituent for the laxative effect of *Aquilaria* species (Hara et al., 2008; Kakino et al., 2010; Ito et al., 2012). Flavonoids (or bioflavonoids) are secondary metabolites of plants and fungi and are the most abundant polyphenolic compound found in photosynthesising plant cells and human diet (Havsteen, 2002). Flavonoids, come from the Latin word *flavus*, meaning yellow, and are mostly known as plant pigments for producing the many colours found in flowers, fruits, and leaves. For example, anthocyanin pigments are mainly responsible for the fruit colouration of red-skinned grapevines (Castellarin and Di Gaspero, 2007). Besides that, some flavonoids such as kaempferol 3-O- $\beta$ -D-glucopyranosyl (1  $\rightarrow$  2)-O- $\beta$ -D-glucopyranoside and kaempferol 3-O-rutinoside isolated from carnation flower cultivar *Esperia* have shown antifungal activity against *Fusarium oxysporum*, a fungal species pathogenic to plants, especially carnation (Galeotti et al., 2008).

### 1.5.2 Classification

More than 5000 different flavonoids have been identified and isolated from different plant sources. A review by Kristanti et al. (2018) presented a total of 22 flavonoids previously isolated from *A. sinensis*. The basic structure of

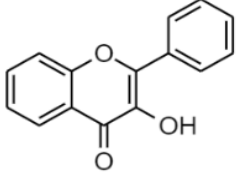
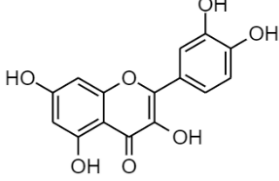
flavonoids is made up of a 15-carbon skeleton comprised of a heterocyclic ring and two phenyl rings which are joined up by a linear 3-carbon chain. Flavonoids can be divided into six main groups based on the substitution patterns of ring C (heterocyclic ring), while the flavonoids within the same group can be differentiated by the substitution patterns of ring A and B (the two phenyl rings) (Prasain et al., 2010). Figure 1.6 shows the 15-carbon skeleton of a flavonoid.

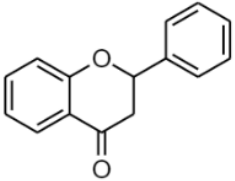
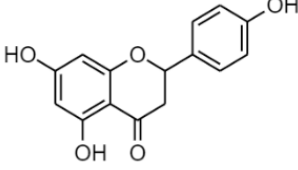
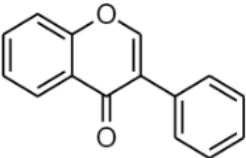
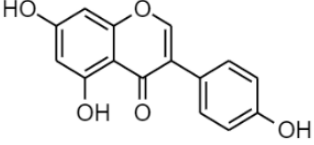
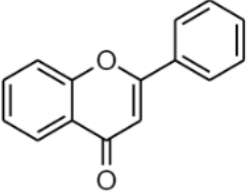
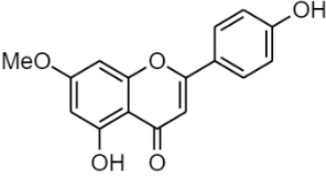
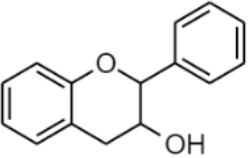
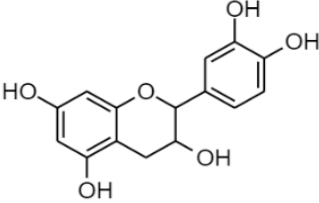
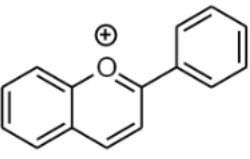
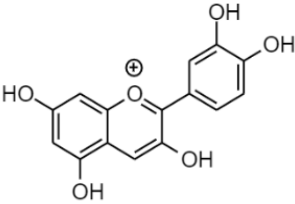


**Figure 1.6** – The 15-carbon skeleton of a flavonoid.

There are six major groups of flavonoids based on the substitution patterns on ring C. Table 1.2 summarises the substitution patterns of all these groups, with one example from each group given, together with its dietary source.

**Table 1.2** – Six major groups of flavonoids (Hossain et al., 2016).

Group	Structure description	Compound	Dietary source
Flavonol	 3-hydroxy-2-phenyl-4H-chromen-4-one	 Quercetin	Red onion

Flavanone	 <p>2-phenyl-2,3-dihydro-4H-chromen-4-one</p>	 <p>Naringenin</p>	Citrus
Isoflavone	 <p>3-phenyl-4H-chromen-4-one</p>	 <p>Genistein</p>	Soy
Flavone	 <p>2-phenyl-4H-chromen-4-one</p>	 <p>Genkwanin</p>	<i>Daphne genkwa</i>
Flavan-3-ol	 <p>2-phenyl-3,4-dihydro-2H-chromen-3-ol</p>	 <p>Catechin</p>	Green tea
Anthocyanin	 <p>2-phenylchromenylium (flavylium)</p>	 <p>Cyanidin</p>	Blueberry

### **1.5.3 Biological activities of flavonoids**

Many of the isolated naturally occurring flavonoids have been reported to show many health benefits over chemical treatments. For example, quercetin was reported to have antioxidant and anti-inflammatory properties (Zhang et al., 2011). Several investigations suggested that naringenin supplementation is beneficial for obesity, diabetes, hypertension, and metabolic syndrome (Alam et al., 2014). A relation between a soy-rich diet and cancer prevention have been shown in some epidemiologic studies, which was attributed to the presence of genistein in soy-based foods (Spagnuolo et al., 2015). Wang et al. (2015) had tested the activity of genkwanin on HT-29 and SW-480 human colorectal cancer cell lines *in vitro* and showed promising antitumor activity. Reduction in body fat and malondialdehyde-modified LDL (low-density lipoprotein) was reported through daily consumption of tea rich in catechins for 3 months (Nagao et al., 2005). Cyanidin, an anthocyanidin which is the aglycone form of anthocyanin, was reported to exhibit antioxidant activity on the erythrocyte cell membranes of rabbit (Tsuda et al., 1994). The biological activities shown by genkwanin 5-O- $\beta$ -primeveroside are discussed in the subsequent section (1.5.3.1).

#### **1.5.3.1 Genkwanin 5-O- $\beta$ -primeveroside and its biological activities**

Genkwanin 5-O- $\beta$ -primeveroside is an O-methylated flavone, with a sugar moiety known as  $\beta$ -primeveroside attached to the C5 oxygen atom. The primeveroside is made up of a  $\beta$ -glucose and a  $\beta$ -xylose. So far it has only

been reported to be isolated from *Aquilaria* species (Ito et al., 2012) and *Daphne genkwa* (Lin et al., 2001). The molecular formula of genkwanin 5-O- $\beta$ -primeveroside is  $C_{27}H_{30}O_{14}$ , and it has a molecular weight of 578.43 g/mol. The chemical structure of genkwanin 5-O- $\beta$ -primeveroside is illustrated in Figure 1.7.

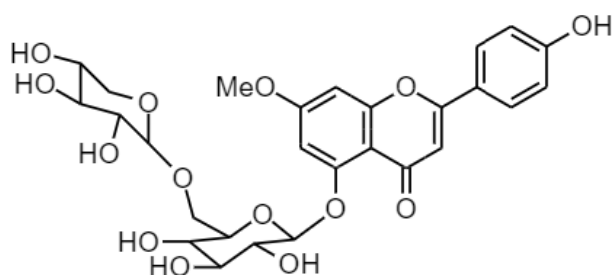


**Figure 1.7** – Chemical structure of genkwanin 5-O- $\beta$ -primeveroside.

Not many biological activity studies were carried out on genkwanin 5-O- $\beta$ -primeveroside. Up to date, only laxative effect (Hara et al., 2008; Kakino et al., 2010; Ito et al., 2012) and potential antioxidant effect (Supasuteekul et al., 2017) were reported. A review by Hossain et al. (2016) has shown that all of the flavonoids from the six groups (except genkwanin) mentioned above may potentially possessed antiobesity and antidiabetic properties.

## 1.6 Diabetes mellitus

One of the traditional uses of *Aquilaria* species is to treat/manage diabetes. Diabetes mellitus is a chronic metabolic disorder characterised with hyperglycaemia (high blood glucose concentration, fasting blood glucose > 7 mmol/L, or plasma glucose > 11.1 mmol/L, 2 hours after meal) due to insulin

deficiency, insulin resistance or both combined. It is one of the most prevalent disease that has high mortality rate if not treated. When there is reduction of glucose uptake by skeletal muscles due to reduced glycogen synthesis (glycogenesis) and uncontrolled hepatic glucose output (gluconeogenesis), hyperglycaemia occurs (Rang et al., 2003).

### **1.6.1 Classification of diabetes**

There are two types of diabetes mellitus: type 1 diabetes and type 2 diabetes. It is estimated that 1 out of 20 of most western countries population suffered from diabetes, and 80% of these diabetic patients have type 2 diabetes (Rang et al., 2003). In 2017, 3.6 million diabetes cases were reported out of 32 million Malaysia populations (“Staggering 3.6 mil Malaysians”, 2017).

#### **1.6.1.1 Type 1 diabetes**

Previously known as insulin-dependent diabetes mellitus (IDDM) as the patients require insulin injection since their pancreas cannot produce any insulin. This is due to complete destruction of the  $\beta$ -cells of the pancreas which may have caused by toxin exposure, viral or bacterial infection, or even autoimmune response that triggers antibodies to destroy the Langerhans cells in genetically predisposed individuals. Most patients do not inherit from their parent as the genetic predisposition of type 1 diabetes is moderate. Type 1 diabetes usually occurs on young individuals and tend to exhibit characteristic

symptoms such as increased hunger (polyphagia), thirst (polydipsia) and urinary frequency (polyuria) (Boarder et al., 2010).

#### **1.6.1.2 Type 2 diabetes**

Previously known as non-insulin-dependent diabetes mellitus (NIDDM) since insulin injection is not compulsory as insulin is still being produced by the pancreas. However, this terminology is no longer valid as majority of the type 2 diabetes patients still require insulin injection when the oral medication fails. Unlike type 1 diabetes, type 2 diabetes has strong genetic predisposition. This means that an individual has higher chances of developing type 2 diabetes if the disease runs within the family members. Prevalence of type 2 diabetes is also influenced by age and ethnicity, with higher incidence being reported to occur on older and non-Caucasians individuals. Due to a combination of impaired functions of their Langerhans cells such as decreased insulin secretion and sensitivity, coupled with increased glucose production in liver, type 2 diabetes patients are often obese (Boarder et al., 2010).

#### **1.6.2 Complications of diabetes**

When diabetes is not properly treated, several complications could arise that could increase the morbidity and mortality rate of patients. The two most common complications are acute complications and long-term complications.

Acute complications are often metabolic emergencies that could be lethal if not treated and occur more commonly for type 1 diabetes patients. The major

disease in this category is diabetic ketoacidosis (DKA), which is a metabolic emergency with high mortality rate. When insulin is absent in cells such as skeletal muscle and adipose tissue that depend on insulin for glucose uptake, the breakdown rate of fat (lipolysis) to acetyl-CoA will increase. In some serious cases where oxygen and aerobic carbohydrate metabolism are absent, the acetyl-CoA will be converted further into acetoacetate, acetone and  $\beta$ -hydroxybutyrate. The  $\beta$ -hydroxybutyrate accounts for the acidosis while acetone causes the patient's breath to smell like ketone (Boarder et al., 2010).

A number of organs and cells can be damaged under long-term hyperglycaemia through several mechanisms such as non-enzymatic glycosylation of proteins and lipids, activation of protein kinase C, and glucose forced through the polyol pathway. All these mechanisms lead to complications such as thickening of blood vessel walls, cell injury through osmosis, microangiopathy and macrovascular disease (Rang et al., 2003; Boarder et al., 2010).

### **1.6.3 Management of diabetes mellitus**

Diabetes mellitus is fatal if not properly managed and the management of this disease often involves diet modifications and pharmacological agents. Diet modifications involve eating moderate amounts of proper healthy foods at regular mealtimes, whereas pharmacological agents involve the use of insulin and oral antidiabetic drugs. Insulin is compulsory for type 1 diabetes patients, but only required at later stages for type 2 diabetes patients when their



pancreatic insulin stores have completely depleted. For type 2 diabetes patients, their primary treatment involves diet modifications and oral antidiabetic drugs. Therapy of diabetes is monitored using measures such as blood glucose level (BGL) and percentage of glycated haemoglobin (HbA1c). Even though there is no absolute target value of the measurements for diabetic patients, general consensus now is that the closer the value to normal BGL and HbA1c, the better the long-term outcomes. The normal BGL and HbA1c values are < 6 mmol/L and < 7%, respectively (Boarder et al., 2010).

#### **1.6.3.1 Insulin**

Insulin is a protein composed of 51 amino acids and contain two amino acid chains called A chain and B chain. A chain contains 21 amino acids whereas B chain contains 30 amino acids, and both chains are linked together by disulphide bridges. Insulin is synthesised as a precursor (preproinsulin) in the rough endoplasmic reticulum of the  $\beta$ -cells in pancreas. The preproinsulin is transported to the Golgi apparatus where it undergoes proteolytic cleavage into proinsulin, then to insulin and a fragment of C-peptide molecules with unknown function. Insulin and C-peptide are stored in the granules of  $\beta$ -cells in equimolar concentrations, ready for cosecretion by exocytosis together with small amount of proinsulin. When glucose enters the  $\beta$ -cells through a glucose transporter 2 (GLUT2) membrane transporter, it is metabolised into pyruvate which in turn increases the production of ATP. The increase in intracellular ATP causes a closure of ATP-sensitive potassium channels, which

causes a reduction in potassium influx. This leads to depolarisation of the  $\beta$ -cells membrane and opening of the voltage-dependent calcium channels, leading to calcium influx. This signals the translocation and exocytosis of the secretory granules of insulin to the  $\beta$ -cell surface, but only in the presence of other amplifying messengers such as diacylglycerol (DAG) and non-esterified arachidonic acid (Rang et al., 2003; Boarder et al., 2010).

Even though insulin is a life-saving medication, it is not without some adverse effects. Repeated injections at the same spot could cause lipodystrophy (abnormal changes in fat distribution) and scarring. Besides looking unsightly, this could affect the absorption efficacy of insulin. Therefore, patients are advised to rotate the injection sites. Another potentially more life-threatening side effect is hypoglycaemia, which could occur from over injection of insulin or sudden changes in eating pattern. In severe cases where the patient become unconscious, intravenous glucose injection or parenteral therapy with glucagon is required (Boarder et al., 2010).

#### **1.6.3.2 Oral antidiabetic drugs**

Oral antidiabetic drugs are only used for management of type 2 diabetes. Several classes of oral antidiabetic drugs are now available in the market, these include  $\alpha$ -glucosidase inhibitors (acarbose), insulin sensitisers (metformin), dipeptidyl peptidase 4 inhibitors (sitagliptin), insulin secretagogues (glibenclamide), and peroxisome proliferator activated receptor gamma (PPAR $\gamma$ ) agonists (thiazolidinediones). Each of these drugs

produces hypoglycaemic effect through different mechanism of actions (Boarder et al., 2010). Even though these drugs are effective against diabetes, most of the drugs come with side effects. For example, the daily dose of acarbose need to be taken in a gradually increasing manner to avoid gastrointestinal complications such as bloating and flatulence due to unabsorbed sugars serving as substrates for gastrointestinal bacteria (Boarder et al., 2010). Phenformin was one the biguanides under the insulin sensitisers category. However, it was withdrawn due to cases of fatal lactic acidosis. Metformin is currently the only one drug that remained in use under this category of oral antidiabetic drugs, with extremely low prevalence of causing lactic acidosis (0.03 cases in 1000 patients per year) as reported in literature (Bösenberg and Zyl, 2008). The most common adverse effect of glibenclamide is hypoglycaemia and weight gain. Given that most type 2 diabetes patients are overweight, sulphonylureas are not the first choice of drugs.

### **1.6.3.3 Traditional herbal medicines as antidiabetic remedies**

Due to the multiple side-effects that come together with synthetic antidiabetic drugs, there is increasing demand by patients on the use of natural products with antidiabetic activity. There have been a number of traditional herbal medicines that are used to treat diabetes mellitus since ancient time. These traditional herbal medicines can be categorised into four categories based on their mechanism of action:

**(a) Medicines acting like insulin**

Polypeptide-P was isolated from the seeds and other tissues of the fruit of *Momordica charantia* (bitter melon) which was reported to possess hypoglycaemic effect when administered subcutaneously to humans and langurs (Joseph and Jini, 2013).

**(b) Medicines acting on insulin-secreting  $\beta$ -cells**

Aqueous extract of *Allium cepa* (onion) was found to exhibit promising hypoglycaemic and hypolipidaemic effects in alloxan-induced diabetic rats by stimulating the release of insulin (Ozougwu, 2011).

**(c) Medicines that modify glucose utilisation**

*Cyamopsis tetragonolobus* (Gowar plant) was reported to exhibit hypoglycaemic activity through modification of glucose utilisation by increasing the viscosity of the gastrointestinal contents and slowing the gastric emptying (Wadkar et al., 2008).

**(d) Miscellaneous mechanisms**

Attele et al. (2002) have found that *Panax Ginseng* berry extract significantly improved glucose homeostasis and systemic insulin sensitivity in obese mice. *Curcuma longa* (turmeric) extracts were found to exhibit potent inhibitory activity on  $\alpha$ -glucosidase activities and glycation reactions (Lekshmi et al., 2014).

## 1.7 Gaharu Technologies Sdn Bhd (GTSB)

GTSB undertakes intensive cultivation of gaharu-producing *Aquilaria* plants on a commercial scale at Gaharu Tea Valley Gopeng. GTSB has become successful in large-scale gaharu plantation and its management with full support from its subsidiary, Envirotech Management Sdn Bhd. GTSB also has an R&D laboratory to perform tests on *Aquilaria* plants for the purpose of enhancing the quality of the agarwood and the commercial products derived from the *Aquilaria* trees. Specifically, GTSB has an array of tea products (mixture of different plant parts from the cultivated *Aquilaria* trees) marketed under the brand name HOGA. Selected tea products include HOGA Gaharu Tea, HOGA Fruit Tea, and GOGA Drink, of which the former is one of the first local agarwood tea products marketed locally (Figure 1.8). HOGA Gaharu Tea and HOGA Fruit Tea come in tea bags, while GOGA Drink is sold as bottled drinks. For the present study, Gaharu Tea, Gaharu Cool Tea (raw material of HOGA Fruit Tea) and GOGA Drink Powder (to be made into GOGA Drink) were used for analyses.



**Figure 1.8** – HOGA Gaharu Tea, HOGA Fruit Tea, and GOGA Drink that are being sold in the market (Gaharu Tea Valley Gopeng, n.d.).

A lot of health beneficial claims are associated with the HOGA Gaharu Tea products, which are illustrated in Figure 1.9.

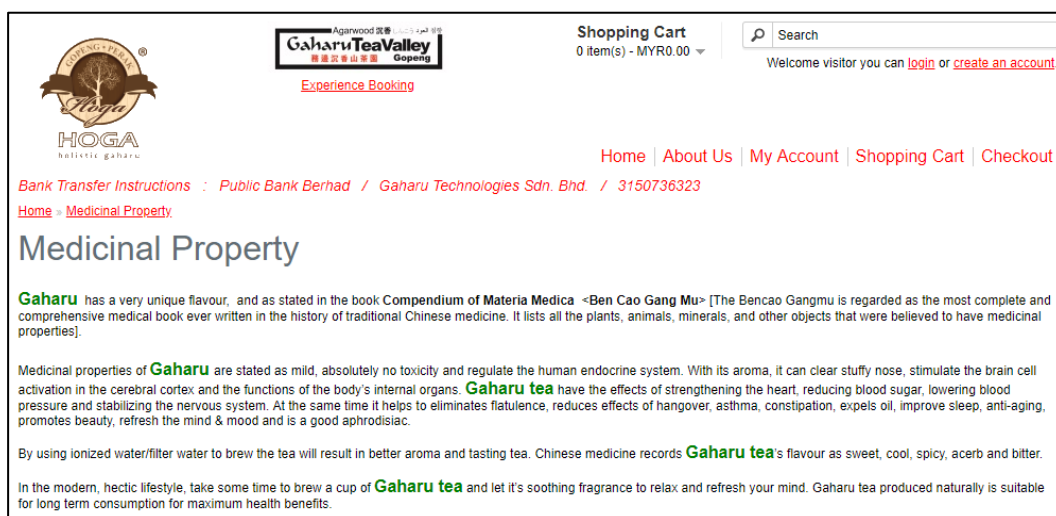


**Figure 1.9** – Screenshot of the GTSB homepage about the health beneficial claims of the HOGA Gaharu Tea Products (Gaharu Tea Valley Gopeng, n.d.).

Recent research activities on the leaves of *A. sinensis* and *A. crassna* have revealed that mangiferin and genkwanin 5-O- $\beta$ -primeveroside played major roles for their associated biological activities, which are anti-diabetic and laxative, respectively (Hara et al., 2008; Kakino et al., 2010; Ito et al., 2012). In order to increase the commercial value of the tea products, which are claimed to help in reducing blood sugar levels and constipation, GTSB proposed to carry out detailed chemical analyses on the extracts of their raw materials (e.g. bark, leaf, twig, and young shoot) and HOGA tea products to determine the presence of the two bioactive phytochemicals. These two bioactive phytochemicals can also be used as biomarkers in the future to ensure the tea products manufactured are maintained at an acceptable standard.

## **1.8 Biological assays**

Three biological assays, namely, MTT assay, gluconeogenesis assay and Bradford protein assay, were undertaken in this research project to determine the hepatic glucose production-lowering effect of two of the major phytochemicals isolated from *A. sinensis*, the water extracts of the raw materials (plant parts), as well as three HOGA Gaharu Tea products.

### **1.8.1 MTT assay**

MTT [3-(4,5-dimethylthiazol-2-yl)-2,5-diphenyltetrazolium bromide] assay is a colorimetric assay to determine the cytotoxicity of potential medicinal agent and to establish a safe concentration range of treatment to be used on cell in experiment. Yousefi et al. (2017) have used MTT assay to assess anticancer activity of fucoxanthin-containing extracts on breast cancer cells line and normal human skin fibroblast cells line to specify the cytotoxic effects. In this research, it was performed to determine a safe concentration range of treatments (above  $IC_{50}$ , where more than 50% of the cells are still viable) that can be used for gluconeogenesis assay. Viable cells are capable of reducing the tetrazolium dye MTT to its insoluble formazan through NADPH-dependent cellular oxidoreductase enzyme (Berridge et al., 2005). Since reduction of MTT is dependent on the cellular metabolic activity of cells, a high absorbance reading at 560 – 570 nm indicates high concentration of formazan, which translate to high amount of rapidly dividing viable cells which exhibit high rates of MTT reduction (Brescia and Banks, 2009).

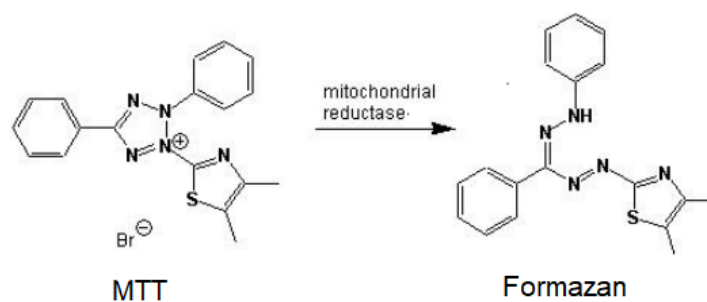


**Figure 1.10** – Reduction of yellow tetrazolium dye MTT into purple formazan (Bresciaa and Banks, 2009).

### 1.8.2 Gluconeogenesis assay

Gluconeogenesis assay is an easy and sensitive colorimetric assay that is commonly used by researchers to determine the amount of glucose produced by the cell. Berasi et al. (2006) used the assay to measure the amount of glucose produced in an experiment about inhibition of gluconeogenesis through transcriptional activation of EGR1 and DUSP4 by AMP-activated kinase. It is reflected by the conversion of Amplex Red reagent into resorufin (red fluorescence compound) through glucose oxidase and peroxidase enzymes activity. In the presence of glucose, glucose oxidase converts the glucose molecule into D-gluconolactone and hydrogen peroxide ( $H_2O_2$ ). The  $H_2O_2$  then reacts with Amplex Red reagent to form red-fluorescent oxidation product, resorufin in the presence of horseradish peroxidase (Debski et al., 2016). The absorbance intensity at 560 nm is proportional to glucose concentration. Figure 1.11 illustrates the mechanism for glucose detection using Amplex Red Glucose Assay Kit for the gluconeogenesis assay.



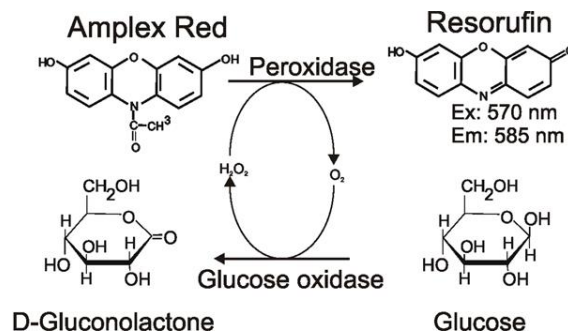


**Figure 1.11** – Illustration on the conversion of Amplex Red reagent into resorufin in gluconeogenesis assay (Thermo Fisher Scientific, n.d.).

### 1.8.3 Bradford Protein assay

In 1976, Marion Mckinley Bradford developed a quick and accurate spectroscopic analytical procedure to measure protein concentration in a solution, which was known as Bradford protein assay (Bradford, 1976). Moridikia et al. (2018) have used this assay to quantify the lyophilised venom of *Vipera latifii*. The assay was also used by Sahin et al. (2018) to quantify the allergenic pollen protein content of *Cupressus arizonica* Greene., *Cupressus sempervirens* L. and *Juniperus oxycedrus* L. in Turkey. The Coomassie Brilliant Blue G-250 is a red-brown solution (cation) in its acidic solution when not bound with protein. Once bound with protein, the dye is converted to blue solution (anion) which is detected at 595 nm. The dye-protein complex is stabilised through non-covalent interactions such as Van der Waals force with the protein's carboxyl group and electrostatic interaction with the protein's amino group. The amount of complex present in a solution is proportional to the protein concentration, which can be estimated through absorbance reading (Spector, 1978).

Bradford protein assay was run in parallel with gluconeogenesis assay and was used to determine protein concentration of individual well of the same 24-well plate used in the gluconeogenesis assay. The calculated protein concentration was then used to normalized the result from gluconeogenesis assay so as to eliminate variable such as glucose concentration difference due to different number of cells in the well.

### **1.9 Isolation, purification and structure characterization of natural products**

The term “natural products” often refer to secondary metabolites produced by an organism that are not absolutely essential for the survival of the organism. Since antiquity, natural products have been an important source of therapeutic agents and about half of the drugs in the present are derived from natural sources. Biodiversity in nature offers a valuable source for novel active lead compound discovery. However, a crude natural product extract is a complex mixture of compounds where a single separation technique is often insufficient to successfully isolate and purify individual compounds. Thus, multiple chromatographic techniques such as vacuum column chromatography (VCC), thin layer chromatography (TLC), centrifugal TLC (CTL), and high performance liquid chromatography (HPLC), coupled with chemical structure characterization techniques such as nuclear magnetic resonance (NMR) and mass spectrometry (MS), need to be employed to allow isolation, purification and identification of natural products in crude extract mixtures.

### **1.9.1 Vacuum column chromatography (VCC)**

Column chromatography (CC) consists of two phases, namely, a solid stationary phase (adsorbent) and a liquid mobile phase. As the mixture of compounds move through the stationary phase, they are separated based on the interaction between the solutes and the stationary phase. There are two types of chromatographic mode, one is adsorption and the other is size exclusion.

In adsorption chromatography, separation is based on the adsorption affinities of the compounds and the surface of the stationary phase. The extent of adsorption affinity is governed by a number of factors such as van der Waal forces, hydrogen bonding, dipole-dipole interactions, and charge transfer (Sarker et al., 2006). For size exclusion chromatography, the separation is based on a sieving effect, where the stationary phase is made up of porous particles. The porous particles provide a continuous decrease in accessibility for compounds of increasing size. Therefore, compounds that are bigger in size will be eluted first. Generally, sample recovery for this type of chromatography is high since the stationary phase is inert (Sarker et al., 2006).

VCC involves the use of vacuum at the end of a column. It is effective for rapid fractionation of crude extracts. The compound fraction eluted together with the mobile phase is collected into a Buchner flask and can be concentrated in vacuo later. Figure 1.12 shows the setup of VCC.

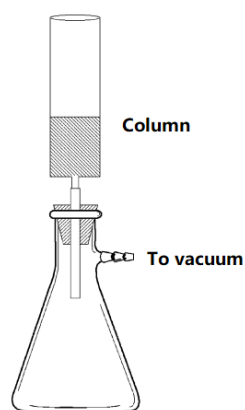


**Figure 1.12** – VCC setup (Sarker et al., 2006).

### 1.9.2 Thin layer chromatography (TLC)

TLC is one of the oldest, easiest and cheapest forms of chromatography. It utilizes the separation of organic compound mixture on a thin layer of adsorbent (silica gel) coated on an aluminium or glass sheet. When a mixture is loaded as a spot onto the bottom of a TLC plate and placed into a tank with a suitable solvent just enough to wet the part below the spot, the solvent front will move up the TLC plate through capillary action. As the plate develops, compounds of different polarity and affinity to the solvent and sorbent will move up different distances, which are quantified in  $R_f$  (retention factor) values.  $R_f$  value is defined as:

$$R_f = \frac{\text{Distance of compound from origin (the spot)}}{\text{Distance of solvent front from origin}}$$

In the case where the sorbent is silica (polar), a polar compound will have higher affinity for the sorbent and thus travels slowly up the plate. This will

give a low  $R_f$  value for that particular compound. The  $R_f$  value can be increased by increasing the polarity of the solvent. Figure 1.13 shows a typical TLC setup.

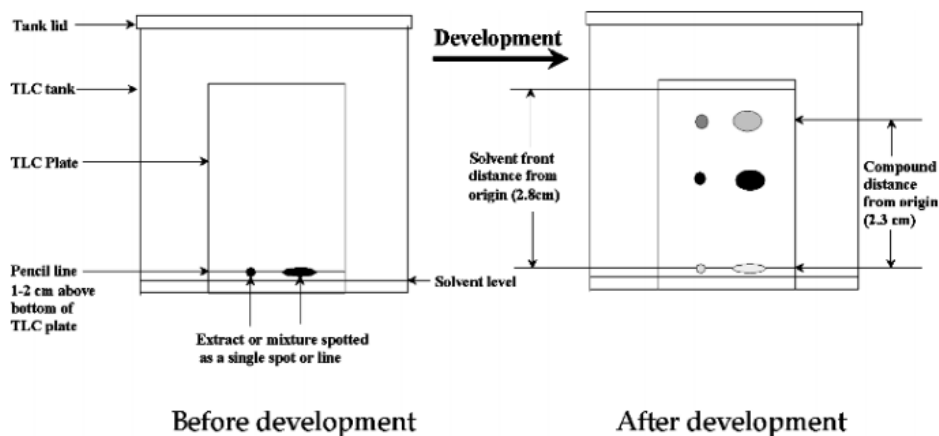


**Figure 1.13** – TLC equipment and development process (Sarker et al., 2006).

### 1.9.3 Centrifugal thin layer chromatography (CTLC)

CTLC is a type of planar chromatography, which is similar to TLC. It is used to separate mixture of compounds through the action of centrifugal force. Figure 1.14 shows the schematic view of a CTLC setup known as Chromatotron.

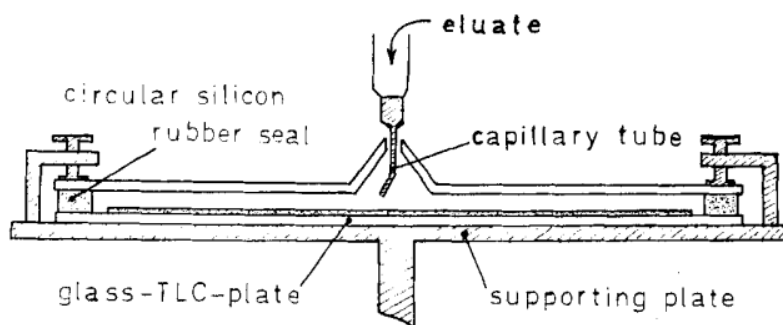


**Figure 1.14** – Schematic view of a Chromatotron (Lepoivre, 1972).

Prior to sample application, the sorbent layer (silica) is saturated with a constant flow rate of starting mobile phase solvent and the sample is dissolved in solvent and filtered. Once the sample is loaded and the plate starts to spin, a centrifugal force is generated. As the mobile phase elutes, compounds with higher affinity to the mobile phase will travel faster to the edge of the spinning plate and then swirled off together with the mobile phase, while components with higher affinity to the sorbent will travel slowly. This will create spherical bands of separated components which allow for separate collection. As time passes, the polarity of the mobile phase can be increased to elute the more polar compounds that are adsorbed to the sorbent layer. Similar to TLC, high polarity solvent will cause the sorbent (silica) to dissolve, which would compromise the whole separation process (Agrawal and Desai, 2015).

#### **1.9.4 High performance liquid chromatography (HPLC)**

HPLC has become a main choice for isolation and purification of natural products. To date, there are various types of HPLC column that operates at different modes such as normal-phase, reverse-phase, size exclusion, and ion-exchange (Valko, 2000). One of the deciding factors for choosing the type of HPLC column is the polarity of the mixture of compounds. Since MeOH extract was involved in the HPLC isolation and purification process in this research project, a reverse-phase HPLC column was used. The stationary phase of the column is packed with C-18 coated on 5  $\mu\text{m}$  silica gel. C-18 is a non-polar

molecule that is covalently bonded (silanization or carbon loading) to the stationary phase particle (silica), thus creating a hydrophobic stationary phase. As a result, polar molecules will be eluted faster together with the polar (aqueous) mobile phase. In order to elute the retained hydrophobic molecules, polarity of the mobile phase need to be reduced by increasing the concentration of non-polar (organic) solvent. Besides that, additives such as buffers, acids, or bases can be added to suppress the ionization of free unreacted silanol group in order to reduce peak tailing (Sarker et al., 2006).

Figure 1.15 shows the schematic diagram of a HPLC system.

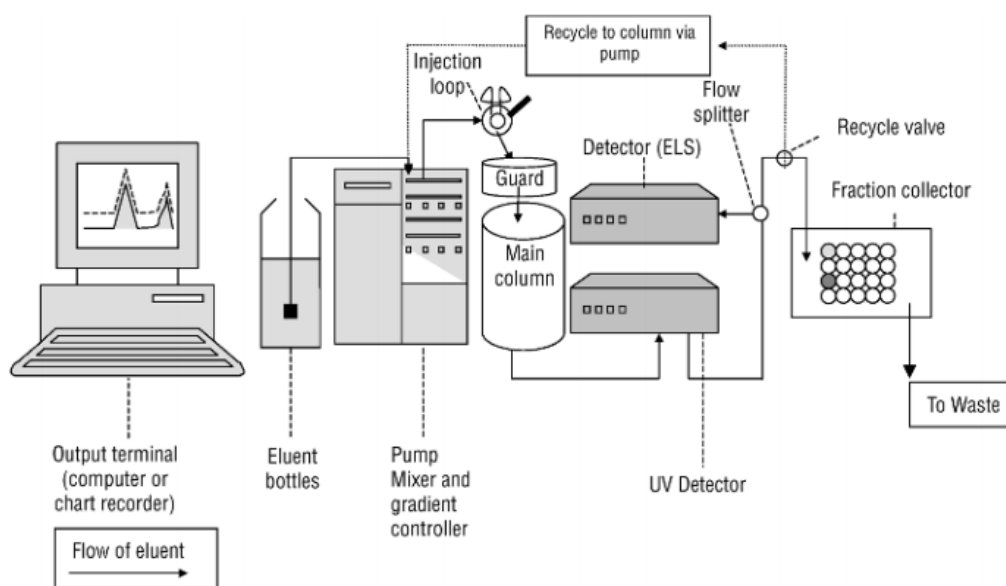


**Figure 1.15** – Schematic diagram of a HPLC system featuring an automated sample collector (Sarker et al., 2006).

### 1.9.5 Nuclear magnetic resonance (NMR)

NMR is regarded as an indispensable tool to investigate the chemical structures of natural products. Besides solving the gross chemical structures, NMR can also be used to study conformation, configuration, molecular interactions and motions. In the field of natural products, the major nuclei (such as  $^1\text{H}$ ,  $^{13}\text{C}$ ,  $^{15}\text{N}$ ,  $^{31}\text{P}$ , and  $^{17}\text{O}$ ) have a spin quantum number ( $I$ ) of  $\frac{1}{2}$ .  $^1\text{H}$  is the most common nucleus to be investigated in NMR spectroscopy due to its high natural abundance. The second common nucleus to be investigated is  $^{13}\text{C}$  due to its carbonaceous nature as the skeleton of most organic compounds (Colegate and Molyneux, 2008).

When atomic nuclei that possess non-zero spin quantum number ( $I$ ) are immersed in a magnetic field of strength  $B_0$ , energy in the range of radio frequency ( $\nu_0$ ) can be absorbed due to a spectroscopic transition that occurs between the two energy levels of a nuclear magnetic dipole. This relationship is defined by the Larmor equation:

$$\nu_0 = \gamma B_0 / 2\pi$$

where  $\gamma$  is a constant known as gyromagnetic ratio, which is dependent on the type of nucleus (Tringali, 2001).

The magnetic resonance of a nucleus is closely related to four major properties, namely chemical shift, spin-spin coupling, intensity, and the nuclear Overhauser effect (NOE). The degree where a nucleus is shielded from external applied magnetic field is dependent on the electron density



surrounding it. Thus, the frequency at which the nucleus absorbs energy will be different in different chemical environments in relative to a reference nucleus and this difference is known as chemical shift ( $\delta$ ). It is expressed in parts per million (ppm) as described in the following equation (Tringali, 2001):

$$\delta \text{ (ppm)} = \frac{10^6(v_{\text{sample}} - v_{\text{reference}})}{v_{\text{reference}}}$$

Tetramethylsilane (TMS) is the most common reference compound used for  $^1\text{H}$  and  $^{13}\text{C}$  NMR, which is assigned a chemical shift at 0.00 ppm. The functional groups of natural products mostly occur in the range of 0 to 12 ppm for  $^1\text{H}$  NMR and 0 to 230 ppm for  $^{13}\text{C}$  (Colegate and Molyneux, 2008).

Due to mutual spin-pairing tendency of two chemically nonequivalent nuclei, they can influence each other by intervening the bonding electrons, which result in the splitting of signals which will appear as two lines (*d*, doublet) in the NMR spectrum. This frequency difference is known as coupling constant (*J*) which is expressed in hertz (Hz). This spin-spin coupling (also known as scalar coupling) only occur when two nuclei are linked within a maximum of three bonds away (Tringali, 2001).

The intensity (integrated area under the peak) of a  $^1\text{H}$  NMR signal is proportional to the number of protons, which is useful in determining the structural formula. As for  $^{13}\text{C}$ , this is not the case due to reasons such as different relaxation times and NOE enhancement (Tringali, 2001).

### 1.9.6 Mass spectrometry (MS)

MS is used to measure the mass of a sample by plotting the ion signal as a function of mass-to-charge ratio. The mass spectrometer typically consists of three parts: ionizer, mass analyser, and detector. Sample is ionized in the ionizer to produce positively charged ions with different mass-to-charge ratios ( $m/z$ ), which are then accelerated into the mass analyser in the form of an ion beam by accelerating the electric field. Ions of different mass-to-charge ratios are separated through electric or magnetic field, which are then filtered and focused on the detector to obtain a mass spectrum. The x-axis of the mass spectrum records the mass (or  $m/z$ ), while the y-axis corresponds to the ion abundance, which is the numbers of individual ions. The peak with the highest ion abundance is known as the base peak, which could relate to the molecular ion or to any fragment ions (Herbert and Johnstone, 2003). Each sample has its own characteristic mass spectrum which can be used as a fingerprint to identify a sample, either by comparison with the library of known spectrum or through interpretation of the spectrum itself. Figure 1.16 shows the schematic diagram for the formation of a simple mass spectrum.

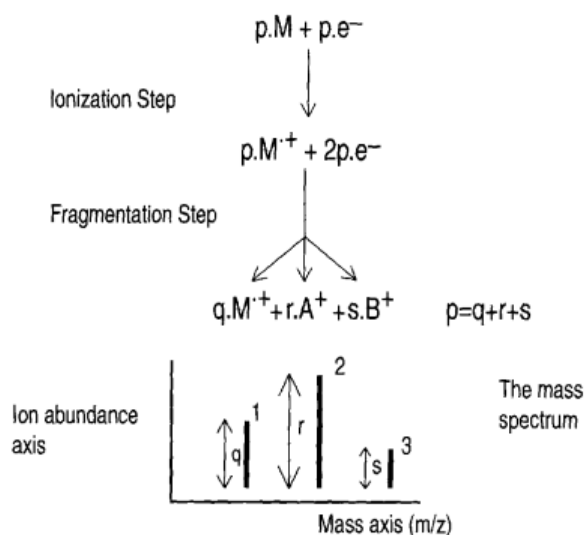


**Figure 1.16** – Schematic diagram of the formation of an electron ionization mass spectrum from a number ( $p$ ) of molecules ( $M$ ) interacting with electrons ( $e^-$ ). Peak 1 indicates the molecular ions ( $M^{*+}$ , the ions with greatest mass), peaks 2 and 3 ( $A^+$  and  $B^+$ ) indicate the fragment ions. Abundance of each peak is indicated by  $q$ ,  $r$  or  $s$ . Peak 2 is the base peak as it has the highest ion abundance (Herbert and Johnstone, 2003).

MS, which is efficient at identifying individual substance but not so well with a mixture, is often used in tandem with liquid chromatography (LC). LC is efficient at separating mixture into individual components. The combination of LC-MS could provide information which could not be extracted by either technique alone. However, an interface is required to convert the liquid flowing from the end of a column into the ion source of a mass spectrometer. Examples of such interface include electrospray, particle beam, thermospray, and atmospheric pressure ionization (Herbert and Johnstone, 2003). Figure 1.17 shows the schematic diagram of an LC-MS system.

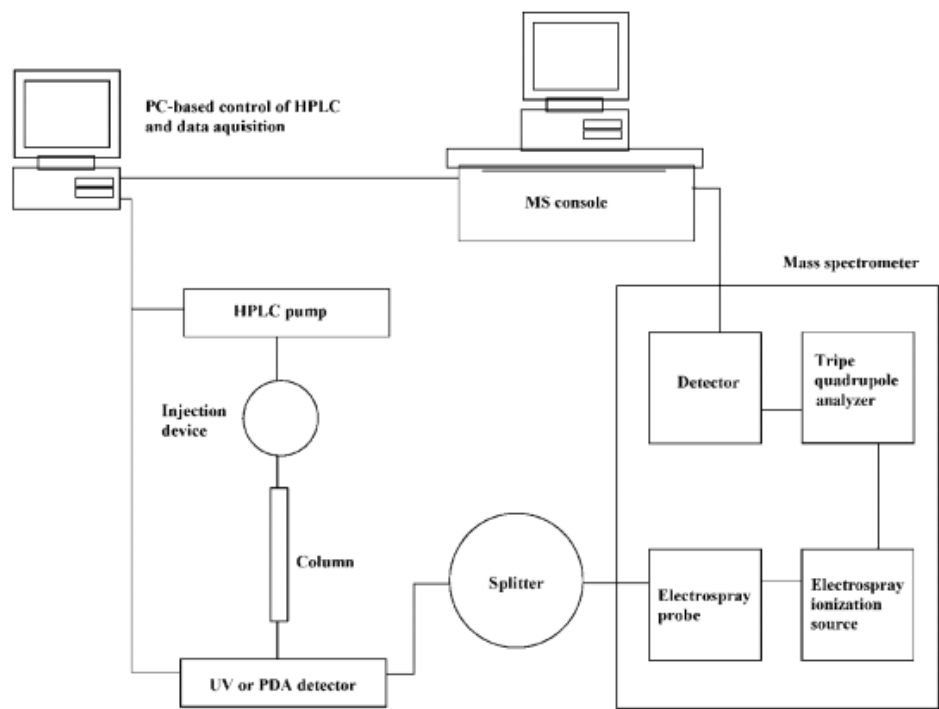


**Figure 1.17** – Schematic diagram of an LC-MS (electrospray ionization interface) system (Sarker et al., 2006).

### **1.10 Research objectives**

The ultimate aim of the present research is to investigate whether the various plant parts and tea products (Gaharu Tea, Gaharu Cool Tea and GOGA Drink Powder) produced by GTSB possess glucose lowering activity in human liver cells HepG2 and if so, whether the effect is attributable to the presence of mangiferin and/or genkwanin 5-*O*- $\beta$ -primeveroside. The specific objectives of the present project are to:

1. Extract and isolate the mangiferin and genkwanin 5-*O*- $\beta$ -primeveroside from the leaf material.
2. Detect and quantify the presence of mangiferin and genkwanin 5-*O*- $\beta$ -primeveroside in the water extracts of the various plant parts and tea products.
3. Examine the effect of mangiferin, genkwanin 5-*O*- $\beta$ -primeveroside, the water extracts of the various plant parts and tea products on glucose production activity in human liver cells (HepG2).

# Chapter Two

## Experimental

### 2.1 Plant source and gaharu tea products

Four ground plant parts of the *A. sinensis* were provided by GTSB. Those parts include the leaf, bark, twig and young shoot. The species was identified by Dr Sam Yen Yen and Mr Mohamad Aidil Noordin (Forest Biodiversity Division, Forest Research Institute Malaysia - FRIM). Three raw materials of gaharu tea products, namely Gaharu Tea, Gaharu Cool Tea and GOGA Drink Powder were also provided by GTSB. The Gaharu Tea is a mixture of ground leaf, twig and bark at a certain ratio, whereas the Gaharu Cool Tea has the young shoot included into the mixture. GOGA Drink Powder, is a modified product where the water extracts of plant parts are spray dried onto the maltodextrin filler and mogroside V is added as a natural sweetener.

### 2.2 Materials

All solvents used throughout this research for extraction, isolation and purification were analytical grade whereas HPLC grade solvents were used for reverse phase HPLC. Absolute ethanol and acetone were from RCI-Labscan (Bangkok, Thailand). Aluminium chloride hexahydrate, methanol, and sulphuric acid were from Merck (New Jersey, United States). Acetic acid, acetonitrile, chloroform, ethyl acetate, and formic acid were from Friendemann Schmidt (Perth, Australia). Purified water was obtained by a Milli-Q® HX 7000 SD (Merck) water purification system.

Human liver cells (HepG2) were purchased from Riken BRC Cell Bank. Bradford Protein Assay Kit, BSA, DMEM (no glucose), DMSO, FBS, L-glutamine (200 mM), MTT, penicillin-streptomycin solution, RIPA buffer (10x), RPMI 1640, sodium DL-lactate, and sodium pyruvate (100 mM) were purchased from Nacalai Tesque (Kyoto, Japan). HEPES solution (1 M) was purchased from Merck. PBS, DMEM (no phenol red, glucose, and L-glutamine), and Amplex Glucose Oxidase Assay Kit were purchased from Bio-diagnostic (Giza, Egypt). Reference drugs used for bioactivity tests were metformin (Merck), insulin, and dexamethasone (Nacalai Tesque).

### **2.3 General experimental procedures used for isolation, purification, and quantitative analysis**

$^1\text{H}$  NMR spectra were recorded in  $\text{CDCl}_3$  with TMS as internal standard on Bruker 600 MHz spectrophotometer. Liquid chromatography – mass spectrometry (LC-MS) result were obtained from FRIM by using LTQ Orbitrap mass spectrometer in negative mode. Purification of genkwanin 5-O- $\beta$ -primeveroside using reverse phase HPLC was performed using Waters Liquid Chromatograph with a Waters 600 controller and a Waters 2998 tuneable absorbance detector. A semi-prep column (10 x 50 mm, Waters X-Bridge, United State) packed with C-18 (ODS, Octadecylsilane) coated on 5  $\mu\text{m}$  silica gel was used, at 40°C, and fractions were collected with Waters Fraction Collector III. The quantitative analysis of mangiferin and genkwanin 5-O- $\beta$ -primeveroside content in different gaharu leaf extracts, plant parts and tea

products were carried out by FRIM and Permulab Sdn Bhd, respectively. FRIM carried out the analysis through means of a HPLC system (Waters 2535 quaternary gradient module, Waters 2707 Autosampler and Waters 2998 photodiode array detector), whereas Permulab Sdn Bhd used Agilent 1220 HPLC with DAD detector. An analytical column (FRIM: Waters X-Bridge C18, 4.6 x 250 mm, 5  $\mu$ m; Permulab Sdn Bhd: Zorbax ODS C18, 4.6 x 250 mm, 5  $\mu$ m) was used and for elution of the constituents, two solvents denoted as A and B were employed. A was 0.1% aqueous acetic acid and B was acetonitrile.

## **2.4 Chromatographic techniques**

Besides HPLC, several chromatographic techniques were used on the crude extracts to obtain pure compounds. These included column chromatography, thin layer chromatography, centrifugal thin layer chromatography.

### **2.4.1 Column chromatography (CC)**

Vacuum column chromatography (VCC) was used to fractionate the acetone (70.27 g) and methanol (129.95 g) extract, respectively, using Merck silica gel 60 (0.040 – 0.063 mm) at approximately 20:1 silica to sample ratio. Slurry method was used to pack the column where measured amount of silica was made into slurry and packed into the column under vacuum condition while gently tapping the column with a thick rubber tube to ensure no trapped air pocket in the column. The column was refilled repeatedly with  $\text{CHCl}_3$  until



sufficient packing and the column was equilibrated. The crude extract was dissolved in minimum amount of solvent of least possible polarity (normally  $\text{CHCl}_3$ , with or without minimum amount of MeOH). The extract solution was then gently pipetted onto the silica bed. The extract was then eluted using  $\text{CHCl}_3/\text{MeOH}$  at 99:1 ratio (acetone extract) and 9:1 ratio (MeOH extract), respectively, while gradually increasing the solvent polarity by increasing the proportion of MeOH. The collected eluents were concentrated and monitored using TLC.

#### **2.4.2 Thin layer chromatography (TLC)**

TLC was one of the most commonly used techniques for qualitative analysis during isolation works. It can be used to check the purity of sample; to determine the optimum starting solvent to be used for CC and CTLC; and to detect the presence of conjugated compounds that are UV active. Fractions collected from CC and CTLC that showed similar TLC profile can be combined together. The TLC plate was an aluminium sheet pre-coated with silica gel 60  $F_{254}$  with a standard thickness of 0.25 mm (Merck). Before use, it was manually cut into a standard size of 2.5 cm x 10 cm. Samples were spotted onto the plate using a glass pipette, and the plate was then placed into a saturated chromatographic tank which contained different solvent systems ( $\text{CHCl}_3/\text{MeOH}$  mixture was commonly used). Once the plate was developed, where the solvent front was 1 cm away from the end of the plate, it was removed from the tank to air-dry for a few minutes. Once dried, it was

sprayed with reagents like aluminium chloride ( $\text{AlCl}_3$ ) or 10% sulphuric acid (heating required). The plate was then examined under a UV lamp using short wave (254 nm) and long wave (365 nm). The spots which reacted with the  $\text{AlCl}_3$  (turned turquoise) or 10% sulphuric acid (turned orange after heated) under long wave UV indicated the presence of mangiferin. As for genkwanin 5-O- $\beta$ -primeveroside, only  $\text{AlCl}_3$  spray was used. The blue spot under long wave UV indicated the presence of genkwanin 5-O- $\beta$ -primeveroside. Other UV active compounds would give different colour. The solvent systems that were commonly used were:

- a) Ethyl acetate: formic acid: acetic acid: water (100:11:11:25)
- b)  $\text{CHCl}_3$ : MeOH (1-30%)

#### **2.4.3 Centrifugal thin layer chromatography (CTLC)**

CTLC was a preparative chromatographic technique used for separation of multi-component system through the action of centrifugal force. It was carried out using an instrument called Chromatotron as well as a 24 cm in diameter circular chromatographic plate that need to be prepared before use. The edge of the plate was secured with cellophane tape to form a mould. To prepare a 1 mm thick plate, 40 g of silica gel (Kieselgel 60 PF<sub>256</sub>, Merck) was added to about 90 mL of cold distilled water, mixed well and poured while manually turning the plate to ensure an even setting. Gentle taping was applied while pouring to ensure all trapped air bubble was released to prevent cracking. The plate was then left to air-dry for at least an hour before being

dried in the oven overnight at 55°C. After the plate was dried, it was shaved down to 1 mm thickness using the 1 mm blade and stored. Prior to use, the plate was activated at 100°C for one hour and left outside to cool down for few minutes. Meanwhile, the Chromatotron and all the tubing were cleaned with acetone before securing the plate in place. The sample was dissolved in minimum amount of suitable solvent and then gently applied on the centre of the spinning plate using a glass pipette to form a thin band. As the solvent flowed across the plate, thin bands were separated and eluted at different time in accordance to the polarity of the solvent system used. Fractions collected were dried by rotary evaporation, examined by TLC and combined for fractions with similar TLC profile. The solvent systems that were commonly used were:

- a)  $\text{CHCl}_3$ : MeOH (1-25%)
- b) Hexane:  $\text{CHCl}_3$  (20-100%)
- c) Diethyl ether: MeOH (1-25%)

## **2.5 Spray reagents**

### **2.5.1 Aluminium chloride ( $\text{AlCl}_3$ )**

$\text{AlCl}_3$  was used to detect the presence of flavonoid within a sample and was made by dissolving 5 g of aluminium chloride hexahydrate in 500 mL of absolute ethanol.

### **2.5.2 10% Sulphuric acid (H<sub>2</sub>SO<sub>4</sub>)**

10% H<sub>2</sub>SO<sub>4</sub> was used to detect the presence of xanthonoid such as mangiferin. It was made by mixing 10 mL of 100% H<sub>2</sub>SO<sub>4</sub> in 100 mL of purified water. Small amount of H<sub>2</sub>SO<sub>4</sub> was added slowly as heat will be developed in contact with water.

### **2.6 Extraction of plant materials**

Ground dried leaves of *A. sinensis* was provided by GTSB. 1 kg of leaf was macerated in 6 L of acetone overnight. The acetone extract was then decanted, filtered and concentrated through rotary evaporation. The same plant material was subjected to the same process for another four times using new and recovered acetone from the rotary evaporation. 70.27 g of crude acetone extract was yielded. The same plant material was air-dried inside a fume hood for 1 week, and the same overall process was repeated using MeOH instead. The yield of crude MeOH extract was 129.95 g.

### **2.7 Isolation and purification**

The crude acetone extract was suspended in a CHCl<sub>3</sub>: MeOH (1:1) mixture for 2 hours. The suspension was passed through a filter paper (Whatman, 25 µm pore size). The insoluble precipitate on the filter paper was scrapped using a spatula and collected in a 100 mL beaker. The insoluble precipitate was recrystallized with MeOH through air-drying in the fume hood to yield 1.022 g

of **compound 1** (mangiferin). The filtrate was subjected to VCC with CHCl<sub>3</sub>: MeOH solvent system (10:1, linear increase of MeOH gradient). Based on TLC, fractions of similar profiles were pooled into several major fractions (13 fractions, F1-F13). F10 was suspected to contain the compounds of interest and thus subjected for further purification by CTLC and yielded 0.021 g of **compound 2** (naringenin) and 0.030 g of **compound 3** (iriflophenone 2-O- $\alpha$ -rhamnoside).

The MeOH extract was subjected to VCC with CHCl<sub>3</sub>: MeOH solvent system (5:1, linear increase of MeOH gradient). Similarly, fractions of similar TLC profile were pooled into 7 major fractions altogether (F1-F7). F4 was eluted during CHCl<sub>3</sub>: MeOH (3:1) and was subjected to decantation and recrystallization and yielded 0.129 g of pale yellow powder. Preliminary NMR result showed characteristic genkwanin peaks with some impurity peaks. Further purification using HPLC was undertaken to yield 0.018 g of **compound 4** (genkwanin 5-O- $\beta$ -primeveroside).

A flow diagram of the overall isolation procedure is shown in Figure 2.1.

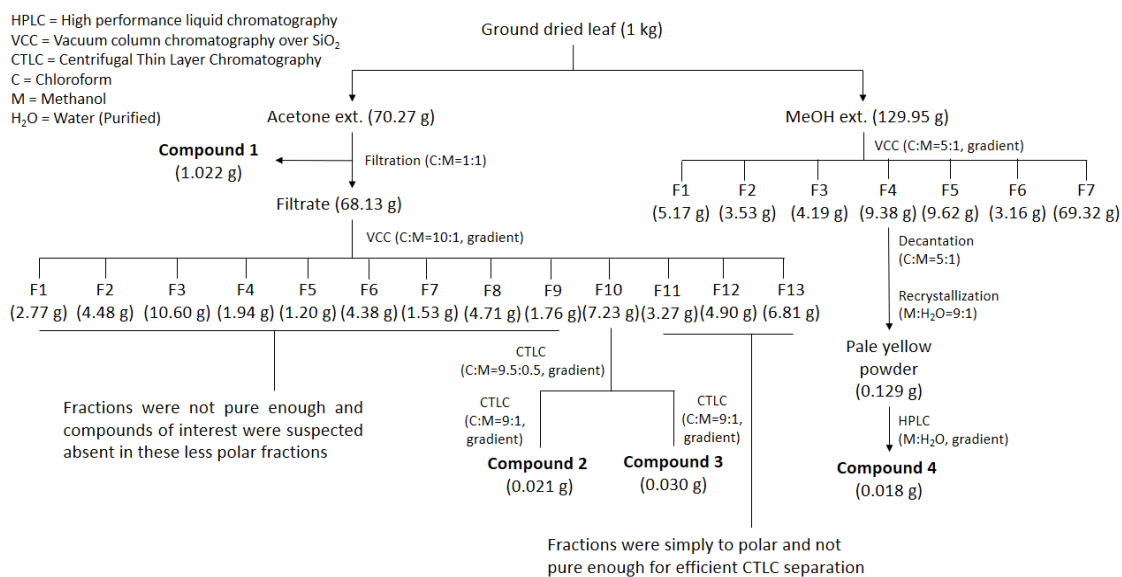


**Figure 2.1** – Isolation of compounds 1-4 from the leaves of *A. sinensis*.

### 2.7.1 Purification of genkwanin 5-O- $\beta$ -primeveroside by reverse phase HPLC

The pale yellow powder (impure compound 4) was dissolved in MeOH (4.0 mg in 2.0 mL each time) and resolved using a reverse phase semi-prep column (eluting solvent: H<sub>2</sub>O/MeOH, 95:5-10:90 from 1-3 min, hold from 3-6 min, 10:90-40:60 from 6-8 min, and back to 95:5 from 8-10 min; flow rate 1.0 mL/min; 30 injections, 50  $\mu$ L each) to yield a fraction (around 2.5 mg) at retention time between 6 min 5 s and 6 min 42 s. A total of 260 injections were made, which yielded 0.018 g of pure compound 4.

## 2.8 HPLC quantitative analyses of mangiferin and genkwanin 5-O- $\beta$ -primeveroside

About 100 mg of seven test samples (i.e., bark, leaf, twig, young shoot, Gaharu Tea, Gaharu Cool Tea, and GOGA Drink Powder) were sent to FRIM and Permulab Sdn Bhd for HPLC quantitative analyses of mangiferin and genkwanin 5-O- $\beta$ -primeveroside contents, respectively. A mixture of methanol (2 mL) and water (1 mL) was added to each test sample and sonicated for 30 minutes. In the HPLC quantitative analysis of mangiferin, two samples, i.e., Gaharu Cool Tea and leaf, were further diluted 3 times and 6 times, respectively, prior to injection to HPLC. The resulting solution was filtered prior to analysis. Table 2.1 shows the HPLC conditions used by FRIM and Permulab Sdn Bhd.

**Table 2.1** – HPLC conditions used for quantitative analyses of mangiferin and genkwanin 5-O- $\beta$ -primeveroside.

HPLC System (Mangiferin)	Instrumentation: Waters 2535 quaternary gradient module Waters 2707 Autosampler Waters 2998 photodiode array detector  Column: WATERS X-Bridge C18, 5 $\mu$ m (4.6 mm i.d. x 250 mm)
HPLC System (Genkwanin 5-O- $\beta$ -primeveroside)	Instrumentation: Agilent 1220 HPLC DAD detector  Column: Zorbax ODS C18, 5 $\mu$ m (4.6 mm i.d. x 250 mm)

Parameter	Setting		
	Time (min)	0.1% Aqueous acetic acid (%)	Acetonitrile (%)
Mobile Phase (Gradient Elution)	0.00	90.00	10.00
	30.00	50.00	50.00
	40.00	50.00	50.00
Flow Rate (mL/min)	1.00		
Injection Volume ( $\mu$ L)	10.00		
Column Temperature ( $^{\circ}$ C)	40.00		
UV Spectra (nm)	330		

Percentage of mangiferin/genkwain 5-O- $\beta$ -primeveroside content was determined using the formula shown below:

$$\text{Concentration (\%)} = (\text{CS} \times \text{D} \times 100) / \text{CE}$$

CS = Concentration of mangiferin from calibration curve (mg/L)

D = Dilution factor

CE = Concentration of test sample extract (mg/L)

## 2.9 Compounds data

**Mangiferin (1):** pale yellow powder; LC-Orbitrap-MS m/z: 421.076 [M-H]<sup>-</sup> (calcd. for C<sub>19</sub>H<sub>18</sub>O<sub>11</sub>-H, 421.334); <sup>1</sup>H NMR data, Table 3.2.

**Naringenin (2):** white powder; LC-Orbitrap-MS m/z: 271.096 [M-H]<sup>-</sup> (calcd. for C<sub>15</sub>H<sub>12</sub>O<sub>5</sub>-H, 271.248); <sup>1</sup>H NMR data, Table 3.3.

**Iriflophenone 2-O- $\alpha$ -rhamnoside (3):** pale yellow powder; LC-Orbitrap-MS m/z: 391.102 [M-H]<sup>-</sup> (calcd. for C<sub>19</sub>H<sub>20</sub>O<sub>9</sub>-H, 391.352); <sup>1</sup>H NMR data, Table 3.4.

**Genkwain 5-O- $\beta$ -primeveroside (4):** pale yellow powder; <sup>1</sup>H NMR data, Table 3.5.



## **2.10 Cell culture**

### **2.10.1 Cell lines and cell culture**

HepG2 was subcultured in RPMI 1640 medium with 10% fetal bovine serum (FBS), 1% sodium pyruvate and 1% Penicillin-Streptomycin solution. All cells were maintained inside an incubator at 37°C and 5% CO<sub>2</sub>.

### **2.10.2 Total dissolved solid (TDS)**

10 g of each tea product (i.e., Gaharu Tea, Gaharu Cool Tea and GOGA Drink Powder) and plant part (i.e., bark, leaf, young shoot and twig) was brewed in 150 mL of hot water (100 °C) for 15 minutes. A brownish solution was obtained upon filtration and this solution was used as the stock solution for further experiments, i.e., MTT and gluconeogenesis assays. 10, 1 and 0.1 mL of each stock solution was dried (by rotavap and desiccator) to determine the total amount of dissolved solid in each respective sample volume. A TDS calibration curve was then plotted to determine the stock concentration as well as the concentrations of all diluted stock solutions. Figure 2.2 shows an example of the TDS calibration curve of Gaharu Tea.

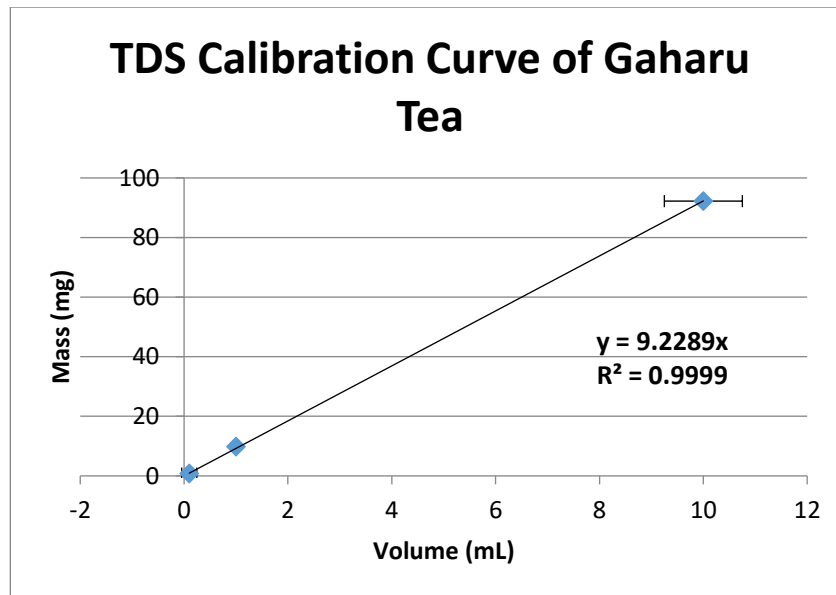


**Figure 2.2** – TDS calibration curve of Gaharu Tea.

### 2.10.3 MTT assay

HepG2 were seeded in a 96-well plate and incubated (37 °C, 5% CO<sub>2</sub>) for 1-2 days. After that, the cells were starved by replacing the media with (200 µL/well) no-serum media (RPMI 1640 and Penicillin-Streptomycin) and incubated for 4 hours. Treatments with different concentration were prepared (dilution with no-serum media) within these 4 hours. After 4 hours, the media was aspirated off and 200 µL of each treatment was added to the respective well. The plate was then incubated for 16 hours. After 16 hours, 50 mg of MTT was dissolved in 10 mL PBS to give a 5 mg/mL MTT solution. The media was aspirated off and 40 µL of MTT solution was added to each well along with 160 µL of no-serum media. The plate was wrapped in foil due to its light sensitivity nature of MTT and incubated for 4 hours. After incubation, the media was aspirated and replaced with 200 µL of DMSO (dimethyl sulfoxide).

The absorbance (abs.) was measured at 560 nm using spectrophotometer. Each assay was performed three times in triplicate. The cell viability was calculated using the formula stated below:

$$\text{Cell viability (\%)} = [(\text{Abs. of treatment} - \text{Abs. of blank}) \times 100 / \text{Abs. of control}]$$

#### **2.10.4 Gluconeogenesis assay**

HepG2 were seeded in a 24-well plate and incubated for 1-2 days. After that, the cells were starved by replacing the media with (1 mL/well) no-serum media and incubated for 2 hours. Following that, the no-serum media was replaced with 1 mL glucose-free media and incubated for 1 hour. Treatments with different concentration were prepared (dilution with glucose production media) within this 1 hour. Glucose production media was made up of 47.75 mL DMEM (no phenol red, glucose, and L-glutamine), 1 mL sodium pyruvate, 0.5 mL L-glutamine, 0.75 mL HEPES and 200  $\mu$ L sodium DL-lactate. After 1 hour, the media was aspirated off and 1 mL of each treatment was added to the respective well. The plate was then incubated for 16 hours. After incubation, 50  $\mu$ L from each well was pipetted into a new 96-well plate. A set of known standard glucose concentrations (0, 12.5, 25, 50 and 100  $\mu$ M) was prepared in separate wells. Amplex Red glucose reagent was prepared according to manufacturer's protocol. After that, 50  $\mu$ L of Amplex Red glucose reagent was added to each of these wells (including standard glucose, control and treatments) and incubated for 30 minutes, wrapped in aluminium foil. The absorbance was then measured at 560 nm. The glucose concentration for

each treatment was determined by interpolating with the calibration curve of the standard glucose solutions. Figure 2.3 shows an example of the standard glucose calibration curve. Each assay was performed three times in triplicate.

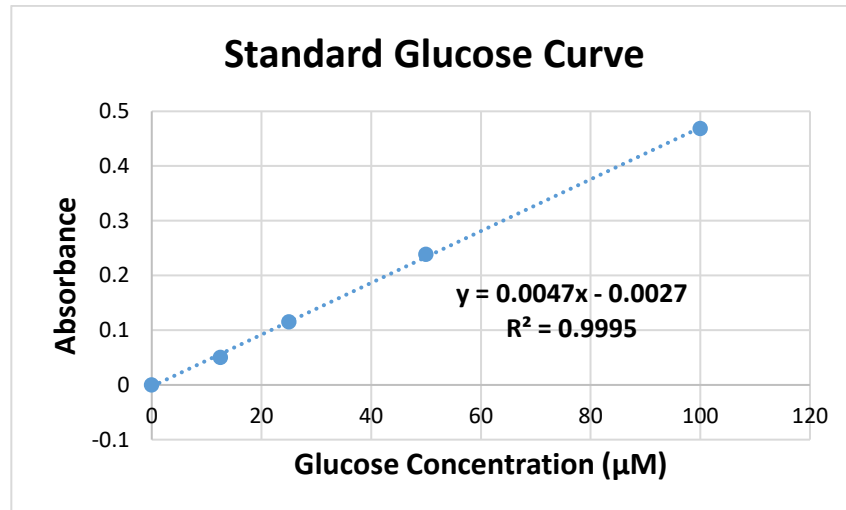


**Figure 2.3** – Standard glucose calibration curve.

#### **2.10.5 Bradford protein assay**

To prepare the RIPA (radioimmunoprecipitation assay) Buffer (1X), the commercially available RIPA Buffer (10X) and SDS (sodium dodecyl sulfate) solutions were thawed at room temperature and then mixed with purified water at the ratio of 1:1:8 respectively. To prepare the standard protein solutions, the BSA stock (bovine solution albumin, 2 mg/mL) was diluted (with water) accordingly as shown in Table 2.2.

**Table 2.2** – Standard protein solution dilution. The volume prepared are enough for triplicate (10  $\mu\text{L}$ /well).

Tube	Standard volume ( $\mu\text{L}$ )	Source	Diluent ( $\text{H}_2\text{O}$ ) volume ( $\mu\text{L}$ ) added	Final protein concentration ( $\mu\text{g}/\text{mL}$ )
1	30	BSA stock	0	2000
2	60	BSA stock	20	1500
3	30	BSA stock	30	1000
4	30	Tube 2	30	750
5	30	Tube 3	30	500
6	30	Tube 5	30	250
7	30	Tube 6	30	125
8	-	-	30	0

In order to prepare the sample solution, the cells attached on the well were detached and lysed. Medium of the cultured cells was removed and then the cells were washed twice with cold PBS (phosphate buffered saline). 100  $\mu\text{L}$  of RIPA Buffer (1X) was added into individual well, and stirred slowly for 5 minutes in a plate shaker. The cells were then scrapped with a cell scraper. The lysate and pellet were transferred into individual microcentrifuge tube. The well was then washed with another 400  $\mu\text{L}$  of RIPA Buffer (1X) and pooled into the respective microcentrifuge tube. The tubes were incubated in ice for 15 minutes to increase protein yield. The lysate was then transferred into a new tube and centrifuged at 10,000 x g for 10 minutes at 4°C. The supernatant containing the total protein extracts was then collected into new tube. This 500  $\mu\text{L}$  sample solution containing 1% SDS Solution was then diluted 5 times with  $\text{H}_2\text{O}$  to yield a solution containing only 0.2% SDS Solution. 10  $\mu\text{L}$  of standard protein solution, sample solution and blank ( $\text{H}_2\text{O}$ ) was

mixed well with 200  $\mu\text{L}$  of the dye per well in a 96-well plate. The plate was wrapped in aluminium foil and incubated at room temperature for 10 minutes. After that, the plate was measured at 595 nm using a spectrophotometer. As shown in Figure 2.4, a sample of standard protein calibration curve was plotted to determine the amount of protein in a well based on UV absorbance, before determining the total amount of protein by incorporating the dilution factor. After the amount of protein ( $\mu\text{g}/\text{mL}$ ) was determined from the equation of the standard curve, the value was then multiplied by 5 (dilution factor) and 0.5 (amount of protein in 500  $\mu\text{L}$ ) to yield total amount of protein ( $\mu\text{g}$ ).

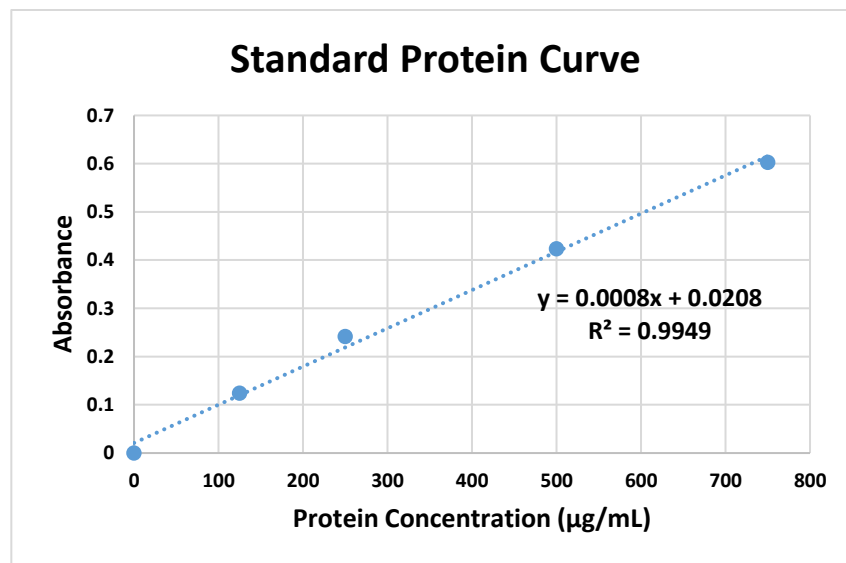


**Figure 2.4** – Standard protein calibration curve.

### **2.10.6 Statistical analysis**

All bioassays were done in triplicate and the data was reported as mean  $\pm$  standard error of mean (SEM). Unpaired t-test was used to determine the differences between test samples against control in the MTT and gluconeogenesis assays. The null hypothesis stated that “no significant difference compared to control”. A p-value of  $<0.05$  was considered as significant. Statistical analysis was conducted using GraphPad Prism software.

# Chapter Three

## Results

### 3.1 Isolation and identification of compounds

The dried leaves (1 kg) were extracted repeatedly in solvents such as acetone and methanol and eventually yielded 70.27 g acetone extract and 129.95 g MeOH extract respectively. Further purification works were taken and four pure compounds were obtained, namely, mangiferin (**1**), naringenin (**2**), iriflophenone 2-O- $\alpha$ -rhamnoside (**3**) and genkwanin 5-O- $\beta$ -primeveroside (**4**). The isolation yields for these compounds from the leaves of *A. sinensis* are shown in Table 3.1.

**Table 3.1** – Isolation yields of compounds from the leaves of *A. sinensis*.

Compound	Yield (g/kg)
Mangiferin ( <b>1</b> )	1.022
Naringenin ( <b>2</b> )	0.021
Iriflophenone 2-O- $\alpha$ -rhamnoside ( <b>3</b> )	0.030
Genkwanin 5-O- $\beta$ -primeveroside ( <b>4</b> )	0.018



### 3.1.1 Mangiferin (1)

Mangiferin (**1**) was obtained as pale yellow powder. LC-Orbitrap-MS (negative mode) measurements yielded a pseudo molecular ion peak at  $m/z$  421.076 ( $C_{19}H_{18}O_{11}-H^+$ ), corresponding to the molecular formula of mangiferin (**1**),  $C_{19}H_{18}O_{11}$ . The  $^1H$  NMR data is shown in Table 3.2 while the NMR spectrum is shown in Figure 3.1.

**Table 3.2** –  $^1H$  NMR data of mangiferin (**1**) compared to those of literature (Hara et al., 2008).

Position	Mangiferin ( <b>1</b> )	Literature
4	6.38 <i>s</i>	6.36 <i>s</i>
5	6.87 <i>s</i>	6.85 <i>s</i>
8	7.39 <i>s</i>	7.37 <i>s</i>
OH-1	-	13.77 <i>s</i>
OH-3	-	10.51 <i>s</i>
OH-6	-	10.58 <i>s</i>
OH-7	-	9.68 <i>s</i>
1'	4.59 <i>d</i> (9.8)	4.58 <i>d</i> (9.8)
2'	4.03 <i>t</i> (9.2)	4.03 <i>dd</i> (9.8, 9.0)
3'	3.22 <i>m</i> <sup>a</sup>	3.22 <i>dd</i> (9.0, 7.8)
4'	3.14 <i>m</i> <sup>a</sup>	3.14 <i>dd</i> (8.2, 7.8)
5'	3.22 <i>m</i> <sup>a</sup>	3.22 <i>dd</i> (8.2, 5.6)
6'	-	3.34 <i>dd</i> (11.2, 5.6)
6'	3.68 <i>d</i> (11.2)	3.67 <i>d</i> (11.2)

<sup>a</sup> signals partially obscured by the DMSO signal.  $CDCl_3$ , 600 MHz ( $^1H$ )

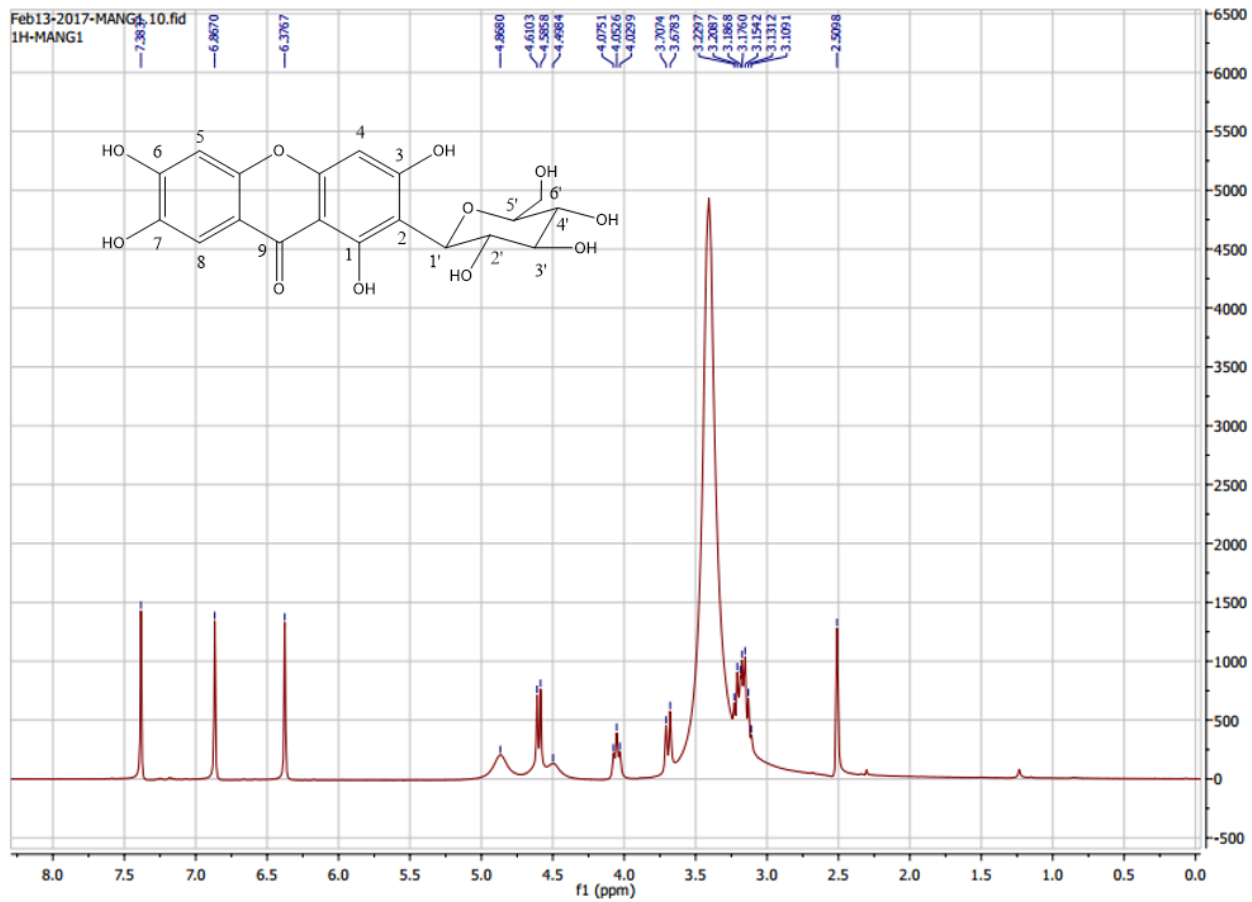


Figure 3.1 – <sup>1</sup>H NMR spectrum and the structure of compound 1

HPLC analysis also confirmed the identity of mangiferin (**1**) when tested against standard mangiferin (Figure 3.2).

HPLC chromatograms of mangiferin (standard) and sample:

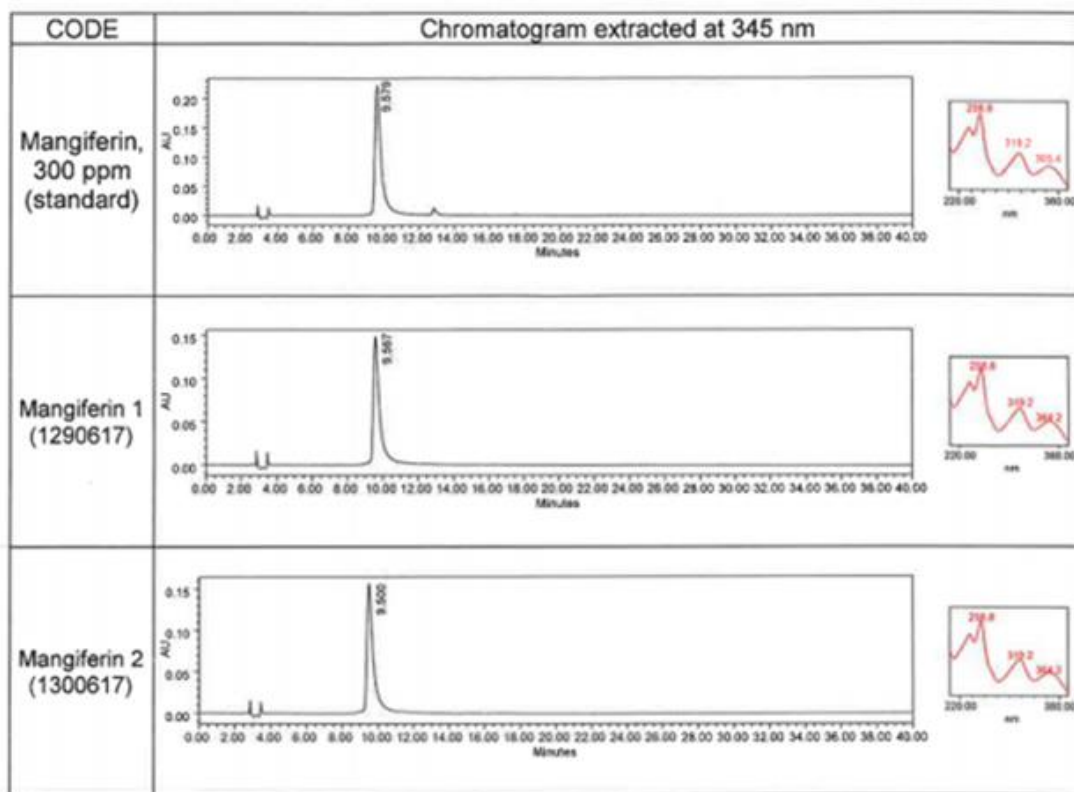


Figure 3.2 – HPLC profiling of the isolated sample (compound **1**).

### 3.1.2 Naringenin (2)

Naringenin (**2**) was obtained as white powder. LC-Orbitrap-MS (negative mode) measurements yielded a pseudo molecular ion peak at  $m/z$  271.096 ( $C_{15}H_{12}O_5-H^+$ ), corresponding to the molecular formula of naringenin (**2**),  $C_{15}H_{12}O_5$ . The  $^1H$  NMR data is shown in Table 3.3 while the NMR spectrum is shown in Figure 3.3.

**Table 3.3** –  $^1H$  NMR data of naringenin (**2**) compared to those of literature (Álvarez-Álvarez et al., 2015).

Position	Naringenin ( <b>2</b> )	Literature
2	5.44 <i>dd</i> (13.1, 3.0)	5.40 <i>dd</i> (13.1, 3.0)
3	2.85 <i>dd</i> (17.2, 3.0)	2.70 <i>dd</i> (17.2, 3.0)
3	3.13 <i>dd</i> (17.2, 13.1)	3.15 <i>dd</i> (17.2, 13.1)
6	6.09 <i>d</i> (2)	5.95 <i>d</i> (2)
8	6.07 <i>d</i> (2)	5.94 <i>d</i> (2)
2',6'	7.45 <i>d</i> (8.6)	7.37 <i>d</i> (8.6)
3',5'	7.21 <i>d</i> (8.6)	6.87 <i>d</i> (8.6)
OH-5	12.02 <i>s</i>	12.15 <i>s</i>

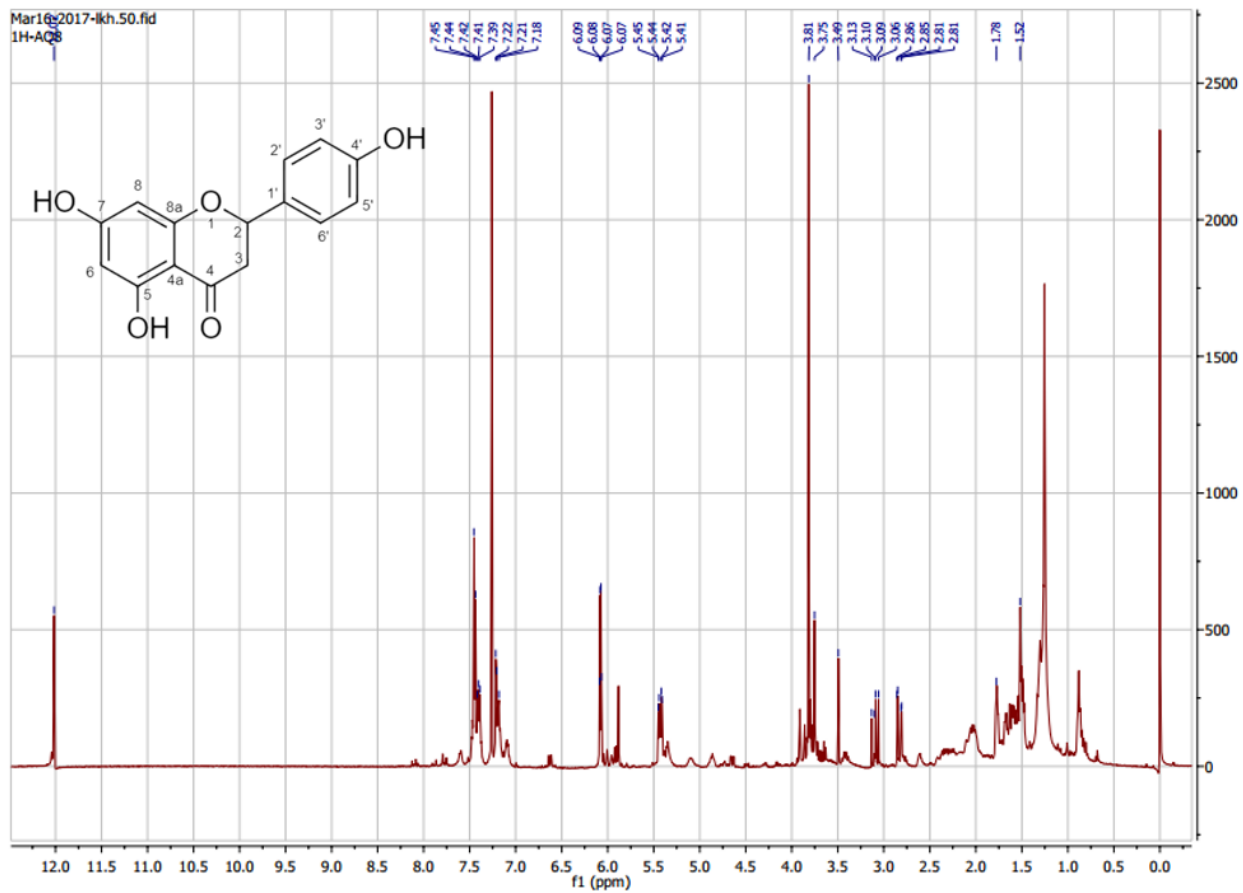


Figure 3.3 - <sup>1</sup>H NMR spectrum and the structure of compound 2

### 3.1.3 Iriflophenone 2-O- $\alpha$ -rhamnoside (**3**)

Iriflophenone 2-O- $\alpha$ -rhamnoside (**3**) was obtained as pale yellow powder. LC-Orbitrap-MS (negative mode) measurements yielded a pseudo molecular ion peak at  $m/z$  391.102 ( $C_{19}H_{20}O_9-H^+$ ), corresponding to the molecular formula of iriflophenone 2-O- $\alpha$ -rhamnoside (**3**),  $C_{19}H_{20}O_9$ . The  $^1H$  NMR data is shown in Table 3.4 while the NMR spectrum is shown in Figure 3.4.

**Table 3.4** –  $^1H$  NMR data of iriflophenone 2-O- $\alpha$ -rhamnoside (**3**) compared to those of literature (Hara et al., 2008).

Position	Iriflophenone 2-O- $\alpha$ -rhamnoside ( <b>3</b> )	Literature
3	6.14 <i>d</i> (2)	6.30 <i>d</i> (2)
5	6.04 <i>d</i> (2)	6.07 <i>d</i> (2)
2',6'	7.55 <i>d</i> (8.7)	7.61 <i>d</i> (8.6)
3',5'	6.80 <i>d</i> (8.7)	6.81 <i>d</i> (8.6)
Rha-H-1	5.11 <i>d</i> (0.8)	5.22 <i>d</i> (0.8)
Rha-H-2	<sup>a</sup>	3.41 <i>dd</i> (3.0, 0.8)
Rha-H-3	3.09 <i>br d</i> (9.1)	3.10 <i>dd</i> (9.6, 3.0)
Rha-H-4	3.28 <i>m</i> <sup>b</sup>	3.29 <i>dd</i> (9.6, 3.6)
Rha-H-5	3.45 <i>m</i> <sup>b</sup>	3.44 <i>dd</i> (6.2, 3.6)
Rha-H-6	1.19 <i>d</i> (6.4)	1.19 <i>d</i> (6.4)

<sup>a</sup> completely obscured by the DMSO signal; <sup>b</sup> signals are overlapping.  $CDCl_3$ ,

600 MHz ( $^1H$ )

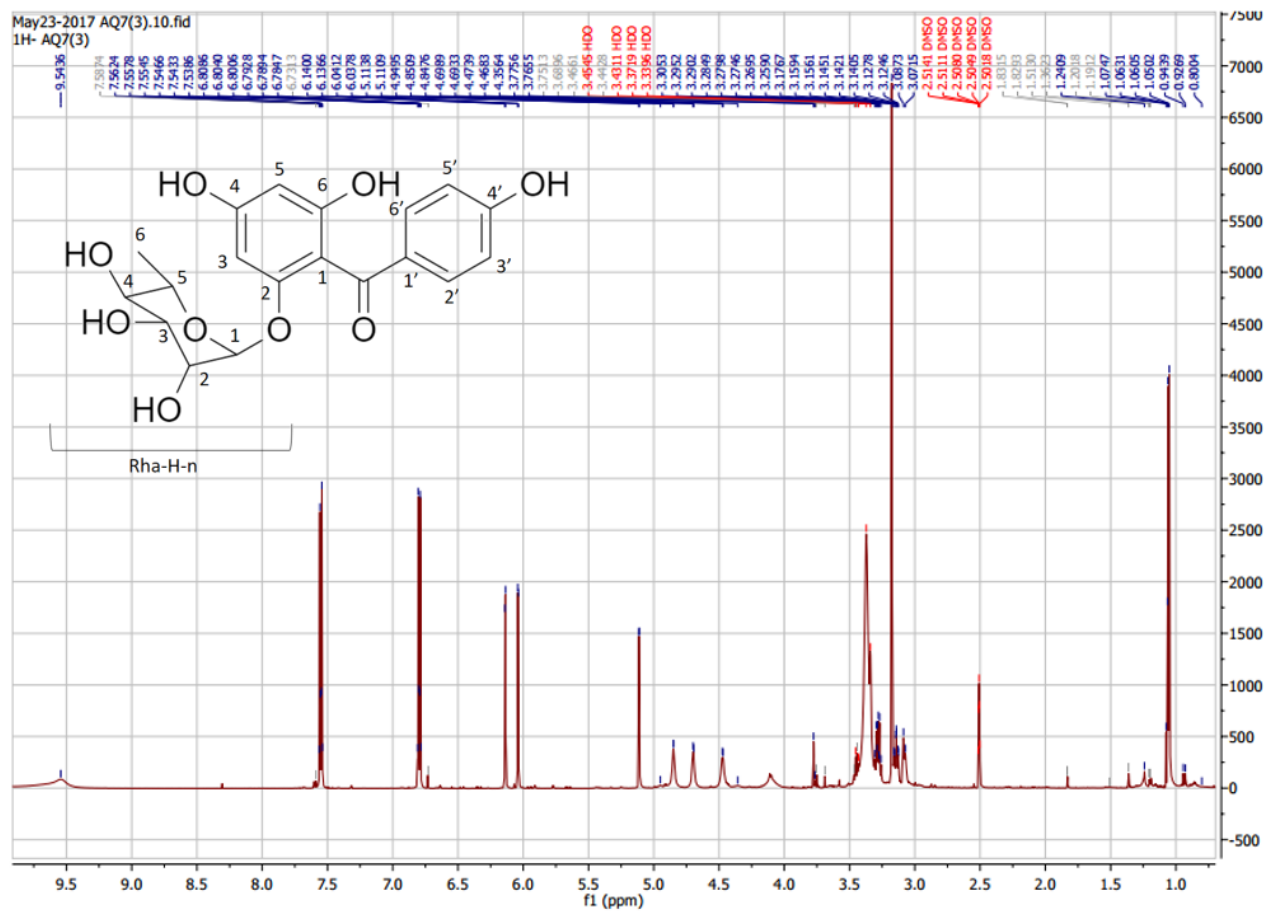


Figure 3.4 -  $^1\text{H}$  NMR spectrum and the structure of compound 3

### 3.1.4 Genkwanin 5-O- $\beta$ -primeveroside (4)

Genkwanin 5-O- $\beta$ -primeveroside (4) was obtained as pale yellow powder. The  $^1\text{H}$  NMR data is shown in Table 3.5 while the NMR spectrum is shown in Figure 3.5.

**Table 3.5** –  $^1\text{H}$  NMR data of genkwanin 5-O- $\beta$ -primeveroside (4) compared to those of literature (Hara et al., 2008).

Position	Genkwanin 5-O- $\beta$ -primeveroside (4)	Literature
Aglycone Moiety - Genkwanin		
3	6.72 <i>s</i>	6.69 <i>s</i>
6	6.87 <i>d</i> (2.4)	6.85 <i>d</i> (2.4)
8	7.05 <i>d</i> (2.4)	7.02 <i>d</i> (2.4)
OMe	3.90 <i>s</i>	3.89 <i>s</i>
2',6'	7.93 <i>d</i> (8.8)	7.91 <i>d</i> (8.8)
3',5'	6.92 <i>d</i> (8.8)	6.91 <i>d</i> (8.8)
4'-OH	10.33 <i>s</i>	10.31 <i>s</i>
Sugar Moiety – 5-O- $\beta$ -primeveroside		
Glc-H-1	4.78 <i>d</i> (7.6)	4.79 <i>d</i> (7.6)
Glc-H-2	<sup>a</sup>	3.39 <i>dd</i> (8.8, 7.6)
Glc-H-3	<sup>a</sup>	3.34 <i>dd</i> (9.6, 8.8)
Glc-H-4	3.28 <i>m</i> <sup>a</sup>	3.28 <i>dd</i> (9.6, 9.2)
Glc-H-5	3.56 <i>dd</i> (9.2, 5.2)	3.56 <i>dd</i> (9.2, 5.2)
Glc-H-6	3.67 <i>m</i> <sup>b</sup>	3.67 <i>dd</i> (10.6, 1.2)
Glc-H-6	3.97 <i>dd</i> (10.6, 5.2)	3.97 <i>dd</i> (10.6, 5.2)
Xyl-H-1	4.18 <i>d</i> (7.6)	4.18 <i>d</i> (7.6)
Xyl-H-2	3.00 <i>m</i> <sup>b</sup>	3.00 <i>dd</i> (8.1, 7.6)
Xyl-H-3	3.10 <i>m</i> <sup>b</sup>	3.10 <i>dd</i> (8.8, 8.7)
Xyl-H-4	3.23 <i>m</i> <sup>b</sup>	3.24 <i>dd</i> (8.8, 5.5)
Xyl-H-5	3.03 <i>m</i> <sup>b</sup>	3.03 <i>dd</i> (10.8, 5.5)
Xyl-H-5	3.70 <i>dd</i> (11, 5)	3.69 <i>dd</i> (10.8, 1.5)

<sup>a</sup> completely obscured by the DMSO signal; <sup>b</sup> signals are overlapping.  $\text{CDCl}_3$ , 600 MHz ( $^1\text{H}$ )



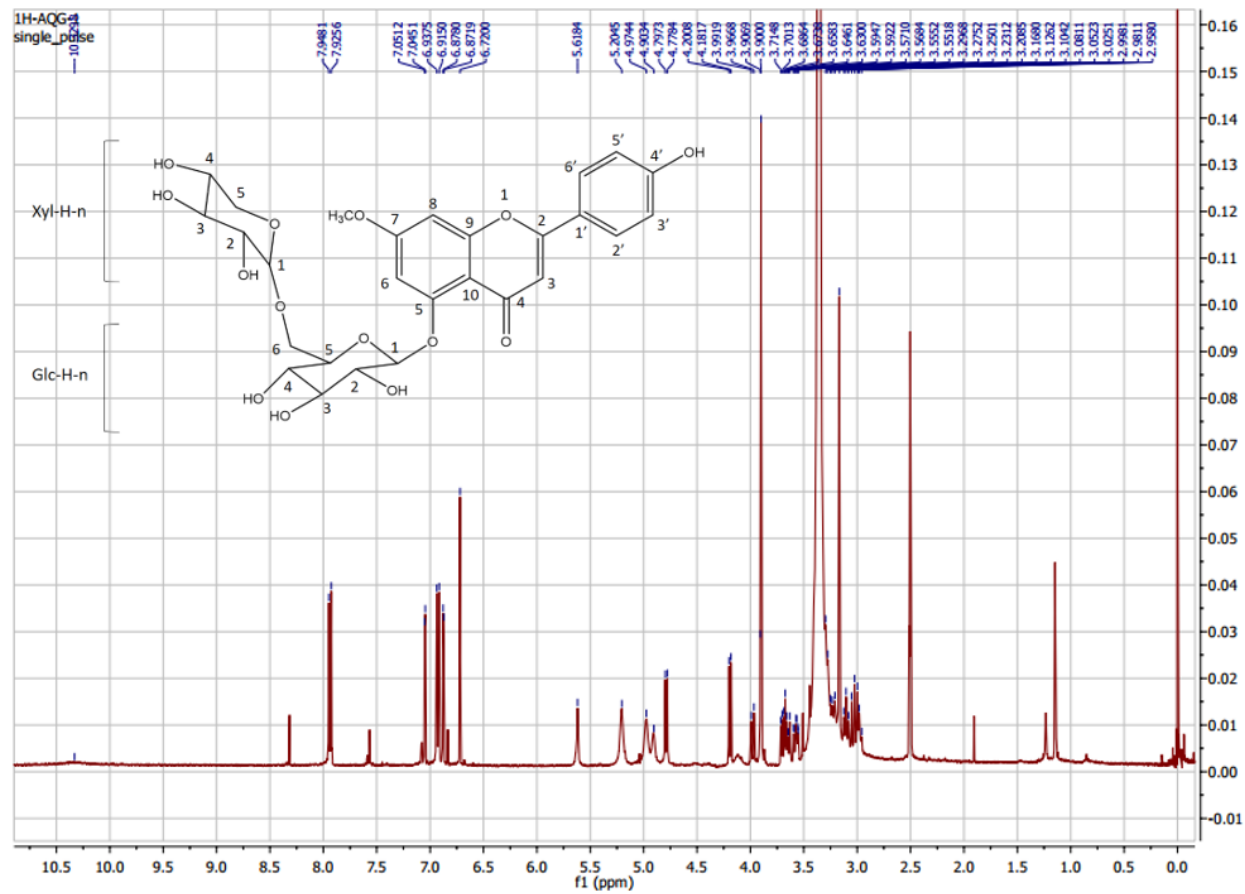
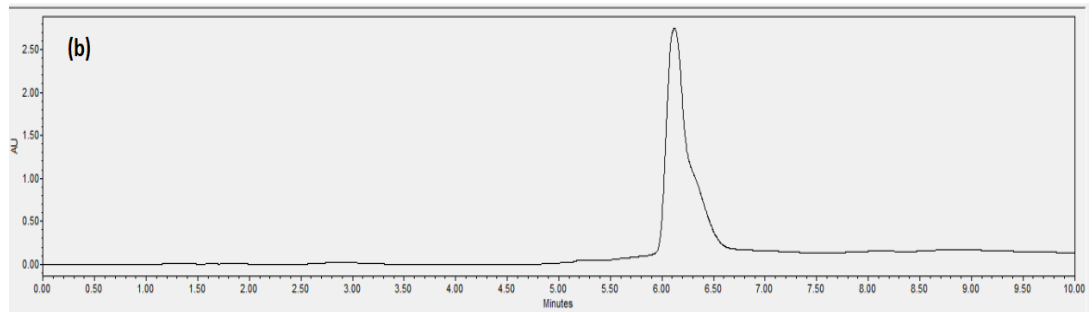
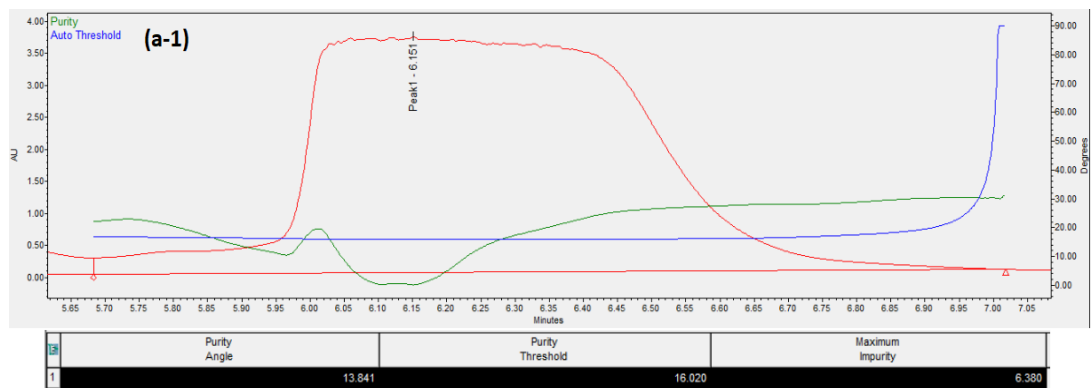
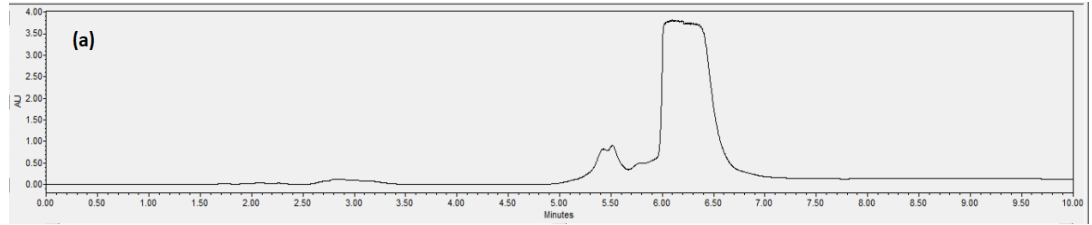
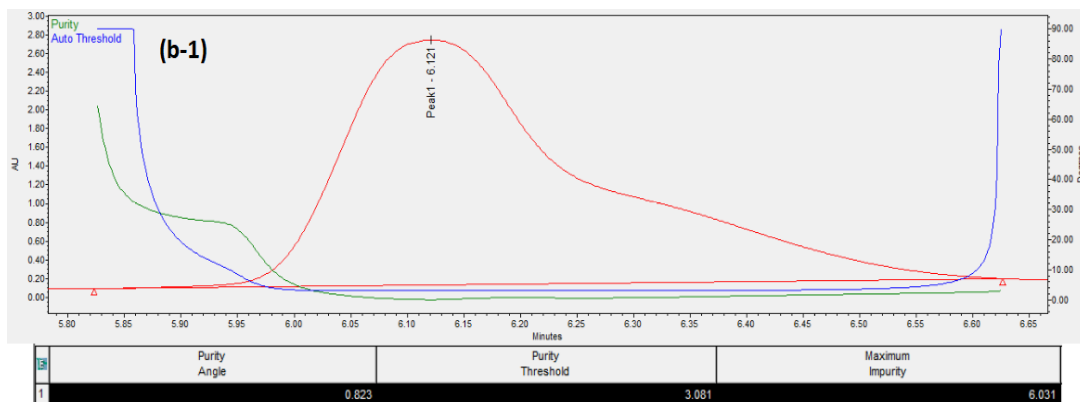


Figure 3.5 -  $^1\text{H}$  NMR spectrum and the structure of compound 4

Figure 3.6 shows the HPLC chromatogram of genkwanin 5-O- $\beta$ -primeveroside before and after purification, as well as the purity plot.





**Figure 3.6** – HPLC chromatogram on the purification of genkwanin 5-O- $\beta$ -primeveroside. (a) Before purification; (a-1) Purity plot before purification; (b) Isolated peak between 6.08 min and 6.70 min; (b-1) Purity plot of the isolated peak. When the purity angle is smaller than the purity threshold, the peak is considered spectrally homogenous (i.e., pure) (Waters Corporation, 1999). (b-1) has smaller purity angle relative to purity threshold compared to that of (a-1), which indicates (b-1) is purer than (a-1).

### 3.2 Extraction yields from TDS

As mentioned in the method part, 10 g of each tea product (Gaharu Tea, Gaharu Cool Tea and GOGA Drink Powder) and plant part (bark, leaf, young shoot and twig) were brewed in 150 mL of hot water (100 °C) for 15 minutes and filtrated to be used as the stock solution for further experiments. In order to determine the concentration of the stock solution, 10.0, 1.0 and 0.1 mL of each stock solution were dried (by rotavap and desiccator) to determine the total amount of dissolved solid in each of the respective sample volume. A TDS calibration curve was then plotted (mass, mg against volume, ml) to determine the stock concentration as well as the concentrations of all diluted stock solutions. Table 3.6 shows the TDS of all the water extracts (tea products and plant parts), final stock concentrations as well as the % yield of dissolved solid. Batch 1 and 2 were used for Attempt 1 and 2 gluconeogenesis assays, respectively.

**Table 3.6** – TDS of two batches of water extracts of various plant parts and tea products.

Sample	Batch	Total mass dissolved (mg)			Stock Concentration (mg/ml)	Dissolved solid yield (%)
		10 ml	1 ml	0.1 ml		
Gaharu Tea	1	89.5	9.0	0.8	9.05	13.71
		90.7	10.3	1.0		
		91.0	10.1	0.7		
	2	93.5	9.9	0.5	9.23	
		90.9	9.8	1.0		
		92.3	9.7	0.8		

Gaharu Cool Tea	1	100.9	10.9	1.2	10.04	15.26
		99.5	11.3	1.2		
		100.5	10.7	1.2		
	2	102.2	11.0	0.7	10.29	
		103.3	12.0	1.1		
		103.0	10.0	0.9		
GOGA Drink Powder	1	660.8	68.5	7.0	65.90	79.88
		656.1	70.3	6.8		
		659.4	67.0	7.1		
	2	406.4	39.8	4.2	40.607	
		406.4	41.0	4.0		
		405.7	38.2	4.0		
Bark	1	117.9	13.1	1.2	11.92	18.06
		120.4	12.4	1.3		
		119.1	12.3	1.3		
	2	122.0	12.4	1.2	12.16	
		121.1	12.6	1.5		
		121.5	12.7	1.3		
Leaf	1	116.2	11.6	1.4	11.44	17.12
		112.8	11.1	1.6		
		114.3	11.0	1.5		
	2	111.3	10.4	1.3	11.37	
		115.9	10.7	1.5		
		114.2	9.9	1.2		
Twig	1	53.0	5.4	0.7	5.22	7.70
		51.1	5.9	1.0		
		52.2	5.7	0.8		
	2	49.6	5.4	0.5	5.03	
		50.0	5.7	0.8		
		51.1	5.6	0.7		
Young Shoot	1	94.5	10.0	1.2	9.45	14.13
		93.7	10.1	1.2		
		95.1	9.8	1.3		
	2	96.4	9.6	1.2	9.38	
		91.4	10.5	1.2		
		93.5	9.8	1.1		

### 3.3 HPLC quantitative analyses of mangiferin and genkwanin 5-O- $\beta$ -primeveroside

Water extract samples of the various plant parts and tea products were subjected to HPLC quantitative analyses for the amount of mangiferin and genkwanin 5-O- $\beta$ -primeveroside present in the individual samples. The results are shown as mean  $\pm$  S.D. (n=3) (Table 3.7).

**Table 3.7** – Quantitative analysis of mangiferin and genkwanin 5-O- $\beta$ -primeveroside. The mangiferin content of MeOH extract is highest (9.76 g of mangiferin/100 g of extract), followed by leaf (6 g/100 g). Content of genkwanin 5-O- $\beta$ -primeveroside is highest in leaf (0.55 g/100 g), followed by Gaharu Tea (0.15 g /100g), and the least in Gaharu Cool Tea (0.11 g/100 g).

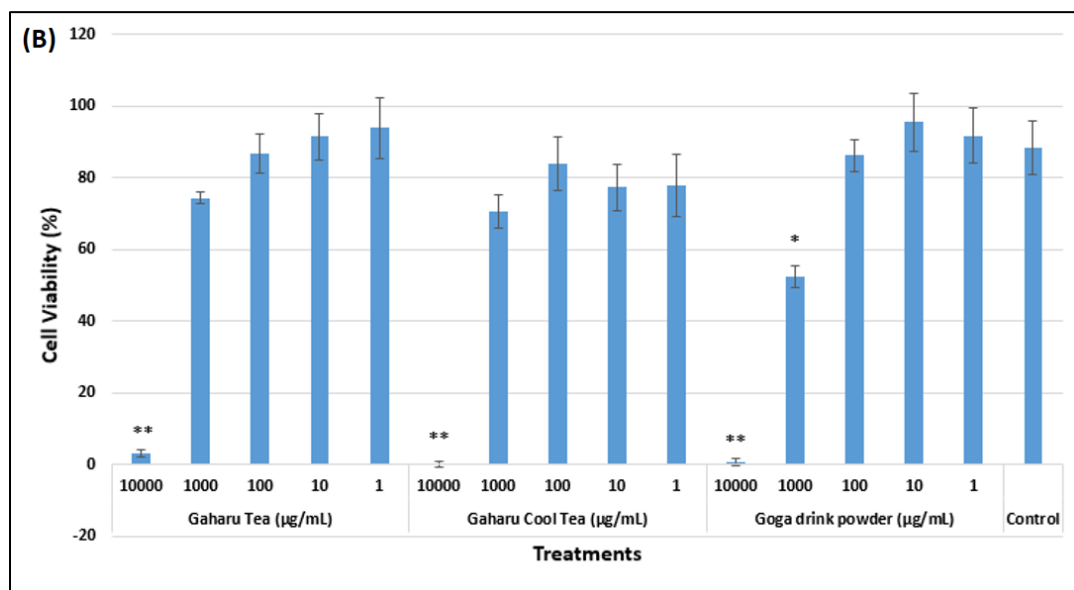
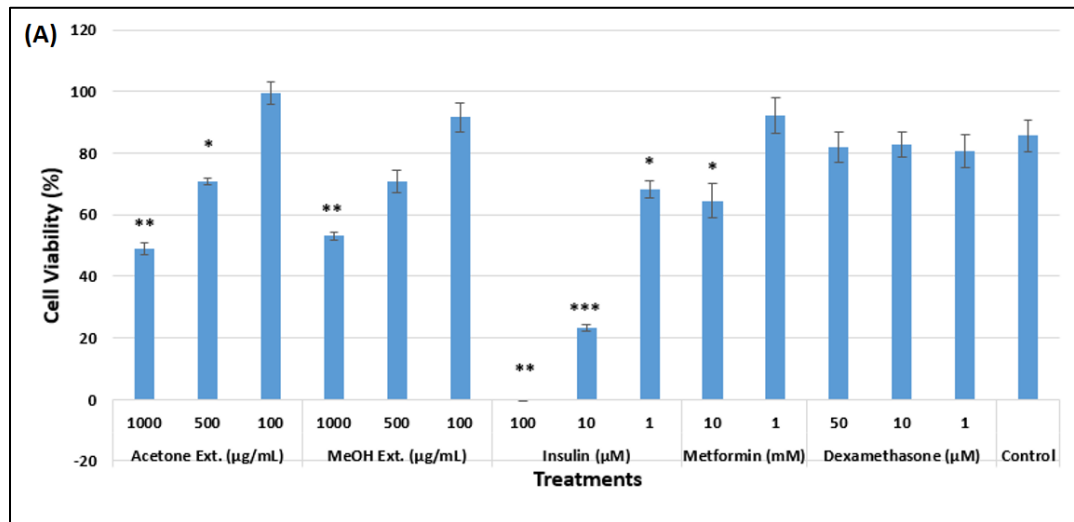
Sample	Code	Average amount of mangiferin (% w/w) $\pm$ S.D.	Average amount of genkwanin 5-O- $\beta$ -primeveroside (% w/w) $\pm$ S.D.
Gaharu Tea	AQGT	1.33 $\pm$ 0.03	0.15 $\pm$ 0.00
Gaharu Cool Tea	AQGCT	1.66 $\pm$ 0.25	0.11 $\pm$ 0.00
GOGA Drink Powder	AQGDP	0.18 $\pm$ 0.01	ND
Twig	AQT	0.50 $\pm$ 0.02	ND
Bark	AQB	ND	ND
Leaf	AQL	6.00 $\pm$ 0.40	0.55 $\pm$ 0.01
Young Shoot	AQYS	ND	ND
Acetone Extract	AQAE	5.45 $\pm$ 0.00	NM
MeOH Extract	AQME	9.76 $\pm$ 0.01	NM

\* ND - Not detectable; NM – Not measured.

### 3.4 Biological assays

#### 3.4.1 MTT assay

MTT assay was performed to determine a safe concentration range of treatments (above  $IC_{50}$ ) that could be used to conduct the gluconeogenesis assays. Figure 3.7 shows the average cell viability percentages for all test samples from the MTT assays. All samples were evaluated three times, each in triplicate.



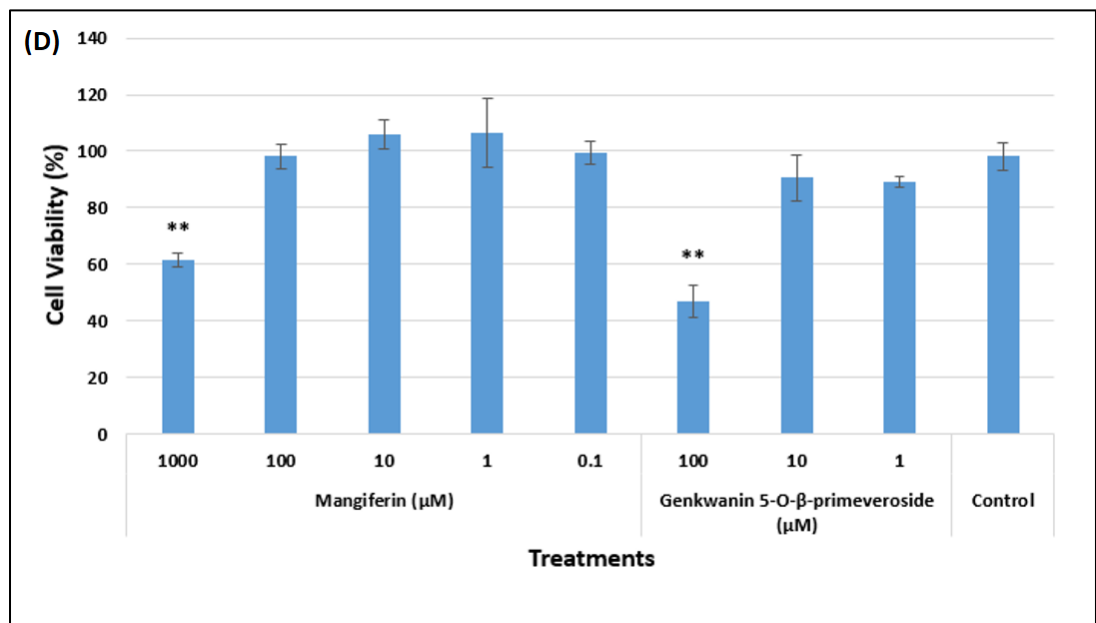
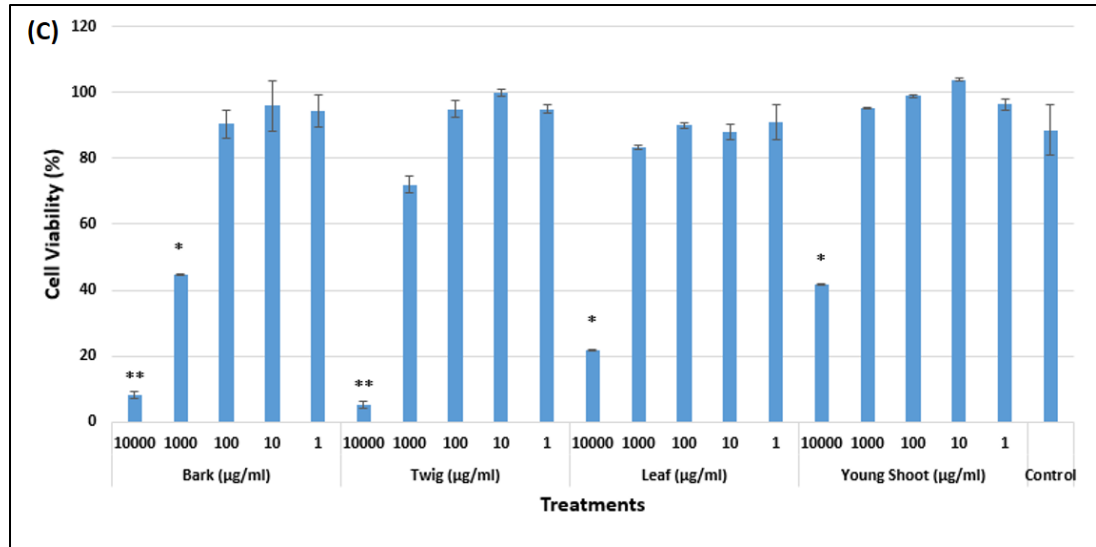


**Figure 3.7** – MTT assays for: (A) Acetone and methanol extracts of leaves, positive (insulin and metformin) and negative (dexamethasone) drug controls; (B) Water extract of tea products; (C) Water extracts of plant parts; (D) Mangiferin and genkwanin 5-O-β-primeveroside. Data are expressed as mean ± SEM (n=3). \*, p<0.05, \*\*, p<0.01 and \*\*\*, p<0.001.



Based on Figure 3.7 (A), acetone and MeOH extracts showed significant reduction in cell viability relative to control at concentration of 1000  $\mu\text{g/ml}$  (49%,  $p < 0.01$  and 53%,  $p < 0.01$  respectively). At 500  $\mu\text{g/ml}$ , both acetone and MeOH extracts showed comparable cell viability reduction with cell viability being well above 50%. Thus, safe concentration ranges for these two extracts were determined to be below 500  $\mu\text{g/ml}$ . For insulin, significant cell viability reduction was determined at concentration above 1  $\mu\text{M}$  (69%,  $P < 0.05$ ), where 10  $\mu\text{M}$  (23%,  $p < 0.001$ ) and 100  $\mu\text{M}$  (0%,  $p < 0.01$ ) killed more than half of the cells. Therefore, maximum concentration of insulin to be used for gluconeogenesis was 1  $\mu\text{M}$ . At 10 mM, although metformin showed significant cell viability reduction (65%,  $p < 0.05$ ), cell viability is still above 50%. Thus any concentration below 10 mM was considered safe for gluconeogenesis assay. Last but not least, dexamethasone showed no significant cell viability reduction from 1 to 50  $\mu\text{M}$ . Therefore, concentration within this range was used in gluconeogenesis assay. For comparability purpose, the concentration used in gluconeogenesis assay for the acetone and MeOH extracts was 100  $\mu\text{g/ml}$ , whereas concentration for the three drug controls was set at 1  $\mu\text{M}$ .

From Figure 3.7 (B), Gaharu Tea and Gaharu Cool Tea showed significant reduction in cell viability relative to control at 10,000  $\mu\text{g/ml}$  (3%,  $p < 0.01$  and 0.1%,  $p < 0.01$ , respectively). At 1000  $\mu\text{g/ml}$ , both Gaharu Tea and Gaharu Cool Tea showed comparable cell viability reduction but not significant. Thus, safe concentration range for these two extracts was determined as below 1000  $\mu\text{g/ml}$

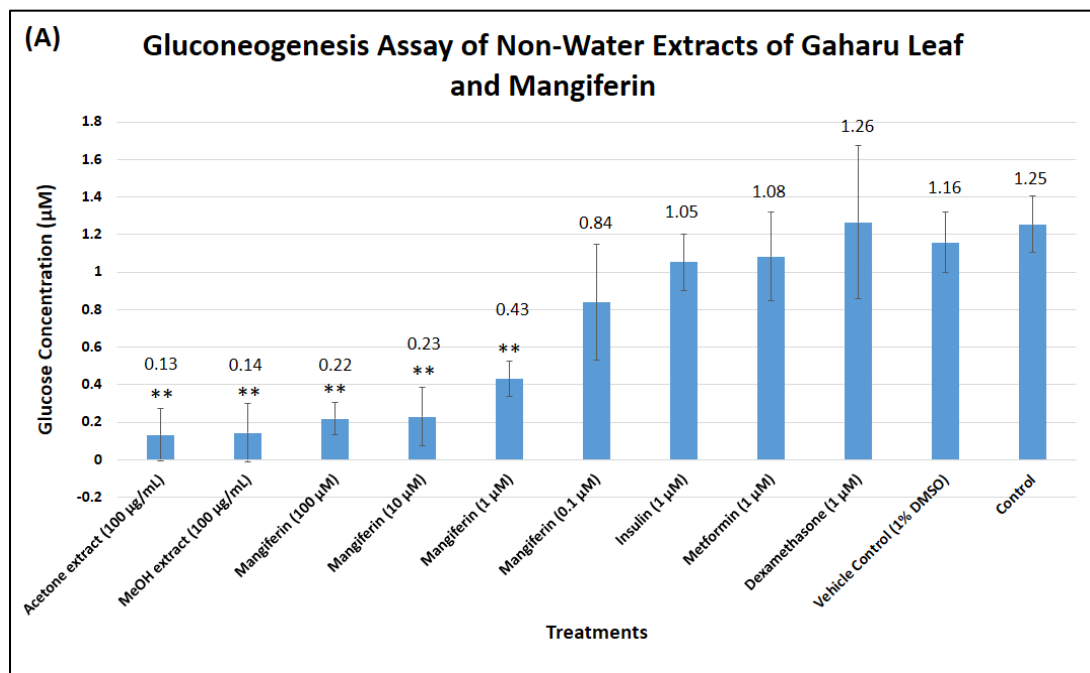
(maximum). As for GOGA Drink Powder, concentrations at 10,000 and 1000  $\mu\text{g}/\text{ml}$  showed significant cell viability reduction (0.6%,  $p<0.01$  and 52%,  $p<0.05$  respectively). Thus, safe working concentration range was determined at 100  $\mu\text{g}/\text{ml}$  or below. For comparability purpose, the concentration used in gluconeogenesis assay for these three tea products was 10  $\mu\text{g}/\text{ml}$ .

From Figure 3.7 (C), bark showed significant reduction in cell viability relative to control at 10,000 and 1000  $\mu\text{g}/\text{ml}$  (8%,  $p<0.01$  and 45%,  $p<0.05$ , respectively). Twig also showed significant cell viability reduction at 10,000  $\mu\text{g}/\text{ml}$  (5%,  $p<0.01$ ). As for leaf and young shoot, significant reduction in cell viability was only observed at 10,000  $\mu\text{g}/\text{ml}$  (22%,  $p<0.05$  and 42%,  $p<0.05$ , respectively). For comparability purpose, the concentration used in gluconeogenesis assay for these four plant parts was 10  $\mu\text{g}/\text{ml}$ .

From Figure 3.7 (D), both mangiferin and genkwanin 5-O- $\beta$ -primeveroside only showed significant reduction in cell viability at 1000  $\mu\text{M}$  (62%,  $P<0.01$ ) and 100  $\mu\text{M}$  (46%,  $p<0.01$ ) respectively. Safe concentration ranges for mangiferin and genkwanin 5-O- $\beta$ -primeveroside were determined at 100  $\mu\text{M}$  or below and 10  $\mu\text{M}$  or below, respectively. For comparability purpose, the concentration ranges used in gluconeogenesis assay for mangiferin and genkwanin 5-O- $\beta$ -primeveroside were 0.1 to 100  $\mu\text{M}$  and 0.1 to 10  $\mu\text{M}$ , respectively.

### 3.4.2 Gluconeogenesis assay

Gluconeogenesis assays were performed to investigate the glucose production-suppression effect of the plant extracts and tea products. For the water extract of tea products and plant parts, two separate attempts were performed using batch 1 and batch 2 test samples, respectively (refer Table 3.6). The average results from these two attempts were illustrated in Figure 3.8 (C). Figures 3.8 (A), 3.8 (B) and 3.8 (C) show the average glucose concentrations for all test samples based on the gluconeogenesis assays. Each assay was performed three times in triplicate.



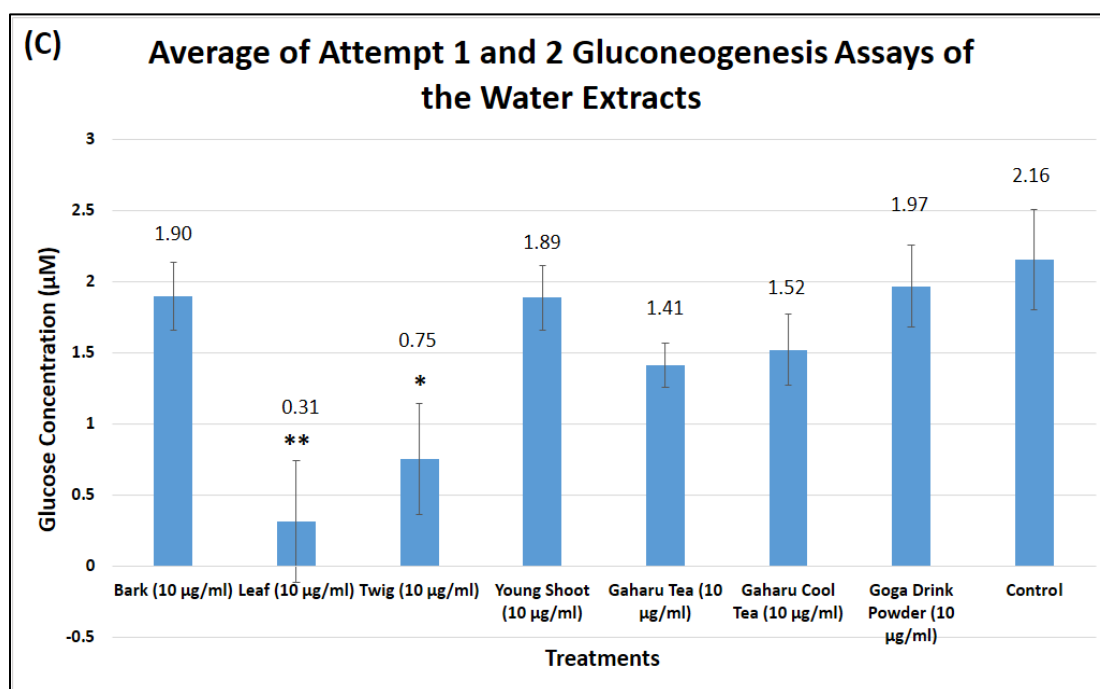
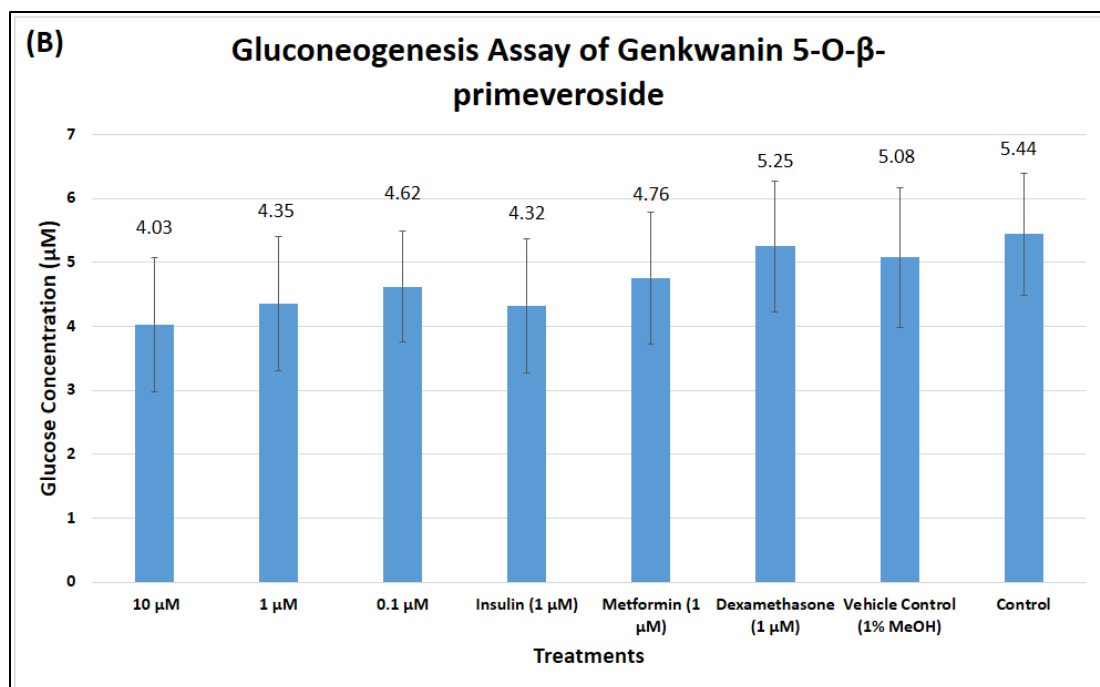


**Figure 3.8** – Gluconeogenesis assays for: (A) Non-water extracts of gaharu leaf, mangiferin, positive (insulin and metformin) and negative (dexamethasone) drug controls, as well as vehicle control (1% DMSO); (B) Genkwanin 5-O- $\beta$ -

primeveroside, the negative and positive drug controls, and vehicle control (1% MeOH); (C) Water extracts of plant parts and tea products. Data are expressed as mean  $\pm$  SEM (n=3 for A and B; n=6 for C). \*, p<0.05, \*\*, p<0.01 and \*\*\*, p<0.001. Control was well not treated with an extract.

### 3.4.3 Bradford Protein assay

Bradford protein assay was performed to determine the total amount of cells in each well that were responsible for glucose production in the respective gluconeogenesis assay. The glucose concentration of each well was divided by the total amount of cells (measured in  $\mu\text{g}$  amount of protein) in that particular well to give a normalised glucose concentration. Table 3.8 – 3.10 shows the total amount of protein ( $\mu\text{g}$ ) determined for all the gluconeogenesis assays that were carried out.

**Table 3.8** – Total amount of protein determined for the gluconeogenesis assay for acetone extract, methanol extract, mangiferin, insulin, metformin, dexamethasone, vehicle control, and control.

Treatments	Total amount of protein ( $\mu\text{g}$ )								
	1st experiment			2nd experiment			3rd experiment		
Acetone extract (100 $\mu\text{g}/\text{mL}$ )	729.79	673.54	554.79	786.04	548.54	546.54	614.17	645.42	551.67
MeOH extract (100 $\mu\text{g}/\text{mL}$ )	857.92	929.79	786.04	920.42	764.17	895.42	757.92	873.54	823.54

Mangiferin (100 $\mu$ M)	417.29	657.92	429.79	454.79	657.92	429.79	661.04	642.29	448.54
Mangiferin (10 $\mu$ M)	761.04	289.17	514.17	401.67	273.54	579.79	473.54	804.79	664.17
Mangiferin (1 $\mu$ M)	1092.29	470.42	329.79	779.79	442.29	436.04	448.54	551.67	398.54
Mangiferin (0.1 $\mu$ M)	1161.04	679.79	767.29	751.67	942.29	851.67	786.04	726.67	645.42
Insulin (1 $\mu$ M)	723.54	923.54	867.29	720.42	873.54	636.04	811.04	823.54	598.54
Metformin (1 $\mu$ M)	626.67	776.67	570.42	667.29	751.67	748.54	728.54	632.92	757.92
Dexamethasone (1 $\mu$ M)	1023.54	398.54	542.29	598.54	470.42	804.79	511.04	482.92	548.54
Vehicle Control (1% DMSO)	568.20	445.64	462.20	583.52	570.27	607.33	515.20	458.89	561.58
Control	726.67	486.04	436.04	536.04	420.42	432.91	739.17	529.79	667.29

**Table 3.9** – Total amount of protein determined for the gluconeogenesis assay for genkwanin 5-O- $\beta$ -primeveroside, insulin, metformin, dexamethasone, vehicle control, and control.

Treatments	Total amount of protein ( $\mu\text{g}$ )								
	1st experiment			2nd experiment			3rd experiment		
Genkwanin 5-O- $\beta$ -primeveroside (10 $\mu\text{M}$ )	723.54	589.17	639.17	667.29	442.29	642.29	551.67	542.29	548.54
Genkwanin 5-O- $\beta$ -primeveroside (1 $\mu\text{M}$ )	729.79	667.29	567.29	679.79	729.79	661.04	570.42	607.92	629.79
Genkwanin 5-O- $\beta$ -primeveroside (0.1 $\mu\text{M}$ )	664.17	701.67	623.54	645.42	623.54	539.17	554.79	426.67	567.29
Insulin (1 $\mu\text{M}$ )	845.42	748.54	626.67	676.67	657.92	567.29	607.92	536.04	642.29
Metformin (1 $\mu\text{M}$ )	526.67	776.67	570.42	467.29	751.67	548.54	548.54	432.92	557.92
Dexamethasone (1 $\mu\text{M}$ )	1023.54	398.54	542.29	598.54	470.42	804.79	511.04	482.92	548.54



Vehicle Control (1% MeOH)	720.42	717.29	695.42	707.92	557.92	807.92	514.17	632.92	595.42
Control	723.54	532.92	736.04	482.92	729.79	682.92	586.04	429.79	567.29

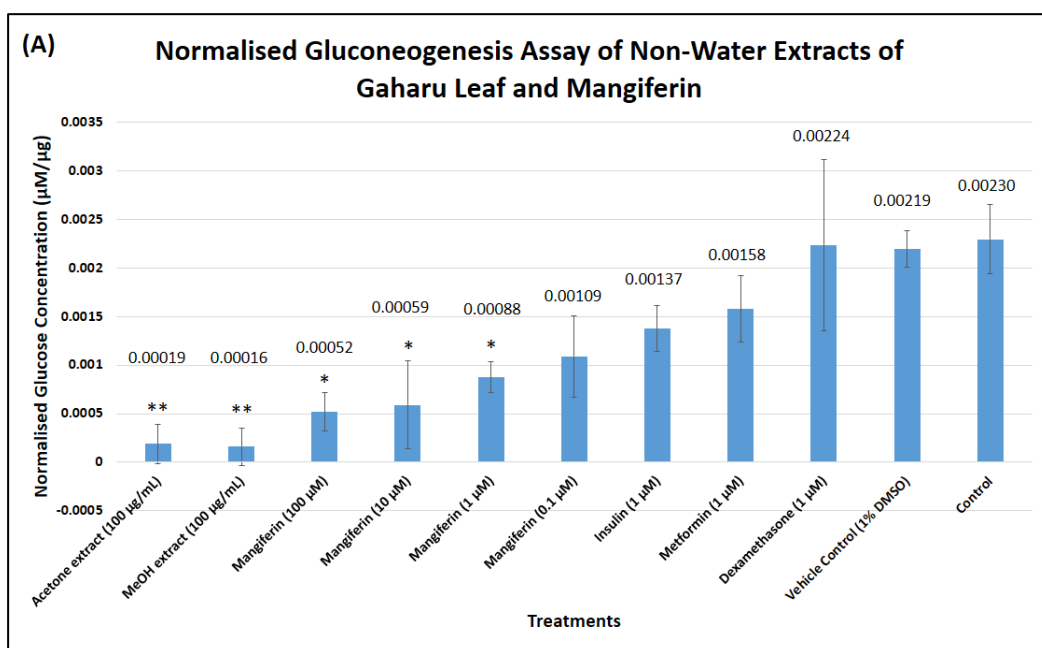
**Table 3.10** – Total amount of protein determined for the gluconeogenesis assay for bark, leaf, twig, young shoot, Gaharu Tea, Gaharu Cool Tea, GOGA Drink Powder, and control.

Treatments	Total amount of protein ( $\mu\text{g}$ )								
	1st experiment			2nd experiment			3rd experiment		
Attempt 1									
Bark (10 $\mu\text{g}/\text{ml}$ )	723.54	714.17	954.79	761.04	904.79	757.92	936.04	923.54	920.42
Leaf (10 $\mu\text{g}/\text{ml}$ )	914.17	829.79	970.42	786.04	882.92	932.92	898.54	776.67	892.29
Twig (10 $\mu\text{g}/\text{ml}$ )	804.79	689.17	882.92	945.42	861.04	798.54	1311.04	951.67	654.79
Young Shoot (10 $\mu\text{g}/\text{ml}$ )	961.04	879.79	882.92	904.79	879.79	1139.17	754.79	773.54	892.29
Gaharu Tea (10 $\mu\text{g}/\text{ml}$ )	901.67	1242.29	973.54	773.54	1029.79	423.54	992.29	732.92	673.54
Gaharu Cool Tea (10 $\mu\text{g}/\text{ml}$ )	664.17	461.04	1348.54	1698.54	842.29	1420.42	1279.79	242.29	998.54

µg/ml)									
GOGA Drink Powder (10 µg/ml)	801.67	729.79	823.54	767.29	911.04	861.04	867.29	689.17	1048.54
Control	1011.04	1004.79	901.67	654.79	961.04	1120.42	686.04	879.79	748.54
Attempt 2									
Bark (10 µg/ml)	745.42	736.04	976.67	782.92	926.67	779.79	957.92	945.42	1045.42
Leaf (10 µg/ml)	936.04	851.67	992.29	807.92	904.79	954.79	920.42	798.54	914.17
Twig (10 µg/ml)	826.67	711.04	904.79	967.29	882.92	820.42	1332.92	973.54	676.67
Young Shoot (10 µg/ml)	982.92	901.67	904.79	926.67	901.67	1161.04	776.67	795.42	914.17
Gaharu Tea (10 µg/ml)	923.54	1264.17	995.42	795.42	1051.67	445.42	1014.17	754.79	695.42
Gaharu Cool Tea (10 µg/ml)	686.04	482.92	1139.17	1198.54	239.17	889.17	1301.67	436.04	1020.42
GOGA Drink Powder (10 µg/ml)	823.54	1064.17	845.42	789.17	932.92	882.92	889.17	1179.79	1132.92
Control	1032.92	1339.17	923.54	676.67	982.92	1142.29	707.92	901.67	770.42

### 3.4.4 Normalised gluconeogenesis assay

The normalised glucose concentration was calculated by dividing the glucose concentration ( $\mu\text{M}$ ) determined for each well with the total amount of protein ( $\mu\text{g}$ ) of the same well as illustrated in Tables 3.8 – 3.10. The normalised data is a more accurate representation of glucose production activity as it is presented as amount of glucose produced ( $\mu\text{M}$ ) per amount of protein ( $\mu\text{g}$ ), which eliminate misinterpretation arose from different cell concentration in each well. Figures 3.9 (A), 3.9 (B) and 3.9 (C) show the average normalised glucose concentrations based on the gluconeogenesis assay results.



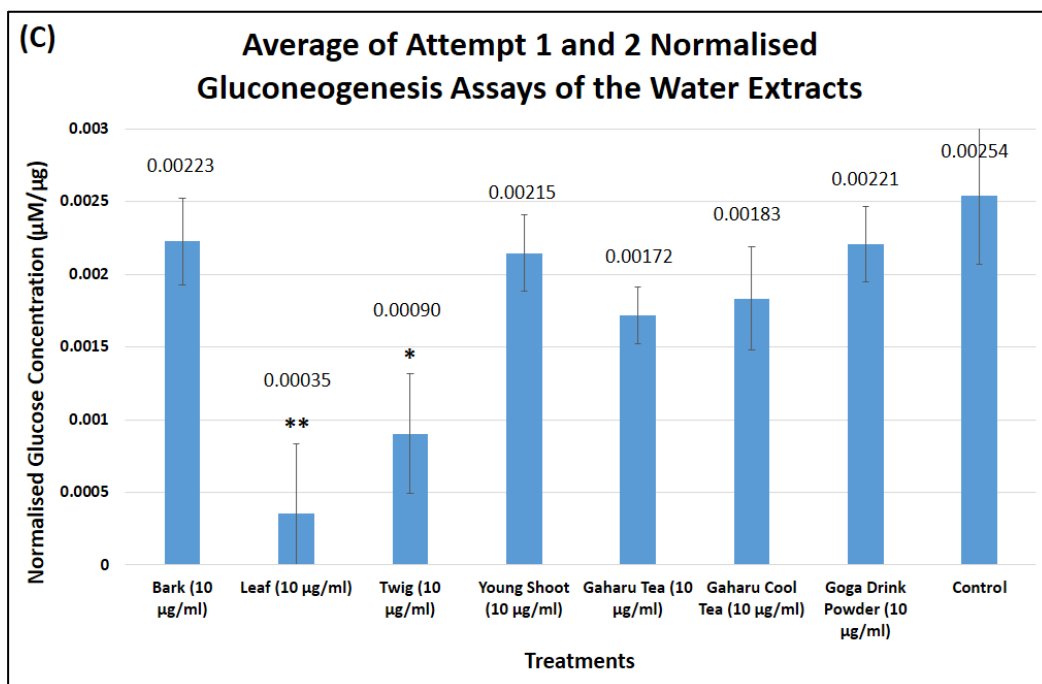
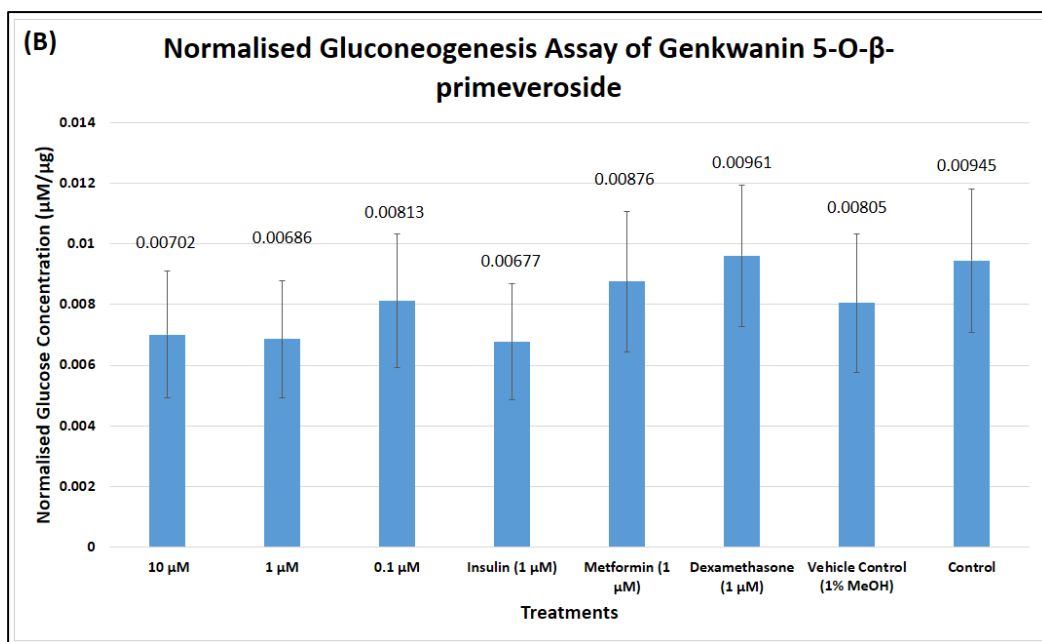


**Figure 3.9** – Normalised gluconeogenesis assays for: (A) Non-water extracts of gaharu leaf, mangiferin, positive (insulin and metformin) and negative (dexamethasone) drug controls, as well as vehicle control (1% DMSO); (B) Genkwanin 5-O- $\beta$ -primeveroside, the positive and negative drug controls, and vehicle control (1% MeOH); (C) Water extracts of plant parts and tea products.

Data are expressed as mean  $\pm$  SEM (n=3 for A and B; n=6 for C). \*, p<0.05, \*\*, p<0.01 and \*\*\*, p<0.001. Control was well not treated with an extract.

From Figure 3.9 (A), cells treated with 100  $\mu$ g/ml of acetone and MeOH extract showed significant glucose production-suppression effect relative to control. As for mangiferin, its concentrations used (0.1  $\mu$ M to 100  $\mu$ M) corresponded well to its glucose-suppression effect, i.e., the highest concentration at 100  $\mu$ M corresponded to the lowest amount of glucose detected, while the lowest concentration at 0.1  $\mu$ M corresponded to the highest amount of glucose detected. 1  $\mu$ M of insulin also showed significant glucose suppression activity. As for metformin and dexamethasone, no significant difference in glucose production compared to control were measured. The vehicle control (1% DMSO) also showed no significant difference in glucose production compared to control.

From Figure 3.9 (B), 10, 1 and 0.1  $\mu$ M of genkwanin 5-O- $\beta$ -primeveroside showed no significant difference in glucose production relative to control. 1  $\mu$ M of insulin, metformin and dexamethasone also showed no significant glucose suppression activity. The vehicle control (1% MeOH) also showed no significant difference in glucose production compared to control.

Figure 3.9 (C) showed the average normalised glucose concentration of Attempts 1 and 2 gluconeogenesis assay results for the water extracts of tea products and plant parts. Both leaf and twig showed significant glucose production-suppression effect compared to control, while both bark and

young shoot showed no significant glucose suppression activity. Among the tea products, both Gaharu Tea and Gaharu Cool Tea showed comparable normalised glucose concentration values (0.00172 and 0.00183  $\mu\text{M}/\mu\text{g}$ , respectively), while GOGA Drink Powder showed a much higher value (0.00221  $\mu\text{M}/\mu\text{g}$ ). Generally, it appears that the order of glucose suppression activity from highest to lowest is Gaharu Tea > Gaharu Cool Tea > GOGA Drink Powder.

The normalised gluconeogenesis assay results for all test samples showed identical trend to the results before normalisation (Figure 3.8 *versus* Figure 3.9).

# Chapter Four

## Discussion

### 4.1 Isolation and structure determination

In the present study, four compounds were obtained from 1 kg of dried ground leaves of *A. sinensis* provided by GTSB, which was first exhaustively extracted with acetone followed by methanol, giving 70.27 g of crude acetone extract and 129.95 g of methanol extract.

As mentioned in chapter 2.6, mangiferin (**1**) was obtained from the crude acetone extract using the precipitation method with  $\text{CHCl}_3$ :MeOH (1:1) as the precipitating solvent. Subsequent recrystallization of the precipitate in methanol gave pure mangiferin (**1**). Following the successful isolation of mangiferin (**1**) based on the TLC profile that showed no other visible impurities,  $^1\text{H}$  NMR and LC-Orbitrap-MS data were acquired for the sample. Visual inspection of the  $^1\text{H}$  NMR spectrum of **1** (see Figure 3.1 and Table 3.2) showed characteristic peaks that correlated to those reported for mangiferin (Hara, 2008). The LC-Orbitrap-MS data further supported the identity of **1** to be mangiferin, which showed a pseudomolecular ion peak at  $m/z$  421.076 ( $\text{C}_{19}\text{H}_{18}\text{O}_{11} - \text{H}^+$ ).

Our initial focus was to locate flavonoid containing fractions, which showed yellowish-green spots when sprayed with ethanolic  $\text{AlCl}_3$  and viewed under UV at 365 nm (longwave). This characteristic was observed in F10 (see Figure 2.1) of the crude acetone extract filtrate that has been subjected to VCC. After

repeated fractionation of F10 using CTLC, compounds **2** and **3** were obtained and their  $^1\text{H}$  NMR and LC-Orbitrap-MS data were acquired. Visual inspection of the  $^1\text{H}$  NMR spectra (see Figure 3.3 and Table 3.3 for compound **2**; Figure 3.4 and Table 3.4 for compound **3**) showed characteristic peaks that correlated to those of naringenin (Álvarez-Álvarez et al., 2015) and iriflophenone 2-O- $\alpha$ -rhamnoside (Hara et al., 2008), respectively. The identities of compounds **2** and **3** were further confirmed by the LC-Orbitrap-MS data.

Compound **4** (genkwanin 5-O- $\beta$ -primeveroside), which is quite polar, was isolated from the crude MeOH extract instead of the crude acetone extract. Similar to other compounds, it was isolated after subsequent VCC and CTLC. However, repeated CTLC failed to fully purify compound **4** due to its polar nature. Compound **4** was eventually purified using a semi-preparative reverse phase HPLC. The  $^1\text{H}$  NMR spectrum was then acquired for the purified sample. Unfortunately, the LC-Orbitrap-MS data is unavailable for **4** as the instrument was out of service. Visual inspection of the  $^1\text{H}$  NMR spectrum of **4** (see Figure 3.5 and Table 3.5) showed characteristic peaks that correlated to those of genkwanin 5-O- $\beta$ -primeveroside as reported in the literature (Hara et al., 2008).

#### **4.2 Biological assays**

Gluconeogenesis is the production of glucose from pyruvate and other non-carbohydrate precursors such as amino acid, glycerol, and lactate (Rang et al.,



2003). Gluconeogenesis mainly takes place in the liver when the blood glucose level is low. In this research, gluconeogenesis assay was employed on human liver cell HepG2 to simulate and measure hepatic glucose production *in vitro*. Besides mangiferin and genkwanin 5-O- $\beta$ -primeveroside, different plant parts and tea products extracts were tested to investigate their effect on glucose production level of HepG2 cells in the gluconeogenesis assay. There were four individual plant parts from the *A. sinensis* tree, namely, bark, leaf, twig, and young shoot. As for the tea products, raw materials of these three products were used, namely, Gaharu Tea, Gaharu Cool Tea, and GOGA Drink Powder. Gaharu Tea and Gaharu Cool Tea are made up of raw plant parts, whereas GOGA Drink Powder is made by spray drying the water extracts of plant parts on the maltodextrin filler. These raw materials of the tea products are made up of different ratio of ground plant parts, which are summarised in Table 4.1.

**Table 4.1** – Tea products composition.

Tea Products	Composition (%)				
	Bark	Leaf	Twig	Young Shoot	Additives
Gaharu Tea	30.00	20.00	50.00	-	-
Gaharu Cool Tea	27.00	18.00	45.00	10.00	-
GOGA Drink Powder	26.25	17.81	44.06	5.63	Mogroside V (6.25) Maltodextrin (1:1 Filler)

Multiple studies have shown that mangiferin possessed an array of antidiabetic properties such as  $\alpha$ -glucosidase inhibition (Feng et al., 2011),

and modulation of GLUT4 expression in the plasma membrane of muscle (Miura et al., 2001). In a study done by Wang et al. (2016) which was similar to this research has shown that mangiferin suppressed gluconeogenesis assay on HepG2 human liver cells. According to Figure 3.9 (A), increasing concentration of mangiferin from 0.1  $\mu\text{M}$  to 100  $\mu\text{M}$  leads to significant reduction in normalised glucose concentration in HepG2 cells. Therefore, it can be deduced that higher amounts of mangiferin corresponded to better glucose suppression activity. As for genkwainin 5-O- $\beta$ -primeveroside, there is no correlation between the concentration of this compound and the glucose suppression activity (see Figure 3.9 (B)). The relationship between glucose suppression activity and the amount of mangiferin detected in each of the water extracts of the plant parts and tea products is presented in Figure 4.1.

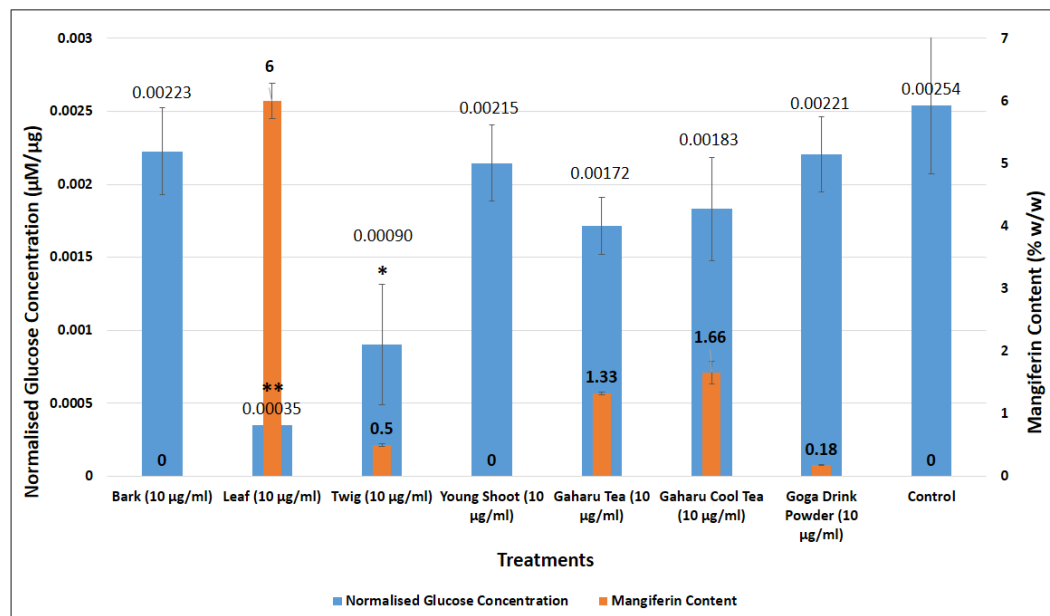


**Figure 4.1** – Normalised gluconeogenesis concentrations and mangiferin contents associated with the water extracts of different plant parts and tea products (see Figure 3.9 (C) and Table 3.7).

The leaf water extract exhibited the highest glucose suppression effect, in agreement with the highest amount of mangiferin detected within the extract (6.00% w/w). Mangiferin was undetectable in the bark and young shoot water extracts (presumably due to very low amounts of mangiferin present), which explained the lack of glucose suppression activity observed. Twig water extract was determined to contain a lower amount of mangiferin (0.50% w/w) compared to that of the leaf. This is consistent with the lower glucose suppression activity observed for the twig water extract, but was more active compared to both the bark and young shoot water extracts.

The amounts of mangiferin present in the water extracts of Gaharu Tea (1.33% w/w) and Gaharu Cool Tea (1.66% w/w) were found to be comparable. This is also consistent with the glucose suppression activity observed for the extracts of both the tea products. Based on the tea product composition data (Table 4.1), Gaharu Tea was made up of 20% leaf, 50% twig and 30% bark, while Gaharu Cool Tea was made up of 18% leaf, 45% twig, 27% bark and 10% young shoot. Since it was observed that only the leaf and twig parts possess appreciable amounts of mangiferin, therefore the varying compositions of the bark and young shoot parts present in Gaharu Tea and Gaharu Cool Tea have little effect on their glucose suppression activity. On the other hand, the low amount of mangiferin detected in the water extract of GOGA Drink Powder (0.18% w/w) corroborated the low glucose suppression activity exhibited by this tea product, of which the activity was almost comparable to that of control (which was not treated with an extract).

According to Table 3.6, the extraction yields (after filtration) of the water extracts of Gaharu Tea and Gaharu Cool Tea are comparable (13.71% and 15.26%, respectively). As for GOGA Drink Powder, the yield is much higher, around 79.88%. This values are analogous to the dissolved content that sipped through the tea bag when brewing the tea. For the commercial products, one tea bag of Gaharu Tea and Gaharu Cool Tea contains an average of 2.25 g of mixed ground plant parts per tea bag. As for GOGA Drink, which is sold as a bottled drink (300 ml), each bottle contains an average of 250 mg of water extract (obtained from a mixed plant parts) in addition to some additives. The amount of mangiferin ingested per serving (one tea bag or one bottle) of each of these tea products is illustrated in Table 4.2.

**Table 4.2** – Mangiferin content per serving of Gaharu Tea, Gaharu Cool Tea, and GOGA Drink.

	Gaharu Tea	Gaharu Cool Tea	GOGA Drink
<b>Averaged weight of tea material per serving<sup>a</sup></b>	2.25 g	2.25 g	250 mg per 300 ml
<b>Averaged TDS yield of water extract (%)<sup>b</sup></b>	13.71	15.26	79.88
<b>Averaged mangiferin content (%)<sup>c</sup> in water extract</b>	1.33	1.66	0.18
<b>Averaged mangiferin content per serving (mg)</b>	4.10	5.70	0.36

<sup>a</sup> These data were provided by GTSB

<sup>b</sup> 1% = 1 g of TDS per 100 g of tea material

<sup>c</sup> 1% = 1 g of mangiferin per 100 g of TDS

As shown in Table 4.2, Gaharu Tea and Gaharu Cool Tea have comparable amount of mangiferin per serving, while for GOGA Drink, a much smaller amount of mangiferin is present per serving. Therefore, it is speculated that consuming Gaharu Tea and Gaharu Cool Tea would result in better glucose suppression activity compared to GOGA Drink per serving.

## Chapter Five

### Conclusion, Research Limitations and Future Works

#### 5.1 Conclusion

1.022 g of mangiferin has been successfully isolated and purified from the acetone extract (70.27 g) of the leaf material (1 kg), while 0.018 g of genkwanin 5-O- $\beta$ -primeveroside was isolated and purified from the MeOH extract (129.95 g) of the same leaf material. Besides the two major compounds of interest, 0.021 g of naringenin and 0.03 g of iriflophenone 2-O- $\alpha$ -rhamnoside have also been isolated from the acetone extract.

The amounts of mangiferin in each plant part and tea product were determined by HPLC quantitative analysis, i.e., Twig 0.50%, Leaf 6.00%, Gaharu Tea 1.33%, Gaharu Cool Tea 1.66%, and GOGA Drink Powder 0.18%. Mangiferin was undetectable in bark and young shoot. Similarly, the amounts of genkwanin 5-O- $\beta$ -primeveroside were determined, i.e., Leaf 0.55%, Gaharu Tea 0.15%, and Gaharu Cool Tea 0.11%. Genkwanin 5-O- $\beta$ -primeveroside was undetectable in twig, bark, young shoot, and GOGA Drink Powder. The acetone and MeOH extracts were also sent for mangiferin content analysis, but not for genkwanin 5-O- $\beta$ -primeveroside. 5.45% of mangiferin was found in the acetone extract, while 9.76% was found in the MeOH extract.

Through MTT assay, safe concentration ranges for all the test samples to be used for gluconeogenesis assay were determined. All gluconeogenesis assay results were normalised with the total amount of protein from the same well plate that was used for gluconeogenesis assay. The normalized data is a more accurate representation of glucose production activity as it eliminates misinterpretation arose from different cell concentration.

Mangiferin in various concentrations showed significant glucose suppression effect, while genkwanin 5-O- $\beta$ -primeveroside was practically ineffective. The acetone and MeOH extracts, which were shown to contain high amounts of mangiferin, showed high glucose suppression effect. The leaf water extract, which has higher amount of mangiferin detected compared to the twig extract, corresponded to a better glucose suppression effect compared to the twig extract. Mangiferin was undetectable in bark and young shoot water extracts, which corresponded to the high glucose concentration produced. Among the tea products, Gaharu Tea and Gaharu Cool Tea have the highest amounts of leaf and twig components (consequently, corresponded to higher amounts of mangiferin present) and this is consistent with higher glucose suppression activity observed. The amount of mangiferin in GOGA Drink Powder was low, which is consistent with its very low glucose suppression activity.

The averaged mangiferin content per serving (mg) for each of the three tea products were also determined, i.e., Gaharu Tea 4.10 mg, Gaharu Cool Tea

5.70 mg, and GOGA Drink 0.36 mg. When viewed from the commercialised tea products perspective, each sachet of Gaharu Tea and Gaharu Cool Tea has comparable amount of mangiferin per serving, whereas a bottle of GOGA Drink (300 ml) has lesser amount of mangiferin per serving.

In conclusion, both mangiferin and genkwanin 5-*O*- $\beta$ -primeveroside have been isolated in the present study. It has been shown that mangiferin, but not genkwanin 5-*O*- $\beta$ -primeveroside, represents the active component that is responsible for the glucose suppression activity observed for the tea products.

## **5.2 Research Limitations and Future Works**

Although this research has successfully yielded four known compounds, two of which are the compounds of interest, namely, mangiferin and genkwanin 5-*O*- $\beta$ -primeveroside, several limitations encountered throughout the research period are listed below:

1. Due to limited resources and time constraint, the bioassays (MTT, gluconeogenesis, and Bradford Protein assays) carried out for the water extracts of the plant parts and tea products provided preliminary results, which require further studies to confirm their antidiabetic effects. For future work, RT-PCR to study gene expression associated with gluconeogenesis assay should be carried out to investigate the effect of mangiferin and the water extracts on gene



expression of PEPCK and G6Pase, which are believed to be downregulated in the presence of mangiferin (Zhang et al., 2009).

2. Concentration-response curve was not done for the water extracts of the plant parts and tea products to determine the optimal concentration that will exhibit the best glucose suppression activity. Instead, the concentration of 10  $\mu\text{g}/\text{mL}$ , which lies within the safe region of cell viability, was used for all the water extracts in this research. For future work, concentration-response curves should be established for all the water extracts of plant parts and tea products.
3. No bioassay was done on naringenin and iriflophenone 2-O- $\alpha$ -rhamnoside as they were isolated in minute quantity. Previous research has shown that iriflophenone 2-O- $\alpha$ -rhamnoside exhibited  $\alpha$ -glucoside inhibitory activity (Feng, 2011). For future work, more naringenin and iriflophenone 2-O- $\alpha$ -rhamnoside should be isolated to assess their antidiabetic effect.

## REFERENCES

- Adam, A. Z., Lee, S. Y., & Mohamed, R. (2018). Pharmacological properties of agarwood tea derived from *Aquilaria* (Thymelaeaceae) leaves: An emerging contemporary herbal drink. *J. Herb. Med.*, *10*, 37-44.
- Agrawal, V., & Desai, S. (2015). Centrifugally accelerated thin layer chromatography for isolation of marker compounds and bioactives. *J. Pharmacog. Phytochem.*, *3*(6), 145-149.
- Alam, M. A., Subhan, N., Rahman, M. M., Uddin, S. J., Reza, H. M., & Sarker, S. D. (2014). Effect of citrus flavonoids, naringin and naringenin, on metabolic syndrome and their mechanisms of action. *Adv. Nutr.*, *5*(4), 404-417.
- Álvarez-Álvarez, R., Botas, A., Albillos, S. M., Rumbero, A., Martín, J. F., & Liras, P. (2015). Molecular genetics of naringenin biosynthesis, a typical plant secondary metabolite produced by *Streptomyces clavuligerus*. *Microb. Cell Fact.*, *14*, 178.
- Apontes, P., Liu, Z. B, Su, K., Benard, O., Youn, D. Y., Li, X. S., Li, W., Mirza, R. H., Bastie, C. C., Jelicks, L. A., Pessin, J. E., Muzumdar, R. H., Sauve, A. A., & Chi, Y. L. (2014). Mangiferin stimulates carbohydrate oxidation and protects against metabolic disorders induced by high-fat diets. *Diabetes*, *63*(11), 3626-3636.
- Attele, A. S., Zhou, Y. P., Xie, J. T., Wu, J. A., Zhang, L., Dey, L., Pugh, W., Rue, P. A., Polonsky, K. S., & Yuan, C. S. (2002). Antidiabetic effects of *Panax*

*ginseng* berry extract and the identification of an effective component. *Diabetes*, 51(6), 1851-1858.

Bahrani, H., Mohamad, J., Paydar, M. J., & Rothan, H. A. (2014). Isolation and characterisation of acetylcholinesterase inhibitors from *Aquilaria subintegra* for the treatment of Alzheimer's disease (AD). *Curr. Alzheimer Res.*, 11(2), 206-214.

Bajpai, M. B., Asthana, R. K., Sharma, N. K., Chatterjee, S. K., & Mukherjee, S. K. (1991). Hypoglycemic effect of swerchirin from the hexane fraction of *Swertia chirayita*. *Pla. Med.*, 57(2), 102-104.

Barros, J., Serrani-Yarce, J. C., Chen, F., Baxter, D., Venables, B. J., & Dixon, R. A. (2016). Role of bifunctional ammonia-lyase in grass cell wall biosynthesis. *Nat. Plant*, 2(6), 16050. doi:10.1038/nplants.2016.50.

Basnet, P., Kadota, S., Shimizu, M., Takata, Y., Kobayashi, M., & Namba, T. (1995). Bellidifolin stimulates glucose uptake in rat 1 fibroblasts and ameliorates hyperglycemia in streptozotocin (STZ)-induced diabetic rats. *Pla. Med.*, 61(5), 402-405.

Berasi, S. P., Huard, C., Li, D., Shih, H. H., Sun, Y., Zhong, W., Paulsen, J. E., Brown, E. L., Gimeno, R. E., & Martinez, R. V. (2006). Inhibition of gluconeogenesis through transcriptional activation of EGR1 and DUSP4 by AMP-activated kinase. *J. Bio. Chem.*, 281(37), 27167-27177.

- Berridge, M. V., Herst, P. M., & Tan, A. S. (2005). Tetrazolium dyes as tools in cell biology: New insights into their cellular reduction. *Biotech. Ann. Rev.*, 11, 127-152.
- Biswas, T., Sen, A., Roy, R., Maji, S., & Maji, H. S. (2015). Isolation of mangiferin from flowering buds of *Mangifera indica* L and its evaluation of *in vitro* antibacterial activity. *J. Pha. Analy.*, 4(3), 49-56.
- Boarder, M., Newby, D., & Navti, P. (2010). Diabetes mellitus. In *Pharmacology for pharmacy and the health sciences: A patient-centred approach* (1<sup>st</sup> ed., pp. 354-366). New York, NY: Oxford University Press.
- Borris, R. P., Blaskó, G., & Cordell, G. A. (1988). Ethnopharmacologic and phytochemical studies of the Thymelaeaceae. *J. Ethnopharmacol.*, 24(1), 41-91.
- Bösenberg, L. H., & Zyl, D. G. V. (2008). The mechanism of action of oral antidiabetic drugs: A review of recent literature. *JEMDSA*, 13(3), 80-88.
- Bradford, M. (1976). A rapid and sensitive method for the quantitation of microgram quantities of protein utilizing the principle of protein-dye binding. *Analy. Biochem.*, 72, 248-254.
- Brescia, P., & Banks, P. (2009). Quantifying cytotoxicity of Thiostrepton on mesothelioma cells using MTT assay and the Epoch Microplate Spectrophotometer. *Biotek Application Note*.

- Cao, T. W., Geng, C. A., Ma, Y. B., He, K., Wang, H. L., Zhou, N. J., Zhang, X. M., Tao, Y. D., & Chen, J. J. (2013). Xanthonenes with anti-hepatitis B virus activity from *Swertia mussotii*. *Pla. Med.*, *79*(8), 697-700.
- Castellarin, S. D., & Di Gaspero, G. (2007). Transcriptional control of anthocyanin biosynthetic genes in extreme phenotypes for berry pigmentation of naturally occurring grapevines. *BMC Plant Biol.*, *7*, 46.
- Chen, H.Q., Wei, J. H., Yang, J. S., Zhang, Z., Yang, Y., Gao, Z. H., Sui, C., & Gong, B. (2012). Chemical constituents of agarwood originating from the endemic genus *Aquilaria* plants. *Chem. Biodivers.*, *9*, 236-250.
- Colegate, S. M., & Molyneux, R. J. (Eds.). (2008). *Bioactive natural products: Detection, isolation, and structural determination* (2nd ed.). Boca Raton, FL: CRC Press LLC.
- Crous, P. W., Gams, W., Wingfield, M. J., & Wyk, P. S. V. (1996). *Phaeoacremonium* gen. nov. associated with wilt and decline diseases of woody hosts and human infections. *Mycologia*, *88*(5), 786-796.
- Dahham, S. S., Tabana, Y. M., Iqbal, M. A., Ahamed, M. B., Ezzat, M. O., Majid, A. S., & Majid, A. M. (2015). The anticancer, antioxidant and antimicrobial properties of the sesquiterpene  $\beta$ -caryophyllene from the essential oil of *Aquilaria crassna*. *Molecules*, *20*(7), 11808-11829.
- Dall'Acqua, S., Innocenti, G., Viola, G., Piovan, A., Caniato, R., & Cappelletti, E. M. (2002). Cytotoxic compounds from *Polygala vulgaris*. *Chem. Pharmaceu. Bull.*, *50*(11), 1499-1501.

- Debski, D., Smulik, R., Zielonka, J., Michalowski, B., Jakubowska, M., Debowska, K., Adamus, J., Marcinek, A., Kalyanaraman, B., & Sikora, A. (2016). Mechanism of oxidative conversion of Amplex® Red to resorufin: Pulse radiolysis and enzymatic studies. *Free Rad. Bio. Med.*, *95*, 323-332.
- Dewick, P. M. (2002). The mevalonate and deoxyxylulose phosphate pathways: Terpenoids and steroids. In *Medicinal natural products: A biosynthetic approach* [Google Book version]. Retrieved from [https://books.google.com.my/books?id=A4zptjOJfKQC&q=terpenoid&source=gbs\\_word\\_cloud\\_r&cad=5#v=snippet&q=terpenoid&f=false](https://books.google.com.my/books?id=A4zptjOJfKQC&q=terpenoid&source=gbs_word_cloud_r&cad=5#v=snippet&q=terpenoid&f=false)
- Feng, J., Yang, X. W., & Wang, R. F. (2011). Bio-assay guided isolation and identification of  $\alpha$ -glucosidase inhibitors from the leaves of *Aquilaria sinensis*. *Phytochem.*, *72*, 242-247.
- Fester, K., & Kutchan, T. M. (2009). Introduction to the different classes of natural products. In A. E. Osbourn and V. Lanzotti (Eds.), *Plant-derived natural products: Synthesis, function, and application* (pp. 3-50). Retrieved from <https://www.researchgate.net/publication/226934227>
- Forestry Department Peninsular Malaysia. (2015). *Manual to the identification of Aquilaria species in peninsular Malaysia* [PDF file]. Retrieved from <http://www.itto.int/files/user/cites/malaysia/Manual%20Pengecaman%20Spesies%20Aquilaria%20Di%20Semenanjung%20Malaysia.pdf>

Gaharu Tea Valley Gopeng. (n.d.). Medicinal property. Retrieved Aug 10, 2018,  
from

[http://www.gaharu.com.my/shop/index.php?route=product/product  
&path=35&product\\_id=100](http://www.gaharu.com.my/shop/index.php?route=product/product&path=35&product_id=100)

Galeotti, F., Barile, E., Curir, P., Dolci, M., & Lanzotti, V. (2008). "Flavonoids from carnation (*Dianthus caryophyllus*) and their antifungal activity. *Phytochem. Lett.*, 1(1), 44–48.

Ghosal, S., Biswas, K., & Jaiswal, D. K. (1980). Xanthone and flavonol constituents of *Swertia hookeri*. *Phytochemistry*, 19(1), 123-126.

Ghosal, S., Sharma, P. V., & Chaudhuri, R. K. (1974). Chemical constituents of gentianaceae X: Xanthone-O-glucosides of *Swertia purpurascens* Wall. *J. Phar. Sci.*, 63(8), 1286-1290.

Ghosh, A., Shieh, J. J., Pan, C. J., Sun, M. S., & Chou, J. Y. (2002). The catalytic center of glucose-6-phosphatase. HIS176 is the nucleophile forming the phosphohistidine-enzyme intermediate during catalysis. *J. Biol. Chem.*, 277(36), 32837-32842.

Girón, M. D., Sevillano, N., Salto, R., Haidour, A., Manzano, M., Jiménez, M. L., Rueda, R., López-Pedrosa, J. M. (2009). Salacia oblonga extract increases glucose transporter 4-mediated glucose uptake in L6 rat myotubes: Role of mangiferin. *Clin. Nutr.*, 28(5), 565-574.

Han, J., Yi, J., Liang, F. Y., Jiang, B., Xiao, Y., Gao, S. H., Yang, N., Hu, H. G., Xie, W. F., & Chen, W. S. (2015). X-3, a mangiferin derivative, stimulates

AMP-activated protein kinase and reduces hyperglycemia and obesity in db/db mice. *Mol. Cell. Endocri.*, 405, 63-73.

Hara, H., Ise, Y., Morimoto, N., Shimazawa, M., Ichihashi, K., Ohyama, M., & Iinuma, M. (2008). Laxative effect of agarwood leaves and its mechanism. *Biosci. Biotechnol. Biochem.*, 72(2), 335-345.

Hara, H., Ise, Y., Morimoto, N., Shimazawa, M., Ichihashi, K., Ohyama, M., & Iinuma, M. (2008). Laxative effect of agarwood leaves and its mechanism. *Biosci. Biotechnol. Biochem.*, 72(2), 335-345.

Hardie, D. G., Hawley, S. A., & Scott, J. W. (2006). AMP-activated protein kinase: Development of the energy sensor concept. *J. Physiol*, 547(1), 7-15.

Havsteen, B. H. (2002). The biochemistry and medical significance of the flavonoids. *Pharmacol. Ther.*, 96(2-3), 67-202.

Herbert, G. C., & Johnstone, R. A. W. (2003). Electron ionization. In *Mass spectrometry basics* (1st ed., pp. 34-37). Boca Raton, FL: CRC Press LLC.

Horike, N., Sakoda, H., Kushiyama, A., Ono, H., Fujishiro, M., Kamata, H., Nishiyama, K., Uchijima, Y., Kurihara, Y., Kurihara, H., & Asano, T. (2008). AMP-activated protein kinase activation increases phosphorylation of glycogen synthase kinase 3 $\beta$  and thereby reduces cAMP-responsive element transcriptional activity and phosphoenolpyruvate carboxykinase C gene expression in the liver. *J. Biol. Chem.*, 283(49), 33902-33910.



- Hossain, M. K., Dayem, A. A., Han, J. H., Yin, Y. F., Kim, K. S., Saha, S. K., Yang, G. M., Choi, H. Y., & Cho, S. G. (2016). Molecular mechanisms of the anti-obesity and anti-diabetic properties of flavonoids. *Int. J. Mol. Sci.*, *17*(4), 569.
- Hostettmann, K., & Miura, I. (1977). A new xanthone diglucoside from *Swertia perennis* L. *Helv. Chim. Acta.*, *60*, 262-264.
- Hu, H. G., Wang, M. J., Zhao, Q. J., Liao, H. L., Cai, L. Z., Song, Y., Zhang, J., Yu, S. C., Chen, W. S., Liu, C. M., & Wu, Q. Y. (2007). Synthesis of mangiferin derivatives as protein tyrosine phosphatase 1B inhibitors. *Chem. Nat. Comp.*, *43*(6), 663-666.
- Huang, T. H. W., Peng, G., Li, G. Q., Yamahara, J., Roufogalis, B. D., & Li, Y. (2006). Salacia oblonga root improves postprandial hyperlipidemia and hepatic steatosis in Zucker diabetic fatty rats: Activation of PPAR-alpha. *Tox. App. Phar.*, *210*(3), 225-35.
- Ito, T., Kakino, M., Tazawa, S., Watarai, T., Oyama, M., Maruyama, H., Araki, Y., Hara, H., & Inuma, M. (2012). Quantification of polyphenols and pharmacological analysis of water and ethanol-based extracts of cultivated agarwood leaves. *J. Nutr. Sci. Vitaminol*, *58*, 136-142.
- Ito, T., Kakino, M., Tazawa, S., Watarai, T., Oyama, M., Maruyama, H., Araki, Y., Hara, H., & Inuma, M. (2012). Quantification of polyphenols and pharmacological analysis of water and ethanol-based extracts of cultivated agarwood leaves. *J. Nutr. Sci. Vitaminol*, *58*, 136-142.

Joseph, B., & Jini, D. (2013). Antidiabetic effects of *Momordica charantia* (bitter melon) and its medicinal potency. *Asian Pac. J. Trop. Disc.*, 3(2), 93-102.

Kakino, M., Izuta, H., Ito, T., Tsuruma, K., Araki, Y., Shimazawa, M., Oyama, M., Iinuma, M., & Hara, H. (2010). Agarwood induced laxative effects via acetylcholine receptors on loperamide-induced constipation in mice. *Biosci. Biotechnol. Biochem.*, 74(8), 1550-1555.

Kakino, M., Izuta, H., Ito, T., Tsuruma, K., Araki, Y., Shimazawa, M., Oyama, M., Iinuma, M., & Hara, H. (2010). Agarwood induced laxative effects via acetylcholine receptors on loperamide-induced constipation in mice. *Biosci. Biotech. Biochem.*, 74(8), 1550-1555.

Kakino, M., Izuta, H., Ito, T., Tsuruma, K., Araki, Y., Shimazawa, M., Oyama, M., Iinuma, M., & Hara, H. (2010). Agarwood induced laxative effects via acetylcholine receptors on loperamide-induced constipation in mice. *Biosci. Biotechnol. Biochem.*, 74(8), 1550-1555.

Kamonwannasit, S., Nantapong, N., Kumkrai, P., Luecha, P., Kupittayanant, S., & Chudapongse, N. (2013). Antibacterial activity of *Aquilaria crassna* leaf extract against *Staphylococcus epidermis* by disruption of cell wall. *Ann. Cli. Microb. Antimicrob.*, 12, 20.

Kavitha, M., Nataraj, J., Essa, M. M., Memon, M. A., & Manivasagam, T. (2013). Mangiferin attenuates MPTP induced dopaminergic neurodegeneration and improves motor impairment, redox balance

and Bcl-2/Bax expression in experimental Parkinson's disease mice.  
*Chem. Bio. Inter.*, 206(2), 239-247.

Korinek, M., Wagh, V. D., Lo, I. W., Hsu, Y. M., Hsu, H. Y., Hwang, T. L., Wu, Y. C., Cheng, Y. B., Chen, B. H., & Chang, F. R. (2016). Antiallergic phorbol ester from the seeds of *Aquilaria malaccensis*. *Int. J. Mol. Sci.*, 17(3), 398.

Kristanti, A. N., Tanjung, M., & Aminah, N. S. (2018). Review: Secondary metabolites of *Aquilaria*, a *Thymelaeaceae* Genus. *Mini-Rev. Org. Chem.*, 15, 36-55.

Lee, J. E., Kang, S. J., Choi, S. H., Song, C. H., Lee, Y. J., & Ku, S. K. (2015). Fermentation of green tea with 2% *Aquilariae lignum* increases the anti-diabetic activity of green tea aqueous extracts in the high fat-fed mouse.

Lee, S. Y., Nazre, M., & Rozi, M. (2013). Vegetative description of three *Aquilaria* (Thymelaeaceae) saplings in Malaysia. *Pertanika J. Trop. Agric. Sci.*, 36(S), 287-294.

Lekshmi, P. C., Arimboor, R., Nisha, V. M., Menon, A. N., & Raghu, K. G. (2014). In vitro antidiabetic and inhibitory potential of turmeric (*Curcuma longa L*) rhizome against cellular and LDL oxidation and angiotensin converting enzyme. *J. Food Sci. Technol.*, 51(12), 3910-3917.

Lepoivre, A. (1972). Centrifugal radial thin-layer chromatography. *Bull. Soc. Chim. Belg.*, 81, 213-219.

- Li, X., Cui, X. B., Sun, X., Li, X., Zhu, Q., & Li, W. (2010). Mangiferin prevents diabetic nephropathy progression in streptozotocin-induced diabetic rats. *Phyto. Res.*, *24*(6), 893-899.
- Lin, J. H., Lin, Y. T., Huang, Y. J., & Liao, C. H. (2001). Isolation and cytotoxicity of flavonoids from *Daphnis Genkwae* Flos. *J. Food. Drug. Analy.*, *9*(1), 6-11.
- Luo, Y, Fu, C. F., Wang, Z. Y., Zhang, Z., Wang, H. X., & Liu, Y. (2015). Mangiferin attenuates contusive spinal cord injury in rats through the regulation of oxidative stress, inflammation and the Bcl-2 and Bax pathway. *Mol. Med. Rep.*, *12*(5), 7132-7138.
- Méndez-Lucas, A., Hyroššová, P., Novellasdemunt, L., Viñals, F., Perales, J. C. (2014). Mitochondrial phosphoenolpyruvate carboxykinase (PEPCK-M) is a pro-survival, endoplasmic reticulum (ER) stress response gene involved in tumor cell adaptation to nutrient availability. *J. Biol. Chem.*, *289*(32), 22090-22102.
- Miura, T., Iwamoto, N., Kato, M., Ichiki, H., Kubo, M., Komatsu, Y., Sasaki, H., Ishida, T., & Tanigawa, K. (2001). Effect of mangiferin on muscle GLUT4 protein content in TSOD (Tsumura, Suzuki, Obese, Diabetes) mouse, a new type 2 diabetic mice. *Biomed. Res. Tokyo*, *22*(5), 249-252.
- Moridikia, A., Zargan, J., Sobati, H., Goodarzi, H. R., & Hajinourmohamadi, A. (2018). Anticancer and antibacterial effects of Iranian viper (*Vipera latifii*) venom; an in-vitro study. *J. Cell. Physio.*, *233*(9), 6790-6797.

- Naef, R. (2011). The volatile and semi-volatile constituents of agarwood, the infected heartwood of *Aquilaria* species: A review. *Flavour Fragr. J.*, *26*, 73-89.
- Nagao, T., Komine, Y., Soga, S., Meguro, S., Hase, T., Tanaka, Y., & Tokimitsu, I. (2005). Ingestion of a tea rich in catechins leads to a reduction in body fat and malondialdehyde-modified LDL in men. *Am. J. Clin. Nutr.*, *81*(1), 122-129.
- Nakashima, E. M. N., Nguyen, M. T. T., Le Tran, Q., & Kadota, S. (2005). Field survey of agarwood cultivation at Phu Quoc Island in Vietnam. *J. Trad. Med.*, *22*, 296-300.
- Neena, V., Devi, C. U., Hema, J., Shahi, V. K., Sharma, V. P., & Shiv, L. (2000). Comparative efficacy of Ayush-64 vs. chloroquine in vivax malaria. *Cur. Sci.*, *78*(9), 1120-1122.
- Negi, J. S., Bisht, V. K., Singh, P., Rawat, M. S. M., & Joshi, G. P. (2013). Naturally occurring xanthenes: Chemistry and biology review article. *J. App. Chem.*, *2013*, 1-9.
- Niu, Y. C., Li, S. T., Na, L. X., Feng, R. N., Liu, L. Y., Li, Y., & Sun, C. H. (2012). Mangiferin decreases plasma free fatty acid through promoting its catabolism in liver by activation of AMPK. *Plos One*, *7*(1), Article ID: e30782.

- Oldenburg, T. B. P., Wilkes, H., Horsfield, B., Van Duin, A. C. T. Stoddart, D., & Wilhelms, A. (2002). Xanthenes-novel aromatic oxygen-containing compounds in crude oils. *Org. Geochem.*, 33(5), 595-609.
- Ozougwu, J. (2011). Anti-diabetic effects of *Allium cepa* (Onions) aqueous extracts on alloxan-induced diabetic *Rattus Novergicus*. *Pharmacologyonline*, 1(7), 270-281.
- Pengsuparp, T., Cai, L., Constant, H., Fong, H. H., Lin, L. Z., Kinghorn, A. D., Pezzuto, J. M., Cordell, G. A., Ingolfssdóttir, K., & Wagner, H. (1995). Mechanistic evaluation of new plant-derived compounds that inhibit HIV-1 reverse transcriptase. *J. Nat. Prod.*, 58(7), 1024-1031.
- Prakash, A., Basumatary, P.C., Ghosal, S., & Handa, S. S. (1982). Chemical constituents of *Swertia paniculata*. *Pla. Med.*, 45(1), 61-62.
- Pranakhon, R., Aromdee, C., & Pannangpetch, P. (2015). Effects of iriflophenone 3-C- $\beta$ -glucoside on fasting blood glucose level and glucose uptake. *Pharmacogn. Mag.*, 11(41), 82-89.
- Prasain, J. K., Carlson, S. H., & Wyss, J. M. (2010). Flavonoids and age-related disease: Risk, benefits and critical windows. *Maturitas*, 66(2), 163-171.
- Putalun, W., Yusakul, G., Saensom, P., Sritularak, B. & Tanaka, H. (2013). Determination of iriflophenone 3-C- $\beta$ -D-glucoside from *Aquilaria* spp. by an indirect competitive enzyme-linked immunosorbent assay using a specific polyclonal antibody. *J. Food. Sci.*, 78(9), 1363-1367.

- Qi, J., Lu, J. J., Liu, J. H., & Yu, B. Y. (2009). Flavonoids and a rare benzophenone glycoside from the leaves of *Aquilaria sinensis*. *Chem. Pharm. Bull.*, 57(2), 134-137.
- Rana, P., Sohel, S. I., Akhter, S., & Islam, J. (2010). Ethno-medicinal plants use by the *Manipuri* tribal community in Bangladesh. *J. Forest. Res.*, 21(1), 85-92.
- Rang, H. P., Dale, M. M., Ritter, J. M., & Moore, P. K. (2003). The endocrine pancreas and the control of blood glucose. In *Pharmacology* (5<sup>th</sup> ed., pp. 380-393). Loanhead, Scotland: Elsevier Science.
- Raval, V., Khare, S. K., Kothari, R., & Singh, S. P. (n.d.). Metabolism of carbohydrates: Gluconeogenesis [PDF]. Retrieved from e-PG Pathshala Website: <https://epgp.inflibnet.ac.in/ahl.php?csrno=2>
- Sahin, A. A., Aslim, B., Tan, S., Alan, S. & Pinar, N. M. (2018). Differences in structure, allergenic protein content and pectate lyase enzyme activity of some Cupressaceae pollen. *Turk. J. Biochem.*, 43(4), 435-446.
- Sam, Y. Y., & Noordin, M. A. (2017). *A report on the plant identification, taxonomic description and botanical illustration of Aquilaria sinensis (family Thymelaeaceae) submitted to Gaharu Technologies Sdn. Bhd.* Forest Research Institute Malaysia: Forest Biodiversity Division.
- Sarker, S. D., Latif, Z., & Gray, A. I. (Eds.). (2006). *Methods in biotechnology: Natural products isolation* (2nd ed.). Totowa, NJ: Humana Press Inc.

- Saxena, P. B. (2007). *Chemistry of alkaloid* [Google Books version]. Retrieved from [https://books.google.com.my/books?id=zZB21wSZpyUC&pg=PA1&source=gbs\\_toc\\_r&cad=3#v=onepage&q&f=false](https://books.google.com.my/books?id=zZB21wSZpyUC&pg=PA1&source=gbs_toc_r&cad=3#v=onepage&q&f=false)
- Shan, W. G., Lin, T. S., Yu, H. N., Chen, Y., & Zhan, Z. J. (2012). Polyprenylated xanthenes and benzophenones from the bark of *Garcinia oblongifolia*. *Helv. Chim. Acta.*, 95(8), 1442-1448.
- Shekarchi, M., Hajimehdipoor, H., Khanavi, M., Adib, N., Bozorgi, M., & Akbari-Adergani, B. (2010). A validated method for analysis of Swerchirin in *Swertia longifolia* Boiss. by high performance liquid chromatography. *Phcog. Mag.*, 6(21), 13-18.
- Shen, B. (2003). Polyketide biosynthesis beyond the type I, II and III polyketide synthase paradigms. *Cur.Opi.Chem.Bio.*, 7, 285-295.
- Spagnuolo, C., Russo, G. L., Orhan, I. E., Habtemariam, S., Daglia, M., Sureda, A., Nabavi, S. F., Devi, K. P., Loizzo, M. R., Tundis, R., & Nabavi, S. M. (2015). Genistein and cancer: Current status, challenges, and future directions. *Adv. Nutr.*, 6(4), 408-419.
- Spector, T. (1978). Refinement of the Coomassie blue method of protein quantitation: A simple and linear spectrophotometric assay for  $\leq 0.5$  to 50  $\mu\text{g}$  of protein. *Analy. Biochem.*, 86(1), 142-146.
- Staggering 3.6 mil Malaysians have diabetes (2017, November 15), *New Straits Times*. Retrieved from



<https://www.nst.com.my/news/nation/2017/11/303305/staggering-36mil-malaysians-have-diabetes>

Supasuteekul, C., Nuamnaichati, N., Mangmool, S., & Sritularak, B. (2017).

Antioxidant activity and upregulation of antioxidant enzymes of phenolic glycosides from *Aquilaria crassna* leaves. *Nat. Prod. Comm.*, *12*(11), 1691-1694.

The International Bank for Reconstruction and Development/THE WORLD

BANK (2008). What's driving the wildlife trade? A review of expert opinion on economic and social drivers of the wildlife trade and trade control efforts in Cambodia, Indonesia, Lao PDR, and Vietnam. *TRAFFIC*.

Thermo Fisher Scientific. (n.d.). Amplex® Red enzyme assays. Retrieved from

<https://www.thermofisher.com/my/en/home/brands/molecular-probes/key-molecular-probes-products/amplex-red-enzyme-assays.html>

Tringali, C. (Eds.). (2001). *Bioactive compounds from natural sources: Isolation, characterisation and biological properties*. New York, NY: Taylors & Francis Inc.

Tsuda, T., Watanabe, M., Ohshima, K., Norinobu, S., Choi, S. W., Kawakishi, S.,

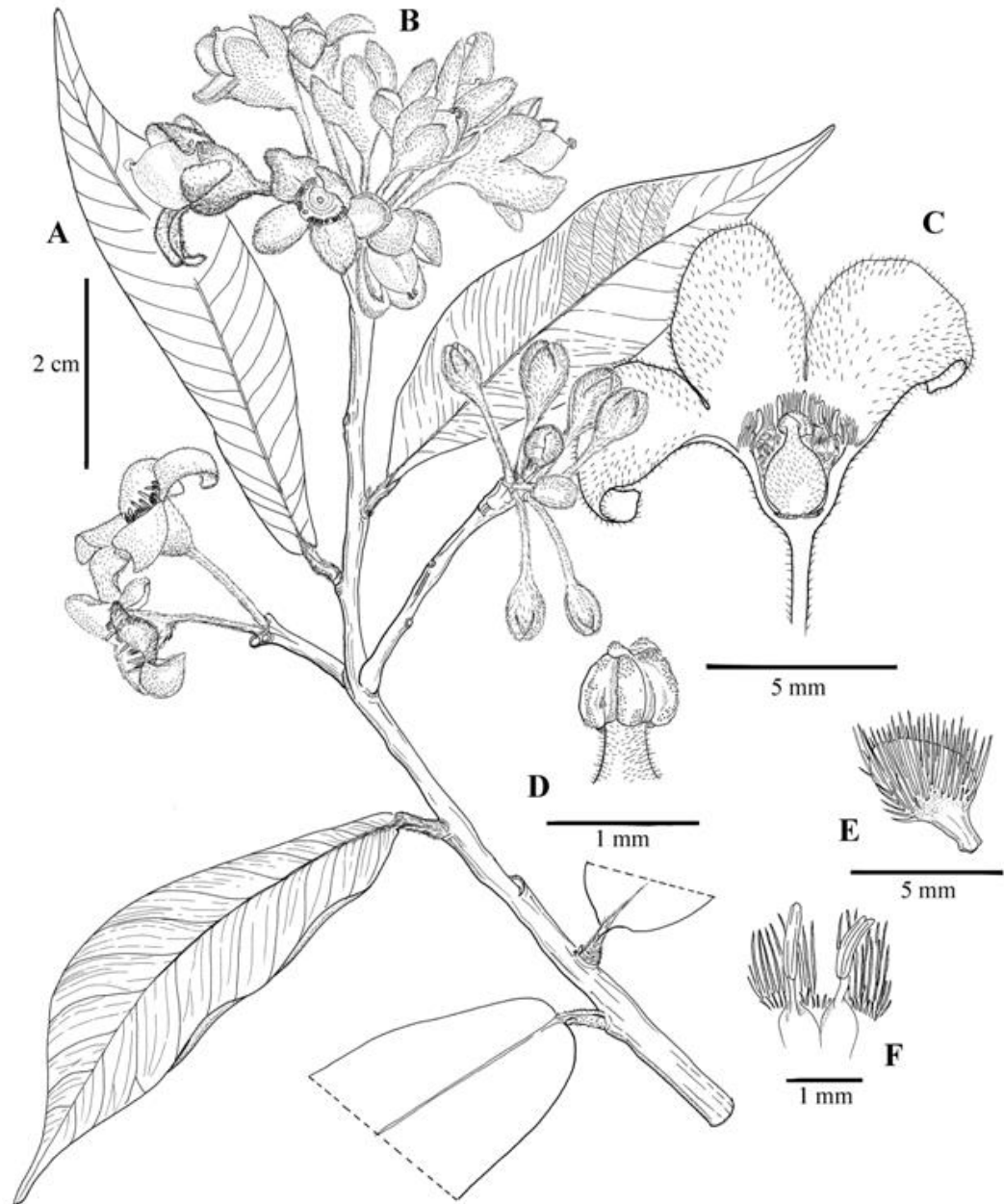
& Osawa, T. (1994). Antioxidative activity of the anthocyanin pigments cyanidin 3-O- $\beta$ -D-glucoside and cyanidin. *J. Agric. Food. Chem.*, *42*(11), 2407-2410.

- Valko, K. (Eds.). (2000). *Separation methods in drug synthesis and purification*. Amsterdam, NL: Elsevier Science B. V.
- Vieira, L. M. M., & Kijjoa, A. (2005). Naturally-occurring xanthenes: Recent developments. *Cur. Med. Chem.*, 12(21), 2413-2446.
- Vogt, T. (2010). Phenylpropanoid biosynthesis. *Mol. Plant*, 3(1), 2-20.
- Wadkar, K. A., Magdum, C. S., Patil, S. S., & Naikwade, N. S. (2008). Anti-diabetic potential and Indian medicinal plants. *J. Herb. Med. Tox.*, 2(1), 45-50.
- Wang, C., Jiang, J. D., Wu, W., & Kong, W. J. (2016). The compound of mangiferin-berberine salt has potent activities in modulating lipid and glucose metabolisms in HepG2 cells. *Biomed. Res. Int.*, 2016, Article ID: 8753436.
- Wang, S., Yu, Z. X., Wang, C. H., Wu, C. M., Guo, P., & Wei, J. H. (2018). Chemical constituents and pharmacological activity of agarwood and *Aquilaria* plants. *Molecules*, 23, 342-362.
- Wang, X., Song, Z. J., He, X., Zhang, R. Q., Zhang, C. F., Li, F., Wang, C. Z., & Yuan, C. S. (2015). Antitumor and immunomodulatory activity of genkwanin on colorectal cancer in the APC<sup>Min/+</sup> mice. *Int. Immunopharm.*, 29(2), 701-707.
- Waters Corporation. (1999). *PDA software: Getting started guide* [PDF file]. Retrieved from <http://www.waters.com/webassets/cms/support/docs/wat053020tpr1.pdf>

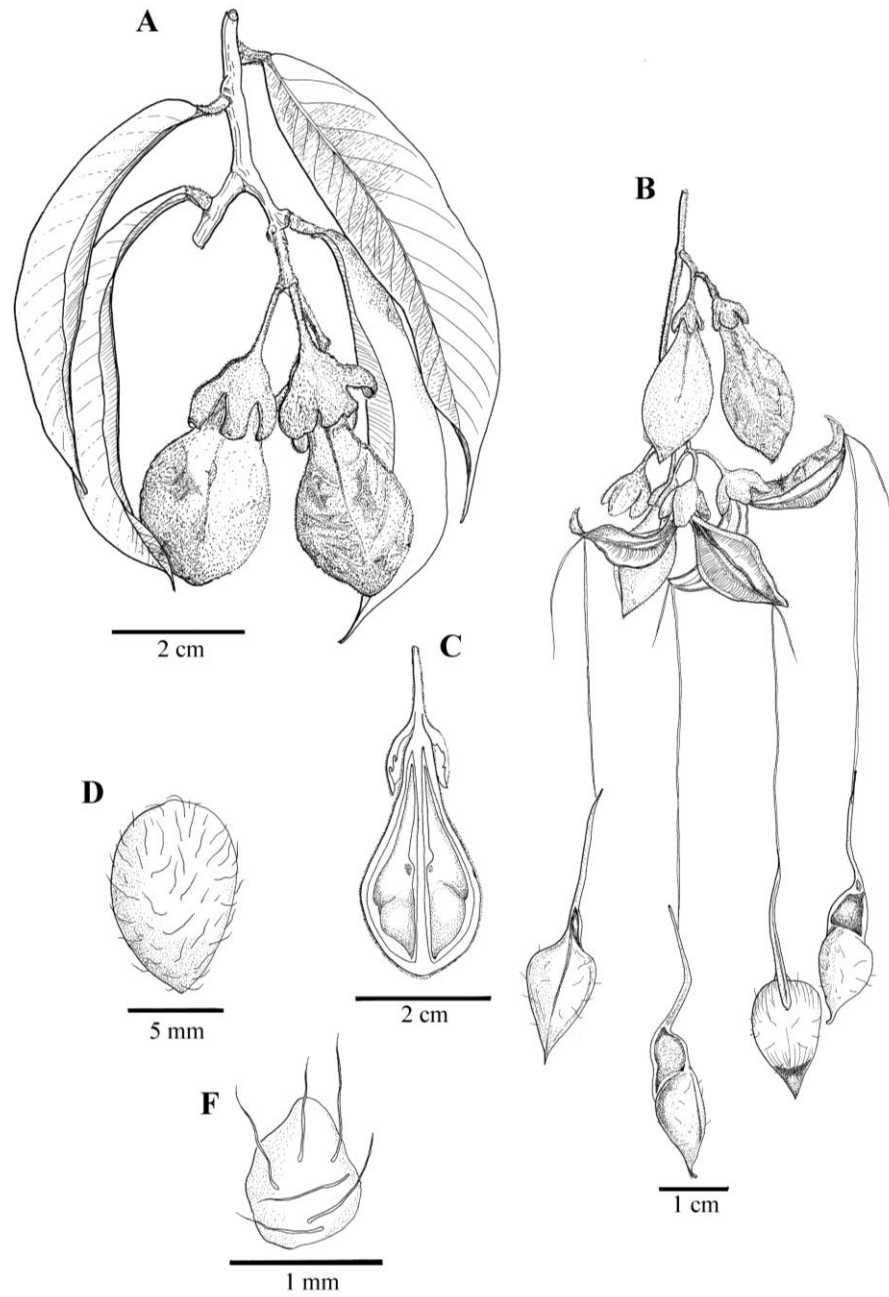
- Xing, F., Tan, Y., Yan, G. J., Zhang, J. J., Shi, Z. H., Tan, S. Z., Feng, N. P., and Liu, C. H. (2012). Effects of Chinese herbal cataplasm Xiaozhang Tie on cirrhotic ascites. *J. Ethnopharmacol.*, 139(2), 343-349.
- Xue, Q. C., Li, C. J., Zuo, L., Yang, J. Z., & Zhang, D. M. (2009). Three new xanthones from the roots of *Polygala japonica* houtt. *J. Asian. Nat. Prod. Res.*, 11(5), 465-469.
- Yang, D. L., Wang, H., Guo, Z. K., Li, W., Mei, W. L., & Dai, H. F. (2014). Fragrant agarofuran and eremophilane sesquiterpenes in agarwood 'Qi-Nan' from *Aquilaria sinensis*. *Phytochem. Lett.*, 8, 121-125.
- Yousefi, M. K., Hashtroudi, M. S., Moradi, A. M., & Ghasempour, A. R. (2017). In vitro investigating of anticancer activity of focuxanthin from marine brown seaweed species. *Glob. J. Environ. Sci. Manag.*, 4(1), 81-90.
- Zhang, B. B., Zhou, G. C., & Li, C. (2009). AMPK: An emerging drug target for diabetes and metabolic syndrome. *Cell Met.*, 9, 407-416.
- Zhang, M., Swarts, S. G., Yin, L., Liu, C., Tian, Y., Cao, Y., Swarts, M., Yang, S., Zhang, S. B., Zhang, K., Ju, S., Olek, D. J. Jr., Schwartz, L., Keng, P. C., Howell, R., Zhang, L., & Okunieff, P. (2011). Antioxidant properties of quercetin. *Adv. Exp. Med. Biol.*, 701, 283-289.
- Zhou, M., Wang, H., Suolangjiba, Kou, J., & Yu, B. (2008). Antinociceptive and anti-inflammatory activities of *Aquilaria sinensis* (Lour.) Gilg. Leaves extract. *J. Ethnopharmacol.*, 117(2), 345-350.

## APPENDICES

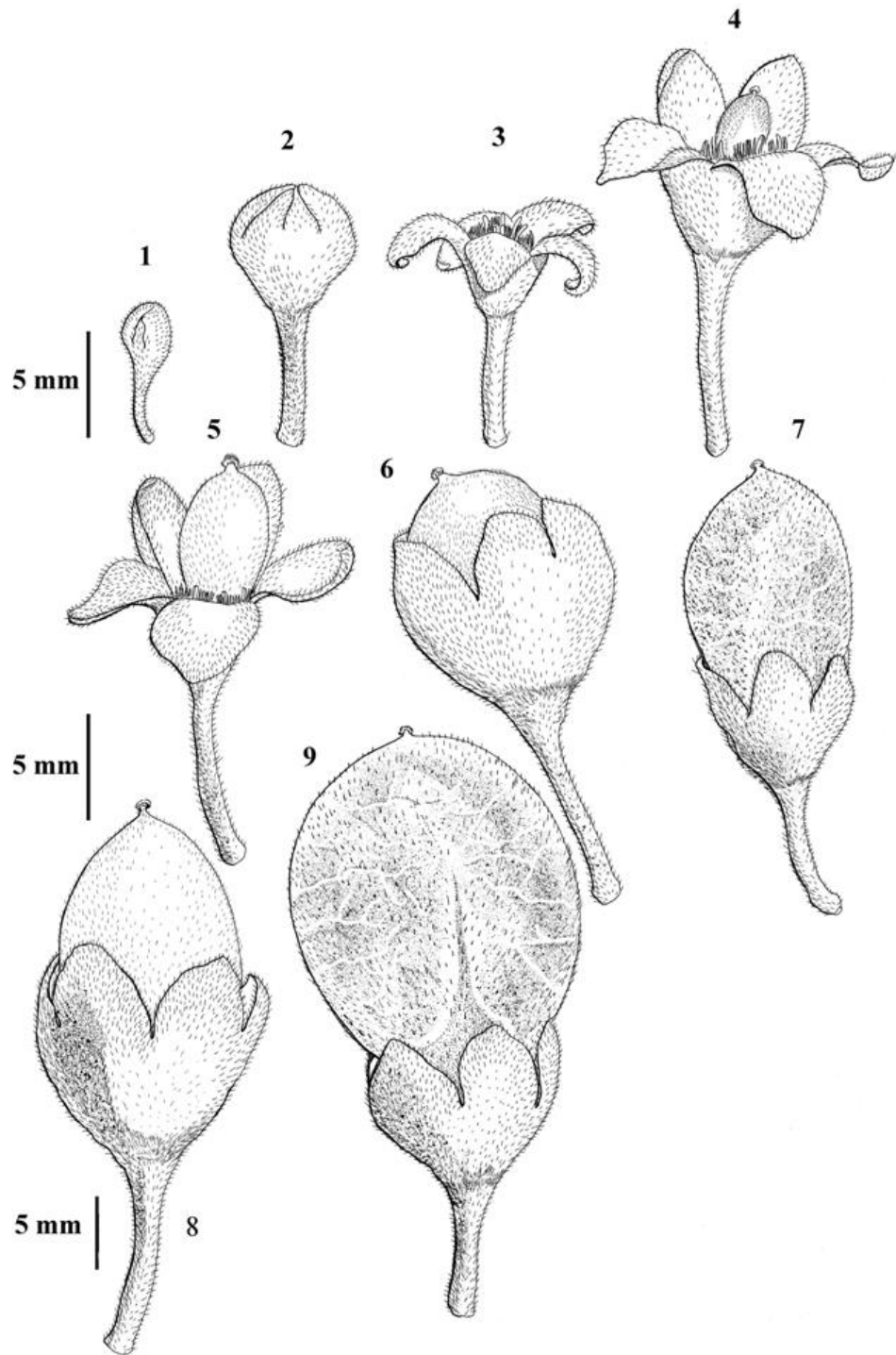
**Appendix 1** – *Aquilaria sienensis*. A. Flowering twig. B. Inflorescence. C. Flower with part of calyx removed. D. Stigma. E. Petaloid appendages. F. Stamens (in front) with petaloid appendages (behind).



**Appendix 2 – *Aquilaria sienensis*.** A. Fruiting bunch. B. Dehisced fruits with seeds hanging on long threadlike funicle. C. Longitudinal section of fruit. D. Seed. F. Hairs on seed surface.



**Appendix 3** – *Aquilaria sinensis*. Stages of development from flower bud to mature fruit.

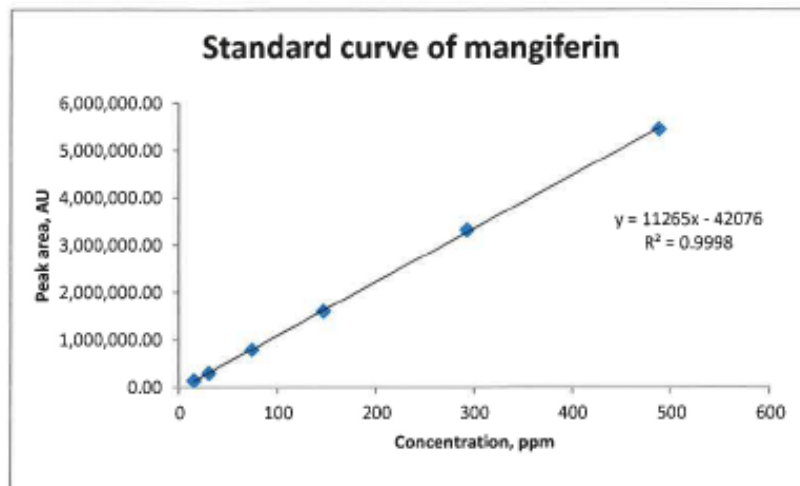


**Appendix 4 – HPLC analysis of mangiferin (1) tested against standard mangiferin.**

PROGRAM FITOKIMIA, BAHAGIAN HASILAN SEMULA JADI  
 INSTITUT PENYELIDIKAN PERHUTANAN MALAYSIA (FRIM)  
 52109 KEPONG, SELANGOR DARUL EHSAN.

**SULIT**

Standard curve of mangiferin:



Quantification of mangiferin in the sample:

Sample	Concentration (ppm)			Average concentration ± SD (ppm)	Concentration in % sample (w/w)			Average concentration in % sample ±SD (w/w)
	Run 1	Run 2	Run 3		Run 1	Run 2	Run 3	
Mangiferin 1 (1290617)	196.49	198.84	201.11	198.81 ± 2.31	98.24	99.42	100.56	99.41 ± 1.16
Mangiferin 2 (1300617)	197.76	193.04	192.81	194.54 ± 2.79	98.88	96.52	96.41	97.27 ± 1.40
AVERAGE (N=6)								98.34 ± 1.64

**Appendix 5 – HPLC quantitative analysis of mangiferin in the water extracts of plant parts and tea products (by FRIM).**

**PROGRAM FITOKIMIA, BAHAGIAN HASILAN SEMULA JADI  
INSTITUT PENYELIDIKAN PERHUTANAN MALAYSIA (FRIM)  
52109 KEPONG, SELANGOR DARUL EHSAN**

**SULIT**

Table 1: Quantitative analysis of mangiferin in the test samples.

Sample (mg) [reference number]	Concentration (ppm)			Average concentration $\pm$ RSD (ppm)	Concentration in % sample (w/w)			Average concentration in % sample $\pm$ RSD (w/w)
	Run 1	Run 2	Run 3		Run 1	Run 2	Run 3	
AQGT (89.8) [0860318]	398.34	423.97	421.71	414.67 $\pm$ 3.42	1.28	1.37	1.36	1.34 $\pm$ 3.42
AQGCT (105.7) [0870318]	208.74	208.32	207.82	208.30 $\pm$ 0.22	1.89	1.89	1.88	1.89 $\pm$ 0.22
AQGDP (103.5) [0880318]	62.00	60.72	60.79	61.17 $\pm$ 1.18	0.18	0.17	0.17	0.17 $\pm$ 1.18
AQT (97.2) [0890318]	179.68	182.16	179.91	180.59 $\pm$ 0.76	0.52	0.52	0.52	0.52 $\pm$ 0.76
AQB (104.8) [0700318]	ND	ND	ND	ND	ND	ND	ND	ND
AQL (99) [0710318]	372.15	370.43	370.22	370.93 $\pm$ 0.29	6.38	6.35	6.35	6.36 $\pm$ 0.29
AQYS (94.6) [0720318]	ND	ND	ND	ND	ND	ND	ND	ND
AQGT (97.2) [0730318]	468.69	468.24	468.97	468.63 $\pm$ 0.08	1.32	1.32	1.32	1.32 $\pm$ 0.08
AQGCT (96.8) [0740318]	174.63	173.18	173.56	173.79 $\pm$ 0.43	1.44	1.43	1.43	1.43 $\pm$ 0.43
AQGDP (96.5) [0750318]	66.74	66.88	67.11	66.91 $\pm$ 0.28	0.18	0.18	0.18	0.18 $\pm$ 0.28
AQT (99.2) [0760318]	185.58	184.91	184.84	185.11 $\pm$ 0.22	0.48	0.48	0.48	0.48 $\pm$ 0.22
AQB (100.2) [0770318]	ND	ND	ND	ND	ND	ND	ND	ND
AQL (98.5) [0780318]	380.62	377.93	379.04	379.20 $\pm$ 0.36	5.65	5.61	5.63	5.63 $\pm$ 0.36
AQYS (109.6) [0790318]	ND	ND	ND	ND	ND	ND	ND	ND

ND – not detected



**Appendix 6** – HPLC quantitative analysis of genkwanin 5-O- $\beta$ -primeveroside in the water extracts of plant parts and tea products (by Permulab Sdn Bhd).

**6.0 Result**

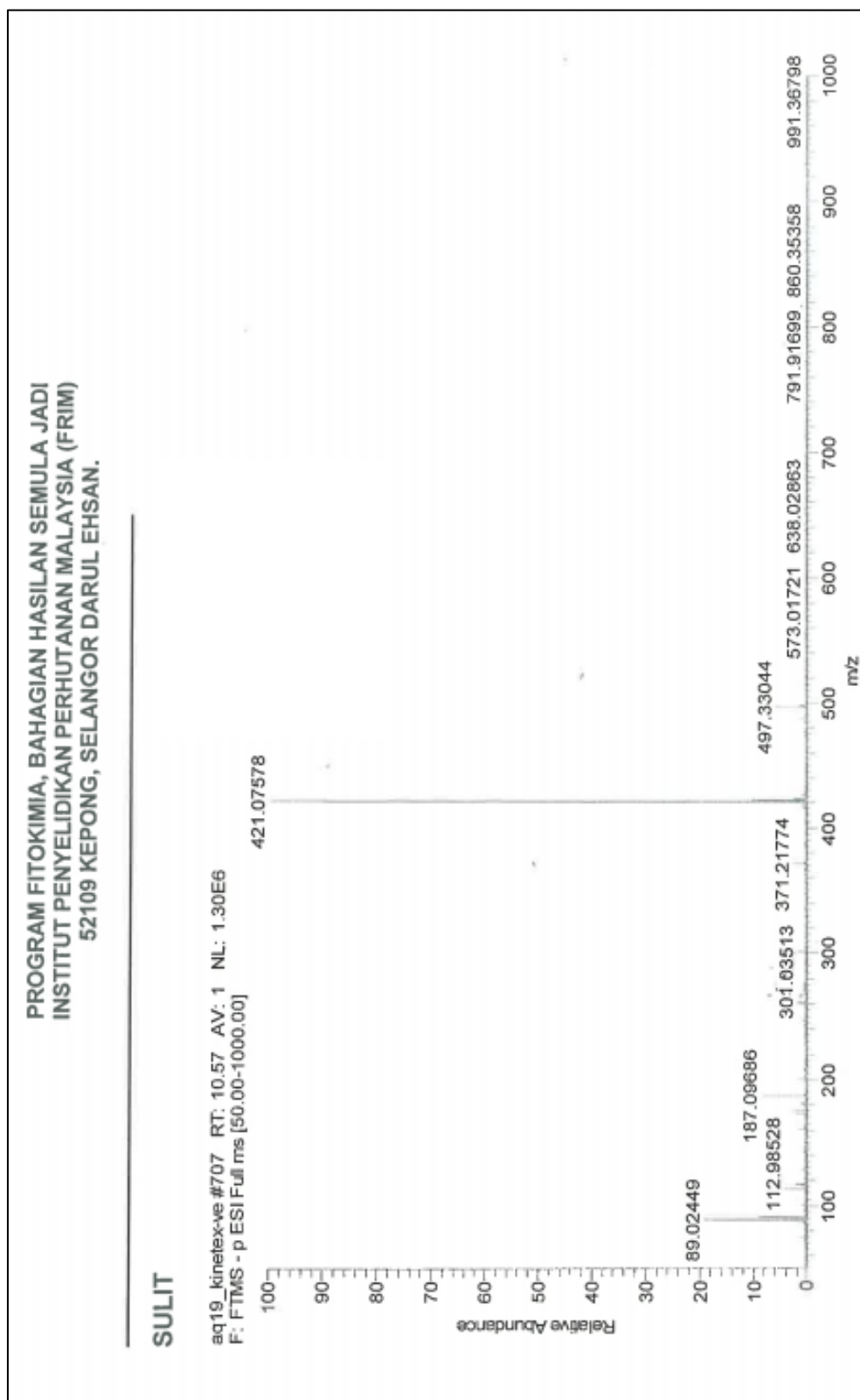
Code	Sample	Sample weight (mg)	Concentration (ppm)			Average (ppm)
			Inj. 1	Inj. 2	Inj. 3	
AQGT	Gaharu Tea	108.2	54.0874	54.0559	54.0187	54.0540
AQGCT	Gaharu Cool Tea	90.9	32.4335	32.4582	32.7986	32.5634
AQGDP	Goga Drink Powder	98.1	ND	ND	ND	ND
AQT	Twig	106.7	ND	ND	ND	ND
AQB	Bark	97.5	ND	ND	ND	ND
AQL	Leaf	97.1	176.353	177.198	177.211	176.920
AQYS	Young Shoot	90.0	ND	ND	ND	ND

Table 1 : Concentration of Genkwanin 5-O- $\beta$ -primeveroside from the chromatogram in ppm.

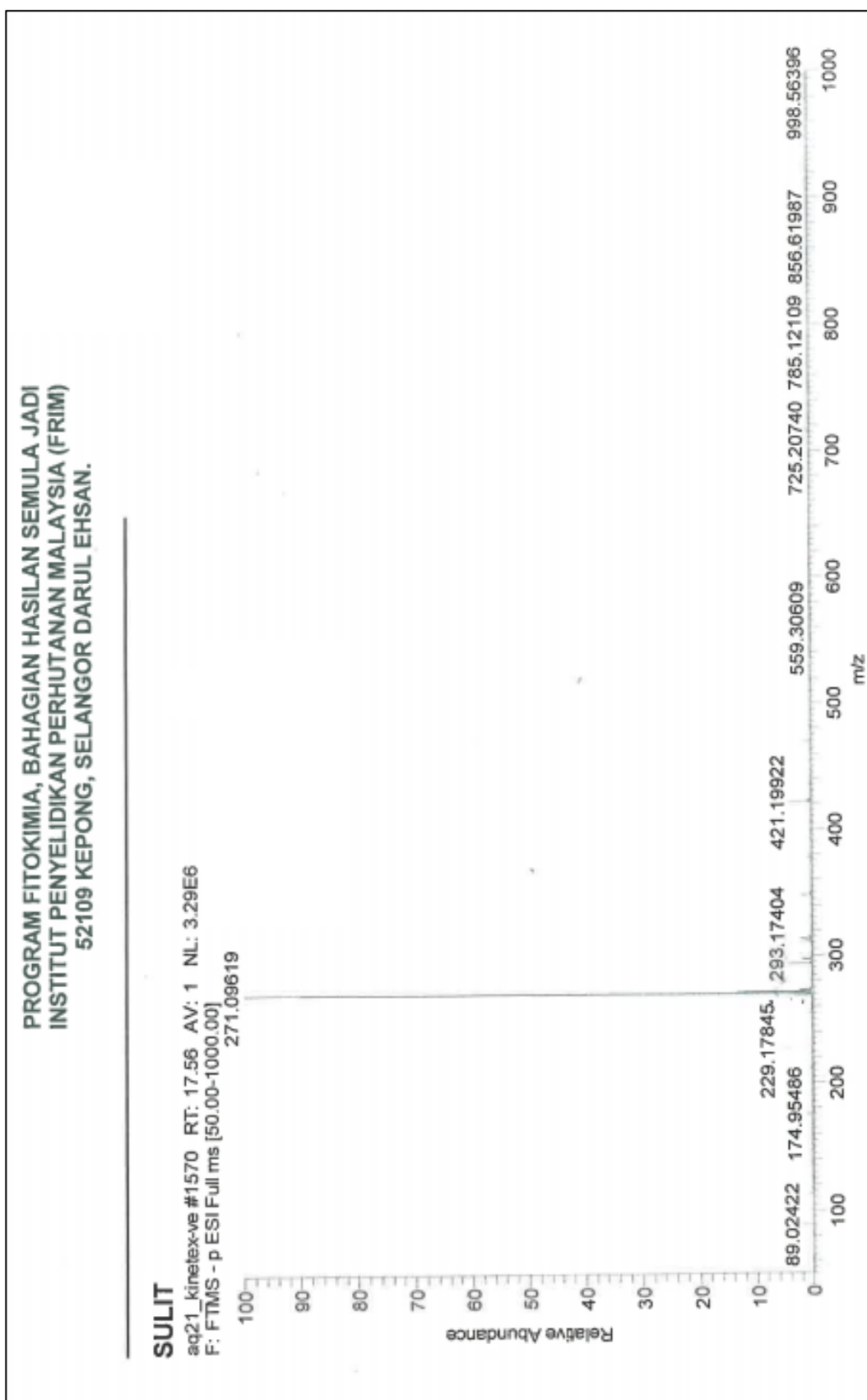
Code	Sample	Sample weight (mg)	Concentration (%)			Average (%)
			Inj. 1	Inj. 2	Inj. 3	
AQGT	Gaharu Tea	108.2	0.15	0.15	0.15	0.15
AQGCT	Gaharu Cool Tea	90.9	0.11	0.11	0.11	0.11
AQGDP	Goga Drink Powder	98.1	ND	ND	ND	ND
AQT	Twig	106.7	ND	ND	ND	ND
AQB	Bark	97.5	ND	ND	ND	ND
AQL	Leaf	97.1	0.54	0.55	0.55	0.55
AQYS	Young Shoot	90.0	ND	ND	ND	ND

Table 2 : Concentration of Genkwanin 5-O- $\beta$ -primeveroside in percentage.

Appendix 7 – LC-Orbitrap-MS (negative mode) of mangiferin (1).



Appendix 8 – LC-Orbitrap-MS (negative mode) naringenin (2).



**Appendix 9** – LC-Orbitrap-MS (negative mode) iriflophenone 2-O- $\alpha$ -rhamnoside (**3**).

